University of Alberta

Acid Catalyzed Aromatic Alkylation in the Presence of Nitrogen Bases

by

Yuhan Xia

A thesis submitted to the Faculty of Graduate Studies and Research
in partial fulfillment of the requirements for the degree of

Master of Science

in

Chemical Engineering

Department of Chemical and Material Engineering

Fall 2012
Edmonton, Alberta

Abstract

Coal pyrolysis liquids are rich in olefinic, phenolic and aromatic compounds, but traditional hydroprocessing destroys their inherent synthetic values. Acid catalyzed processes are not considered, because coal pyrolysis liquids also contain nitrogen bases. We aim to find appropriate catalysts that can conduct acid catalysis in the presence of nitrogen bases.

Catalytic aromatic alkylation using phenol and 1-hexene without and with pyridine was selected as model reaction at 315°C. Different alumina and silica-alumina (1-40 wt% silica) catalysts were characterized. Siral30, the catalyst with the highest medium strength acidity, performed best when the feed contained a nitrogen base. Siral40, the catalyst with the highest strong Brønsted acidity, performed best in the absence of nitrogen bases. Hydration affected the catalysis and had to be controlled. Autocatalysis of phenol alkylation with alkenes can also proceed and was responsible for a minor contribution to the overall conversion. The reaction products were mainly *ortho*-C-alkylphenols.

Acknowledgement

First of all, I would like to give my sincere thanks to my supervisor Dr. Arno De Klerk for all the great guidance and support. It was your remarkable patience, your enthusiastic supervision and your fully trust supported me to overcome the challenges throughout my master study. I will always be grateful and keep your valuable suggestions as I moved forward in my future work.

Secondly, I would like to thank all my colleagues for the kind help and pleasant communication. The encouragements, the accompanying, and the sharing meant a lot to me during the research time. Special thanks to Shaofeng Yang for sharing the lab experiences and providing many suggestions.

Thirdly, I'm very grateful for the financial support received through the Canadian Centre for Clean Coal/Carbon and Mineral Processing Technology (C_5MPT).

Last but not the least, I would like to thank my family for the perpetual faith and love during my research life in Canada. And I would like to thank all my friends being there with me, makes me feel like home.

Table of contents

List of Tables

List of Figures

Chapter 1: Introduction

Tightening oil markets and record high prices have brought oil vulnerability back into focus. The sustainability of conventional crude oil as the raw material for almost all production of liquid transportation fuels and petrochemicals is increasingly being questioned. Conventional crude oil is a finite natural resource and the point of maximum crude oil production is popularly known as “peak oil”. The Hubbert-model successfully predicted peak oil production in the United States In 1970. Since then about half of the crude oil producing countries have passed their peak oil production. Therefore, the challenge that is considered here is to proactively develop refining technology for the conversion of alternative carbon sources when the eventual shortfall in conventional crude oil must be mitigated.

The historical abundance, ease of refining and low price of conventional crude oil gave rise to the almost complete displacement of coal liquids obtained from coal pyrolysis and liquefaction as a source of transportation fuels and chemicals. In future this situation may change if coal regains some importance for the production of liquid products.[1] Doubts about the adequate amounts of crude oil and a steep price hike in petroleum products during the past decade brought more attention to coal-to-liquids conversion. Therefore, serious efforts are being made to produce synfuels and chemical products from coal. Improved processes for pyrolysis (or carbonization), direct and indirect liquefaction, and

solvent extraction of coal are being developed to meet the challenge of the anticipated energy crisis.[2]

Coal is not as localized in its distribution compared to petroleum and natural gas, it is more abundant and the location of coal reserves is more widely spread throughout the world. Coal also plays an important role in the development of the economy throughout the world. Although the demand for coal will be affected by the changing prices of other energy sources, the importance position of coal as energy and carbon source will not change in the future. On the other hand, to compensate for the future shortage of petroleum and natural gas, the use of coal is anticipated to gradually increase. The development of the coal utilization technology will become more and more important, for the supply in transportation fuels and chemicals products.

Table 1-1. Estimated production cost for natural and synthetic crude oils produced from various sources

Oilfields/source	Estimated Production Costs ($/BBL 2008)
Mideast/N.Africa oilfields	6 - 28
Other conventional oilfields	6 - 39
Deep/ultra-deep-water oilfields	32 - 65
Arctic oilfields	32 - 100
CO_2 enhanced oil recovery	30 - 80
Enhanced oil recovery	32 - 82
Heavy oil/bitumen	32 - 68
Oil shales	52 - 113
Gas-to-liquids	38 - 113
Coal-to-liquids	60 - 113

Various factors affect the cost of oil production, including the size and accessibility of the field. Precise cost information is rarely disclosed. The International Energy Agency (IEA) gave the following estimates for the total costs of producing oil from various types of hydrocarbons in different parts of the world in its November 2008 world energy outlook (Table 1- 1).[3]

Because the demand for petroleum and natural gas in the industrialized nations continues to rise, world petroleum supplies are expected to become limiting in the near future and the local distribution of it has resulted in several crises and supply interruptions. Coal can be considered to be one of the most attractive alternative sources. From the energy outlook we can see that the production cost of coal-to-liquids is not low. It is necessary to improve processes for the downstream refining of coal liquids into high quality fuels. And the technologies should meet environmental legislation. One of the key areas of research for this purpose is catalysis.

The composition of coal and coal conversion technology will briefly be described, before the objective of this study is outlined.

1.1 Coal [4-5]

In order to develop efficient technologies, one must be aware of the classification and the structure of coal. Coal is an extremely complex material and displays a wide range of physical properties. It is an organic rock that

contains various amounts of carbon, hydrogen, nitrogen, oxygen, sulfur and traces of other elements, including mineral matter.

Coal contains more than 50% by weight and more than 70% by volume of carbonaceous material (including inherent moisture). The three largest coal reserves are in the United States, the former Soviet Union, and China. Each of The United States and former Soviet Union has about 23% of the world's reserves, and China has about 11%.

1.1.1 Chemistry of coal

Coal is a collective of heterogeneous substances including organic and inorganic materials. Despite decades of research by many outstanding scientists, the fundamental nature of coal is still poorly understood. The structure of coal is still being studied as well as debated. Macerals, the optically homogeneous discrete organic materials in coal, include three major groups: vitrinite, liptinites (exinite), and inertinite. Vitrinite is the most common group, it is developed from woody plant material (mainly lignin), contributing around 80% of the organic matter. Exinite is believed to be derived from lipids and waxy plant substances. Char, a possible origin of inertinites, is said to be formed by prehistoric pyrolysis. The inorganic material in coal is composed mainly of clay minerals, carbonates, quartz, sulfides, and sulfates, as well as traces of other substances.

The structure of coal is a three-dimensional cross-linked polymer, it incorporates aromatic rings linked by aliphatic carbon bridges or ether oxygen

bridges. In low rank coals, the aromatic systems are one ring or two rings systems, containing abundant methoxyl ether, phenol, and carboxylic acid groups. The sizes of the ring systems gradually grow as coal rank increases. When containing about 85% carbon, the rings start to line up on top of each other and the oxygen groups become less. As carbon reaches 90%, there are only a few bridging ether oxygen atoms that remain in coal. In anthracite, which has as high as 95% carbon, the systems comprises of tens of individual rings fused together. Graphite, known as the ultimate coal with an aromaticity of 1, contains neatly stacked fused rings of almost infinite extent.

1.2 Conversion

The conversion of coal to synthetic fuels encompasses a number of catalytic processes and reactions, the most important of which are summarized in Table1-2.[6]

In addition to a variety of current processes of coal conversion to gaseous and liquid fuels, the table includes many catalytic reactions used in the refining of petroleum, similar reactions are anticipated to be applicable for upgrading coal liquids.

Table1-2. Coal conversion processes

Process	General Reactions	Particular Reaction or Products
Direct	Hydrogenation	Aromatics Liquids
Liquefaction	Cracking	Hydrodesulfurization(HDS)
	Hydrofining	Hydrodenitrogenation(HDN)
Direct	Hydrogasification	Methane
Gasification	Oxidative Gasification	Synthesis Gas
CO/H_2 Synthesis	Fischer-Tropsch	Methane
		Hydrocarbon Liquids
		Alcohols
		Chemicals
Water-Gas Shift		Hydrogen
Liquids Refining	Cracking	Hydrogenation
And Upgrading	Reforming	Dehydrogenation
	Hydroforming	Dehydrocyclization
		Isomerization
		Hydrogenolysis
		Hydrodesulfurization(HDS)
		Hydrodenitrogenation(HDN)

1.2.1 Liquefaction

Coal liquefaction means the conversion of solid coal into liquid fuels. Direct liquefaction and indirect liquefaction can be employed.

Direct liquefaction involves the conversion of solid coal to liquids without the process of producing synthesis gas as an intermediate step. Direct coal liquefaction should be the most efficient method of liquid production and this method makes it possible to obtain the highest oil yield. Many technologies were developed for direct coal liquefaction, such as hydropyrolysis, pyrolysis in the presence of high pressure hydrogen and coal extraction using solvent and/or critical gas.

In indirect liquefaction, coal is gasified in the presence of steam and oxygen to produce a synthesis gas (syngas) containing mostly carbon monoxide and hydrogen. The temperature is around 1000°C or higher. Then this syngas is converted to liquid fuels using catalysts. The conversion of syngas to various hydrocarbons and oxygenates that later can be refined to transportation fuels and chemicals is known as Fischer-Tropsch synthesis. A unique characteristic of indirect liquefaction is the ability to produce a broad array of sulfur and nitrogen free products (Table 1- 3).[1]

Table 1- 3. Comparison of direct liquefaction, indirect liquefaction and conventional crude oil conversion

Description	XTL Conversion		Crude Oil
	Direct	Indirect	
Conversion Process			
Feed Properties Affect conversion Technology	Yes	No [a]	-
Feed Properties Affect Product Properties	Yes	No	Yes
Feed C-C Bonding Retained To Some Extent	Yes	No	Yes
Product Phase From Primary Feed Conversion	Liquid	Gas	Liquid [b]
Liquid Products Properties			
Contains Sulfur	Yes	No	Yes
Contains Nitrogen	Yes	No	Yes
Contains Oxygen	Yes	Yes	Yes

a Some technology selection is affected by the nature of the feed, for example, gasifier type
b Primary feed conversion contains desalting and separation by distillation.

1.2.2 Coal liquid refining / upgrading

After the 1973 “Oil Crisis” and second oil crisis at the end of that decade, liquid fuels production from coal by coal-to-liquid (CTL) conversion was actively investigated. In order to produce typical liquid transportation fuels, the hydrogen to carbon (H:C) ratio had to be increased while the heteroatom

content of the coal liquids needed to be decreased. This could be achieved by deep hydrogenation and much of the development work in the 1970's and early 1980's focussed on this approach specifically. Despite words of caution on the comparison of CTL processes,[7] the analysis of Nowacki is insightful in a number of respects and the most important aspects will be highlighted: [8]

(a) The conversion efficiency, expressed as the energy value of liquid product divided by the energy value of the inputs, is much higher for direct liquefaction than indirect liquefaction.

(b) Based on a cost comparison, all of the coal-to-liquids processes are of the same order, with only indirect liquefaction by Fischer–Tropsch synthesis being on the high side.

(c) Based on product quality, CTL via syngas-to-methanol was the most desirable.

(d) The fuel quality from direct coal liquefaction, despite liquid product efficiency and cost advantages, were mostly suitable only as boiler fuel.

The challenge of converting coal liquids to more than just boiler fuel is related to two properties of the coal liquids, namely, the high heteroatom content and high aromatics content, especially in the heavier fractions.[9] Transportation fuels (motor-gasoline, jet fuel and diesel fuel) have specification requirements governing the maximum heteroatom content and there are limitations on the aromatic content too. It has been pointed out that the

removal of heteroatoms requires severe hydrogenation, which is accompanied by high H_2 use.

Reducing the aromatic content is even more hydrogen intensive. The high aromatic content makes coal liquids prone to coking and technologies such as fluid catalytic cracking can only be considered after hydrotreating. Furthermore, nitrogen compounds undermine the efficiency of hydrocracking, which also suffers from high H_2 use and excessive catalyst deactivation. In fact, most of the thinking on coal liquid upgrading centered on hydrogen intensive refinery conversion processes as pretreatment or final product refining steps.[6, 9-10]

Therefore, coal liquids from direct coal liquefaction is potentially an efficient source of liquid products, but that a hydrotreating based approach is fraught with difficulties when considering coal liquid upgrading to higher value products. A clear alternative is not apparent from literature.

1.3 Objective

The refining of coal liquids has historically focused exclusively on hydroprocessing.[6,11] This is understandable, considering the low H:C ratio in coal liquids and high heteroatom (O; N; S) content. But there are opportunities for other types of conversion too. It is proposed to develop alternative approaches to the upgrading of coal liquids to higher value products and specifically through acid catalysis.

Transportation fuels and petrochemicals are not devoid of aromatics and oxygenates, even though the content may be regulated. Retaining aromaticity and oxygenate functionality can be beneficial, it reduces H_2 consumption and may even be mandated in some transportation fuel types, like synthetic jet fuel.[12]

One of the opportunities in coal liquids, especially coal liquids derived by pyrolysis and solvent extraction, is the inherently high phenolic, aromatic and olefinic contents. It was suggested that phenolic alkylation may be a way to add value to the phenols and olefins that otherwise will be converted to aromatic hydrocarbons and paraffins during hydroprocessing.[13] However, alkylation is acid catalyzed and coal liquids contain nitrogen bases. Furthermore, alkylation products are more bulky than the feed. Prospective phenol alkylation catalysts that will be use with real coal liquids therefore need to meet the following criteria:

(a) The acid strength and acid site concentration should be sufficiently high to catalyze phenol alkylation at reasonable rate.

(b) The acid strength should be weak enough so that basic compounds (nitrogen bases) can only inhibit, but not poison the catalyst.

(c) The catalyst should be active at a temperature that is high enough to ensure nitrogen base desorption, but not so high that the alkyl phenol cracking rate exceeds the phenol alkylation rate. (Both acid catalyzed and free radical cracking may be significant >300 °C).

(d) The pore structure of the catalyst must be large, so that the alkyl phenols can desorb and readily diffuse out of the catalyst.

(e) The catalyst must be cheap, or have long cycle lifetime, or be readily regenerable.

In this thesis, we use catalytic alkylation not to remove aromatics form coal liquids, but to retain the longer-chain derivatives that have beneficial fuel properties. Our aim was to find appropriate acid catalysts that would meet the above requirements.

1.3.1 Scope of the investigation

Various catalysts were characterized and tested in order to find catalysts that have sufficient acid strength to perform useful catalysis, but that were not so strongly acidic to be permanently poisoned by nitrogen bases at the conversion conditions.

The acid catalysts were tested through the model reaction of phenol alkylation with 1-hexene in the absence, as well as in the presence of nitrogen bases. Pyridine was employed as nitrogen-base. These tests were conducted in batch and flow reactors.

Although the present work with the model mixtures does not guarantee similar performance with real coal liquids, it provides proof of this concept. In this respect it is the first step towards the ultimate aim of demonstrating the viability of performing aromatic alkylation and other acid catalysed reactions in real coal liquids.

References:

1 D. L. King and A. de Klerk, Overview of feed-to-liquid (XTL) conversion, *ACS Symp. Ser.* 2011, 1084, 1-24.

2 M. Janardanarao, Cracking and Hydrogenation of Low-Temperature Coal Tars and Alkyl Phenols, *Ind. Eng. Chem. Prod. Res. Dev.*, 21 (3), 1982, 375-390

3 International Energy Agency World Energy Outlook, 2008

4 T. Kabe, A. Ishihara, E. W. Qian, I. P. Sutrisna and Y. Kabe, Coal and coal-related compounds structures, reactivity and catalytic reactions (Stud. Surf. Sci. Catal. 150); Elsevier: Amsterdam, 2004.

5 J. G. Speight, Handbook of coal analysis Chemical Analysis: A Series of Monographs on Analytical Chemistry and Its Applications, John Wiley & Sons, 2005, 240

6 J. A. Cusumano, R. A. Dalla Betta and R. B. Levy, Catalysis in coal conversion, Academic Press: New York, 1978.

7 E. C. Mangold, M. A. Muradaz, R. P. Ouellette, O. G. Rarah and P. N. Cheremisinoff, Coal liquefaction and gasification technologies, Ann Arbor Science Publishers: Ann Arbor, 1982.

8 P. Nowacki, Coal liquefaction processes, Noyes Data Corp.: Park Ridge, NJ, 1979.

9 M. L. Gorbaty and B. M. Harney, Eds., Refining of synthetic crudes (Adv. Chem. Ser. 179), ACS: Washington, DC, 1979.

10 R. F. Sullivan, Ed., Upgrading coal liquids (ACS Symp. Ser. 156), ACS: Washington, DC, 1981.

11 J. G. Speight, Synthetic fuels handbook. Properties, process, and performance, McGraw-Hill: New York, 2008.

12 A. de Klerk, Fischer-Tropsch refining, Wiley-VCH: Weinheim, 2011.

13 A. de Klerk and R. J. J. Nel, Phenol alkylation with 1-octene on solid acid catalysts. *Ind. Eng. Chem.* Res. 2007, 46, 7066.

Chapter 2 Literature Review

Coal liquids from non-hydrogenating processes, such as pyrolysis, are on average more heteroatom-rich than crude oils, with sulfur, nitrogen and oxygen usually present at percentage levels.[1,2] As pointed out in the introduction, the high basic nitrogen content has a detrimental impact on refining.

Conversion technology for the refining of coal liquids is consequently dominated by hydroprocessing.[3-5] Once the coal liquids are hydrotreated, the hydrogenated liquid products resemble an aromatic crude oil. Hydrocracking, as well as hydrogenation, plays a vital part in coal conversion technologies. Hydrocracking is the most versatile process and has great flexibility in operation,[6] selection of feedstocks, and product distribution. Hydrogenation is essential to treat feedstocks containing highly condensed polyaromatics and heteroatoms, and where a high degree of saturation is required in the products. The application of these processes to treat coal liquids and coal tars has long been known. The need and importance of hydroprocessing in the refining of coal liquids is consequently clear.

In the introduction (Chapter 1) it was pointed out that the ability to retain some of the useful functionalities present in unhydroprocessed coal liquids, such as aromatic hydrocarbons and phenolics, can reduce refinery H_2 consumption and may even be beneficial for some fuel types.

2.1 Coal liquids

Direct coal liquefaction processes produce a naphtha, gas oil fraction and a heavy high vacuum tower bottom material (residue) from the product separation step, usually 20–30 wt% of coal, which is fed to the liquefaction reactor. The residue usually consists of unreacted coal, ash and 30–50 wt% of heavy liquids.[7,8]

Ordinary coal liquids are high-viscosity black oils or pitches. In comparison with petroleum crudes, they lack of hydrogen, are only partially soluble in benzene, and contain relatively high levels of oxygen and nitrogen. Depending on the efficiency of the mechanical removal of solids achieved in each process, they contain a variable amount of ash and unconverted coal.

These coal liquids were initially intended to serve as boiler fuels. The sulfur content might be sufficiently low to qualify them as substitute for high-sulfur coal, and thereby reduce sulfur dioxide emissions. However, for large boilers, such as some major base load power plants, contamination control through coal liquefaction is probably not cost competitive with stack gas scrubbing.

In other fuel markets, coal liquids can be more competitive. Presently, industrial boilers are not amenable to stack gas scrubbing. For some smaller utility plants in particular, peak load units require a clean, storable liquid fuel as an alternative to natural gas. However, the high viscosity of primary coal liquefaction products is an undesirable factor for many of these applications. Also, the sulfur and nitrogen contents in the residual may exceed the emission

standards, as the emission limitations become more stringent in recent years.[9] The properties of syncrudes from a typical direct coal liquefaction process are shown in Table 2-1.[5] The major improvement in the coal liquefaction technology is in the upgrading of the raw coal liquids and the control of selectivity to higher value products. It shows flexibility to respond to commercial demand, as shown in Table 2- 2, as high as 70% of the raw product from a coal liquefaction process can be made into high-quality motor-gasoline and into diesel fuel is 50%, and alternatively into high density jet fuels is 63%.

Table 2-1. Properties of Direct coal liquefaction liquids

	Direct Coal Liquefaction
Product Mixture	65% Diesel and 35% Naphtha
Diesel Cetane Number	42–47
Diesel Sulfur	<5 ppm
Diesel Aromatics	4.8 wt%
Diesel Specific Gravity	0.87
Naphtha Octane(RON)	>100
Naphtha Sulphur	<0.5 ppm
Naphtha Aromatics	5 wt%
Naphtha Specific Gravity	0.76
Thermal Efficiency (%)	60–70

It was reported by Song et al. that coal-derived JP-8 jet fuel is more thermally stable than petroleum-derived JP-8 fuel, therefore decreasing the chances of forming solid deposits in aircraft engines. Coal derived JP-8 is richer in one- to three-ring cycloalkanes and two-ring hydroaromatics compared to petroleum-derived JP-8 The stability of cycloalkanes is higher than that of long-

chain paraffins. Selective catalytic conversion of polycyclic aromatic hydrocarbons (PAHs) in coal is a very useful way to make polycyclic specialty chemicals that have potential industrial applications. Higher value chemicals and monomers were produced from direct coal liquefaction derived one- to four-ring aromatic compounds, including phenols.

Table 2-2. Selectivities (%) in Upgrading of Raw Coal Liquids[10]

Maximum Product	Reformate	Light Naphtha	Diesel Fuel	Jet Fuel
Motor Gasoline	70	24	6	0
Diesel Fuel	50	11	39	0
Jet Fuel	13	11	13	63

Phenol is an important component in coal liquids, it can be used for synthesising useful products, such as alkyl phenol antioxidants and phenyl ether fuel components, which is applied in industry and add value to the products. These conversions can reduce the need for olefin hydrogenation.[11]

Phenol itself is a valuable petrochemical, but not a desirable fuel component. Phenol can be absorbed through the skin. A number of effects from exposure to phenol have been reported in humans, Including respiratory problems, heart disease and effects on the immune system, red blood cell destruction. Ingestion of very high concentrations of phenol has resulted in death.[12] Refinery streams and refinery wastewater that contains phenolic compounds can be converted to less harmful alkyphenols.

Other aromatic compounds also exist in coal liquids, such as benzene. Benzene is a major commodity chemical, with a market size of 39 million tons

per year in 2005, but in many countries the limitation imposed on the benzene content of fuel is now less than 1%, because benzene is a known human carcinogen, even though it has a high octane number value.[13] To reduce the benzene content in refinery streams, many efforts have been made. Benzene precursors, C_6 hydrocarbons, can be removed from the feed that goes to the catalytic reformer, in order to decrease benzene production. Moreover, hydrogenation can also used to convert benzene to cyclohexane or even cyclohexene. Extraction of benzene, then sold it as a commodity chemical is another way to reduce benzene. However, its high capital and operating cost is a problem, and the motor octane number (MON) then becomes constrained, cyclohexane's MON is 77, lower than that of benzene (MON 115).

2.2. Commercial coal liquids upgrading production

Direct liquefaction technologies require less energy but have higher carbon yields. The liquid products are more difficult to refine to useful final products. The catalysis that required to efficiently refine coal liquids presents many challenges, as the refining of oxygenate-rich syncrudes do.[3] There are also challenges in the design of coal liquid refineries. In fact, much of the gain in liquid yield and efficiency that was found in direct liquefaction is lost when conventional crude oil refining technology is used to convert the syncrude into transportation fuels and petrochemicals.[14]

James A. Cusumano and co-workers reported the catalytic upgrading of different coal liquefaction products. Initial coal liquefaction products from three processes, which were solvent-refined coal, Synthoil, and H-Coal. These products were hydrotreated. Upgrading was measured according to the reduction of heptane and benzene insolubles, the decrease in sulfur, nitrogen, and oxygen, and the increase in hydrogen content. Hydrotreating substantially removed benzene insolubles and sulfur. They obtained an 85% conversion of heptane insolubles and 80% conversion of nitrogen.

The Coalcon process, developed in 1975, produced four main fuel products: liquefied petroleum gas, synthetic natural gas, light and heavy oil products. Aromatics, such as benzene, toluene, phenol and nitrogen bases, were also contained in the coal liquids. Since little data has been reported for Coalcon liquid upgrading, refining challenges must be inferred from the reported chemical and physical properties of Coalcon liquids, and by comparing to processing of similar coal liquids or petroleum fractions.[3]

The highly condensed aromatic character of the liquid product is a particular problem, since the condensed ring compounds should be selectively cracked into one and two-ring compounds, which can reduce molecular weight and thereby give improved burning characteristics. It is also necessary to reduce the concentration of compounds such as phenol and BTX, even though they have a high octane numbers, because there are limitations on their content in transportation fuels.

The existence of nitrogen containing compounds at a high concentration in the heavy oil product is another problem. The nitrogen and sulphur compounds of the coal liquids are concentrated in the heavy ends.

Coal liquid from direct coal liquefaction is potentially an efficient source of liquid products, however, the hydrotreating-based approach is not cost effective. This is one of the main reasons why petroleum derived aromatics displaced coal derived aromatics in the petrochemical market. The aromatics are present in a matrix of heteroatom containing molecules that do not allow the efficient application of conventional petroleum refining technology to coal liquids.

The approach that is advocated in our study is therefore not based on hydrogenation catalysis, although it involves a selective catalytic conversion. One strategy that can be employed is to make use of acid catalysis to alkylate aromatics with alkenes (olefins) that are already present in unhydroprocessed coal liquids. It was reported that for benzene, the acid catalyzed alkylation of it with olefins to produce a high octane number motor-gasoline in the coal-derived processing is especially challenging. The material does not have just pure benzene or pure olefins, it usually has more heteroatom impurities than most crude oil and refinery derived streams. Accomplishing benzene alkylation using an acid catalyst with an olefinic feed component should be possible theoratically.[13]

2.2.1 Aromatic alkylation with olefins

Petrochemical synthesis of vital allied industrial chemicals is accomplished via alkylation of aromatic hydrocarbons with olefins. Catalytic liquefaction of coals can form unsaturated products, such as olefins, if the reaction temperatures do not exceed 400°C.[15] Alkylation of these aromatics with paraffins and α-olefins is the bedrock for producing linear alkylbenzene and branched alkylbenzene utilized for production of detergents, additives, and a diversity of other specialty chemicals.

2.2.1.1 Mechanism

The ring system in aromatics is electron-rich. The aromatic ring usually behaves as the nucleophile in a reaction. This means that the substitution on benzene happens by the addition of an electrophile. This called electrophilic aromatic substitution. The simplified mechanism for the electrophilic aromatic substitution is as follows (Equation2.1):

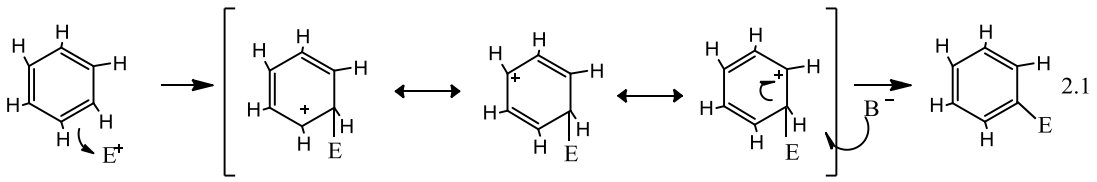

2.1

For example, the benzene is the nucleophile. During the reaction, the electrophile accepts a pair of the aromatic *pi*-electrons. This initial step destroys the aromaticity of the molecule, which results positive charge over the *ortho* and *para* positions. The conjugate base of the initial electrophile then helps to remove the extraneous proton, to gain back the aromaticity. Thus, what we need

is an electrophile, a carbonium ion in the case of olefins, to result in aromatic alkylation.

For Brønsted acid catalysts, take HF for example, the aromatic alkylation with 1-hexene happens as follows (Equation 2.2):

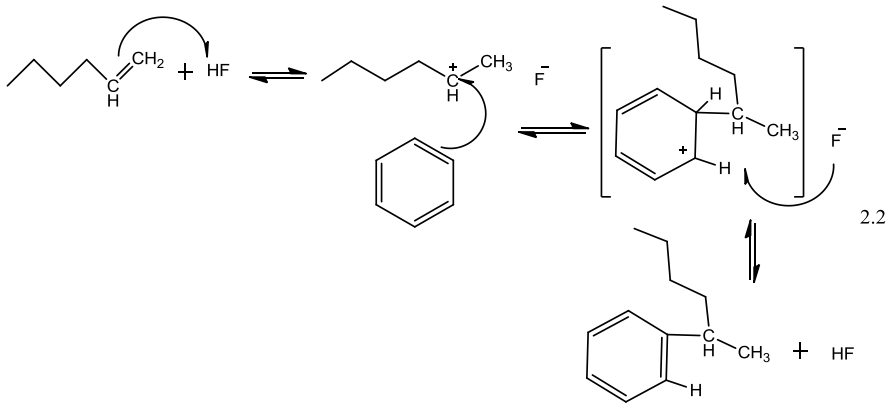

2.2

Phenols are potentially very reactive towards electrophilic aromatic substitution. This is because the hydroxyl group is a strongly activating, *ortho-/ para-* directing substituent, it is an active electron donating group.

For Lewis acid catalysts, $AlCl_3$ for instance, as equation 2.3 shows, the phenol donates an electron to $AlCl_3$, which creates a proton, the proton later reacts with olefins to a carbonium ion. The protonated olefin can then reactor with phenol produce alkylphenol; the process is similar to equation 2.2.

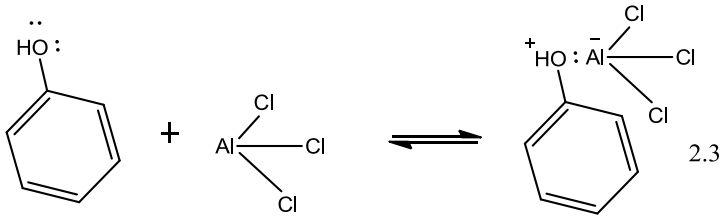

2.3

The behaviour of olefins in acid catalysis is widely understood in terms of the formation and the character of carbonium ion.

The most broadly accepted description of the alkylation of aromatics with olefins in the presence of an acid catalyst involves the addition of carbonium ion, which formed from the olefin, to a pair of pi-electrons of the aromatic nucleus. The acid catalyst converts olefins to the corresponding carbonium ions by adding a proton from the acid to the extra electron pair in the double bond:

$$A + H^+ \rightarrow A^+ \qquad 2.4$$

$$B + A^+ \rightarrow AB + H^+ \qquad 2.5$$

In this general description A stands for an olefin, B is an aromatic hydrocarbon, A^+ denotes a protonated olefin, H^+ is the proton and AB is the product of the reaction.

2.2.1.2 Phenol alkylation with alkene

Aromatic alkylation of phenols is when phenols react with alkylating agents such as olefins, alcohols or alkyl halides, in the presence of an acid catalyst. The alkylation of phenol with an olefin probably accounts for 95% of the commercially produced alkylphenols.[16] Thus, more focus will be given to the alkylation of phenols with olefins. Aromatic alkylation of phenols has been developed for petrochemical production. In a fuels refinery, phenol alkylation can exploit niche opportunities unique to XTL (any feed-to-liquids) facilities to produce anti-oxidants for fuels.

In a coal-to-liquids (CTL) synthetic fuels facility, it is possible to produce a syncrude rich in phenolic material. To avoid elastomer compatibility problems, there are certain limits on phenols in final transportation fuels. However, the

alkylphenols afford different degrees of oxidation stability to the fuel, which depend on the nature and degree of their alkylsubstitution. It is consequently desirable to remove phenol from coal liquids but to retain the longer-chain alkylphenols that have beneficial fuel properties.[11]

The alkenes are commercially available and they do not produce as much by-products as alkylations which use alcohols or alkyl halides. The alkenes being used in aromatic alkylations vary from single species, such as isobutylene, to complicated mixtures, such as propylene tetramers (dodecenes).

Most commercially important alkylphenols which are the typical products from phenol alkylation are of three types, monoalkylphenols, dialkylphenols, and trialkylphenols. Alkylations of phenol can produce three positional isomers, *ortho*, *meta*, and *para*, and multisubstitution products as well. A reaction may yield some of each potential product. The judicious choice of catalyst, as well as reaction conditions, can help control the selectivity. Alkylphenols are widely used, among others as antioxidant. Antioxidants have an important role in protecting foodstuffs, rubbers, resins, and a variety of chemicals, it performs well against atmospheric oxidation on storage and during processing at elevated temperatures.[17] The monoalkylphenols comprise 85% of all alkylphenol production. 2,4-di-*tert*-butyl phenol, 2,6-di-*tert*-butyl phenol are typical dialkyphenols. Pure 2,6-di-*tert*-butyl phenol is used as an antioxidant in oils and greases.

Alkyl phenyl ethers are produced when the unshared electron pairs of the phenol oxygen becomes the nucleophile and reacts with the carbocation.[16]

Some by-products are formed during these alkylation reactions. Alkene oligomers are formed when another alkene becomes the nucleophile in the addition reaction with the carbocation. But these alkene oligomers can in turn react with phenol to produce correspondingly heavier complex alkylphenols. Phenol to alkene ratio is an important operating factor that is used to reduce acid catalysed alkene side reactions. When the phenol:alkene ratio is higher, it may lead to less production, because of less contact between phenols with alkenes.

During the distillation of alkylphenols, higher the temperature, especially in the presence of acidic catalysts, leads to dealkylation, transalkylation, disproportionation and isomerization. Isomerization gives rise to an equilibrium where the thermodynamically more stable 3 or 3,5 isomers occur. The tendency of these reactions' occurrence depends on the nature of the alkyl substituent and increases in the order of primary<secondary<tertiary alkyl.[18]

The alkylation conversion process is equilibrium limited. Over a wide temperature range, the reactions can be completed, as the temperature is getting higher, the reverse reaction may be more significant, and when the temperature is very high, dealkylation leads to lower phenol conversion hence lower alkylphenol production. Because of the highly exothermic nature of these reactions, heat management is crucial; good heat removal capability is needed to

maintain temperature within an acceptable range. The selectivity of alkylation is greatly affected by temperature.

These fast, exothermic reactions are usually carried out under mild conditions in the liquid phase, although, for some substrates, vapor-phase processes with more stringent conditions are applied. During liquid-phase conversion conducted at low temperature, 20-100 °C, proper pressure control is needed to maintain the reagent to be in liquid phase, and to control the temperature. The activity of catalysts used in vapor phase conversion is relatively low, thus higher temperature is needed.

For industrial phenol alkylation, three main types of processes have been developed:

A. Homogeneous liquid-phase alkylation. The alkylating agent is added to the catalyst in the phenol, the solution or suspension of the catalyst must be separated later.

B. Fixed-bed liquid-phase processes. The reactants pass over the catalyst in tubular reactors at elevated pressures, the reactors are cooled externally.

C. Vapor-phase alkylation. The phenol and the alkylating agent are sent to a fixed-bed reactor operating at 300–400 °C. The heat of reaction must be removed effectively.

2.2.1.3 Benzene and Toluene alkylation with alkenes

Benzene as one of the primary aromatic compounds in coal liquids, is also not a desirable transportation fuel component, despite its high octane value. The Mobile Source Air Toxics (MSAT) rule, published on February 26, 2007, claimed the requirement that refiners and importers produce gasoline that has an annual average benzene content of 0.62 vol% or less, beginning in 2011.[19]

Various strategies have therefore been proposed to limit or reduce benzene in fuel refineries. Conventional methods such as benzene extraction and benzene hydrogenation were provided, as well as the Mobil benzene reduction process. Unconventional approaches have also been investigated, including aromatic alkylation units such as benzene alkylation with ethylene or propylene and benzene co-processed in existing olefin refinery units, such as paraffin alkylation, etherification, and olefin oligomerization.

The co-processing of benzene in an existing refinery unit is economically attractive, due to its requirements of less capital and lower operating costs associated with it. The processing of coal-derived benzene, as found in coal-to - liquids (CTL) fuel refineries, is especially challenging, because it usually has more heteroatom impurities compared to most crude oil and refinery derived benzene streams.

For toluene, alkylation of it with long chain 1-alkenes over acid catalysts is a promising technique for the production of the linear alkyltoluenes (LATs). The conventional methods of alkylation with long chain alkenes, chloroalkanes or alcohol are in the presence of HF and H_2SO_4 as catalysts. Because of problems

with corrosion and stringent requirements for feed drying, catalysts selection is critical for a clean petrochemical production processes.[20]

2.3 Equipment for conducting aromatic alkylation

The core equipment in alkylation of aromatics is the reactor. Reactors mostly used to produce alkylated compounds are batch reactors and continuous fix-bed reactors.

A complex batch reactor is a specialized pressure vessel with good liquid-gas contacting capability and heat transfer. Good mixing is required for contacting the olefin and catalyst with the aromatics, to reduce olefin concentration and thus produce desired products, and to control the residence time.

To produce antioxidants, the complex batch reactor is more common, mainly due to their high efficiency and flexibility of operation. There are four basic operating steps for this type of reactor in alkylated aromatics production, take alkylphenol for example: (1) the phenol is loaded; (2) the catalyst is loaded; (3) olefin is added over time, the addition rate depends on two factors, the reactor's heat removal capability is not exceeded and the desired reaction temperature is maintained; and (4) the alkylate is separated.

The downstream use of the product and the physical properties of the alkylated aromatics affect the method being used to recover the alkylation products. Most alkylphenols sold today require purification. Distillation is by far

the most common separation way. Over 80% of the alkylphenol products are recovered using multiple distillation tower separations.

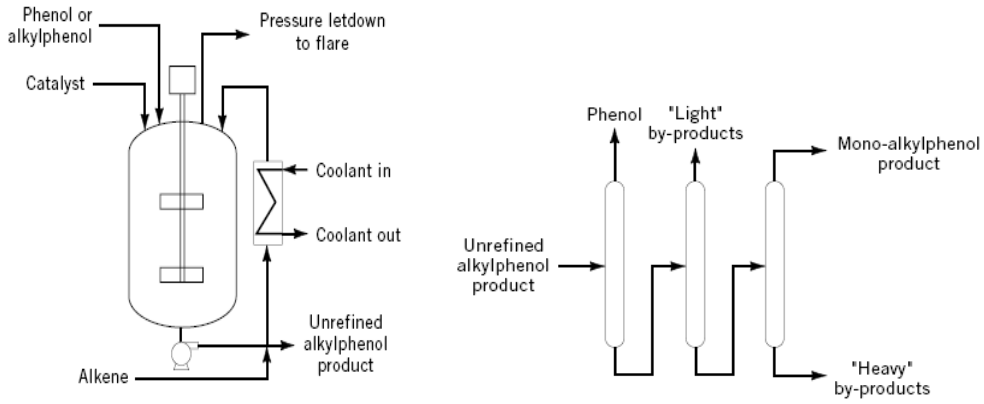

Figure 2- 1 Flow Sheet of Complex Batch Reactor and Monoalkylphenol Distillation route

Monoalkylphenols are commonly produced in plants that have both continuous reactors and continuous vacuum distillation trains. Dialkylphenols are also produced in specialized units. These plants combine complex batch reactors with vacuum distillation trains or other recovery systems. Figure 2-1 (figure 2-1 was reprinted with permission) shows one typical arrangement for a complex batch reactor and a basic alkylphenol distillation route.[16]

The system may need a configuration for utilizing catalyst, a reboiler with product takeoff, and a feed inlet above the catalyst bed. To remove the heat because of the exothermic properties, an overhead condenser may be needed, and a water takeoff may also reasonable when it is a liquid-phase process.

2.3.1 Upflow versus downflow testing

To test catalysts in their commercially applied size and shape under the refinery operation conditions, dilution of the catalyst bed with inert fines is suggested. By diluting the catalyst, the liquid holdup of the bed is increased, leading to more effective catalyst wetting and less risk of channelling. In downflow experiments, poor test reproducibility, a large influence of the method of catalyst packing and deviating reaction orders were reported.[20] To overcome the problems associated with downflow operation, upflow mode was suggested. It is demonstrated that comparable to those in commercial units, reversing the direction of oil flow from downflow to upflow gives a much improved catalyst utilization in small-scale testing and in liquid limited reactions.[21]

In my work, batch reactor and continuous fix bed reactors were both used. The continuous reactor was operated in upflow mode.

2.4 Effect of Nitrogen compounds

We have mentioned that the syncrude from coal liquefaction contains substantial amounts of oxygenates, and has a uniform distribution of nitrogen compounds over the boiling range, which vary from pyridine to complex carbazole structures.

There are two basic problems involved in the upgrading of coal liquids: reduction of the heteroatom content to an acceptable level, and selective cracking of the large polynuclear aromatic compounds to lighter aromatics.[3] The

presence of nitrogen compounds at a high concentration in the heavy oil product must be controlled not only to assure an environmentally acceptable NO_x emission upon combustion, but also to prevent the basic pyridine homologs from poisoning the acidic function of the catalysts used in the upgrading of these liquids to transportation fuels. All types of bases influence the acidity of the catalyst and hence its efficiency, especially for organic nitrogen compounds. If oxygen is present, the catalysts will form heavy resinous materials, even the concentration of oxygen is as low as 20 ppm. The high aromaticity of the various syncrudes makes them difficult to refine, particularly to paraffinic jet and diesel fuels. The molecular compositions of the starting syncrudes and of the three direct liquefaction methods (solvent-refined coal, Synthoil, and H-Coal processes) indicate that there are three major technical requirements: reduction of polynuclear aromatics, more effective ways to decrease the effect of nitrogen coumpounds and the development of catalysts with improved activity maintenance.

Nitrogen compounds present in coal liquids can cause storage and processing problems. The activity of catalysts used in cracking, isomerisation, reforming, and polymerization is known to be decreased due to the presence of nitrogen in the feedstock. They also enhance the chance to form gums, precipitates, and lacquers, and sometimes even pose color instabilities in coal liquids.

Nitrogen-containing heterocyclic compounds can be classified as basic or nonbasic, due to their ability to interact with a perchloric acid-acetic acid.[3] The nitrogen compounds present in the naphtha are primarily aniline and alkyl anilines. Pyridine or alkyl pyridines were found in very small amounts. The middle distillate contains higher alkyl anilines, quinolines, indoles, and some alkyl pyridine, very little dinitrogen compounds such as aniline indoles were also observed in the middle distillate.

Nitrogen can be removed from heterocyclics by hydrogen transfer reactions by a donor solvent or a catalyst. People used model compounds to understand the mechanism of denitrogenation. Studies on denitrogenation of pyridine and a number of its derivatives were reported ant it was found that the effect of gas circulation rate was trival on the rate of hydrodenitrogenation. Various researchers reported that denitrogenation of both the basic and nonbasic compounds follows a pseudo-first –order kinetics.[15]

The nitrogen bases that are present in the unhydroprocessed coal liquids hamper the application of acid catalysis. The nitrogen bases can neutralise the acid sites on acidic catalysts, thereby effectively poisoning the catalysts.

2.4.1 Acid catalysis in presence of N-bases

Acid catalysts used in various of industrial processes are known to be poisoned by basic nitrogen compounds. To better understand the poisoning process, to improve methods for their removal and looking for safe handling

methods of the material, research on the types and concentration of nitrogen compounds in the presence of the coal-derived materials are desirable. Studies of nitrogen bases compounds in coal liquids using GC-MS have been published, also investigations of similar compounds in coal tars, which have been mentioned before. Paul et al. investigated coal liquefaction products using GC-MS to identify nitrogen compounds in basic fractions.[22,23]

The important role of bases as well as coke and alkali poisoning of solid acid catalysts have attracted the interest of many researchers in the past several decades. Basic nitrogen compounds are present in the coal liquefaction environment. The basicity of these compounds can strongly influence their propensity to form coke.

A mechanistic model was described that correlated analysis data obtained for $NiMo/Al_2O_3$ catalysts from the Wilsonville, Alabama coal liquefaction pilot plant.[24] In the model, acid sites on the catalysts rapidly saturate with the nitrogen bases on start-up. The bases can be displaced by sodium, an alkali metal present in coal ash, which also poisoned the acid sites on the catalysts.[24]

Nishijima and co-workers proved that a NiMo/zeolite catalyst produced less distillate-range production when the feed contained higher levels of N-base compounds.[25] Furimsky reported the deactivation of molybdate-based catalysts by nitrogen bases.[26] Hollway, Yoshimura and co-workers reviewed the deposition of nitrogen bases on coal liquefaction catalysts.[27,28]

The nitrogen bases in unhydroprocessed coal liquids are mainly of the aniline, pyridine and quinoline families, which are bases of medium strength (Figure 2-2). It should therefore be possible to find acid catalysts that have sufficient acid sites that are acidic enough to catalyse aromatics alkylation, but weak enough so that the nitrogen bases will only inhibit conversion, but not permanently poison the catalyst.

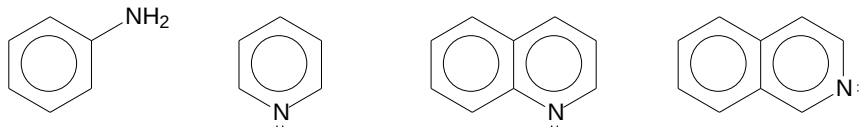

aniline	pyridine	quinoline	isoquinoline
$K_b = 3.7\times10^{-10}$	$K_b = 2.3\times10^{-9}$	$K_b = 3\times10^{-10}$	$K_b = 1.1\times10^{-9}$

Fig. 2- 2 Nitrogen bases commonly found in coal tar and their associated base dissociation constants (Kb)

2.5 Catalysts for aromatics alkylation with olefins

Generally, the alkylation of aromatics proceeds by acid catalysis. The selection of an appropriate catalyst depends on the reactivity of the olefin, cracking propensity of the olefin and the desired product (degree of alkylation and isomer distribution). In our study there was the additional constraint, namely, the presence of nitrogen bases in the feed.

Regioselectivity in alkylation can be influenced by the catalysts. When catalysts such as HF, BF_3, Al_2O_3-SiO_2, or acidic ion-exchange resins are used, the alkylation of phenols with olefins leads mainly to *para*-substituted product.

Whereas $Al(C_6H_5O)_3$, which is formed from phenol and metallic aluminum, especially in the presence of traces of mercury salts, produces almost exclusively *ortho*-alkylated and 2,6-dialkylated products. The reactivity of the alkylating agent also affects selectivity. For example, the reaction between phenol and isobutylene, which has the *tert*-butyl carbocation as the alkylating agent, shows a very high *para*-selectivity.

Various catalysts are commonly used in alkylation of aromatics in industry, which can be basically classified into two types, homogeneous catalysts and heterogeneous catalysts (see also Section 2.2.1.2). The latter includes solid acid catalysts, acidic ion-exchange resins and zeolites.

In the literature, solid acid catalysts, especially silica-alumina catalysts attracted much attention in the aromatic alkylation reactions. During the past two decades, the innovation in zeolite catalysis for aromatic alkylation production was pushed by the growing demand for selected alkyl aromatic products, the characteristics of the aromatic feedstock, and stringent environmental legislation. [29] The improvements the in application of liquid-phase alkylation instead of the gas-phase mode, was facilitated by larger-pore zeolites, such as Beta and MCM-22. Starting with these catalysts, new advances were reported, either by the development of new materials, or by the catalyst formulations. The impact of SiO_2/Al_2O_3 ratio, reactant molar ratios and temperature were all discussed.[29,30,31] The performance of different zeolite

catalysts, such as Beta, ZSM-5 and Beta:ZSM-5 composites for benzene alkylation by propylene, were compared by Laredo and co-workers.[32]

Perego and co-workers discussed the catalytic activity, the selectivity to *o*-, *m*- and *p*-cymenes and the formation of polyalkylates related to catalyst acidity and porosity through liquid-phase alkylation of toluene with propylene. The catalytic behaviour of amorphous silica-aluminas such as MSA, MCM-41, ERS-8, crystalline materials, such as zeolite beta, and also traditional alkylation catalysts ($AlCl_3$–HCl and supported phosphoric acid, SPA) reported in the literature, were compared. The results showed that comparable with zeolite beta, MSA and MCM-41 had higher alkylation activities, while their isomerization and transalkylation activities were lower than those of zeolite beta and $AlCl_3$–HCl, but similar to SPA. [33] Perego and co-workers also reviewed the industrial alkylation of benzene and toluene for ethylbenzene, cumene, linear alkyl benzene and cymene production. They discussed the features of different zeolites considering their activity and selectivity. Much effort have been employed to improve the catalysts performance, which supported the development of environmentally friendly processes of alkylations of aromatics with olefins.[27]

2.5.1 Homogeneous catalysts

In the liquid-phase processes, Lewis acid catalysts, such as $AlCl_3$, BF_3, or Al $(C_6H_5O)_3$ and proton acids (Brønsted acids), such as HF, H_2SO_4, H_3PO_4, or *para*-tolylsulfonic acid are applied. The conventional methods for industrial alkylation are usually performed through homogenous catalytic conversion of hydrocarbons on protonated liquid acid catalysts or their vapors.

Table2- 3 Operating Conditions of Homogeneous Catalysts

Antioxidant	Catalysts	Temperature(°C)
2-*tert*-butylphenol and 2,6-di-*tert*-butylphenol	$Al(C_6H_5O)_3$	100
4-*tert*-butylphenol	H_2SO_4, H_3PO_4, BF_3	80–140
4-*tert*-amylphenol	BF_3 or H_3PO_4	100–120
2,6-di-*tert*-butyl-4-methylphenol	H_2SO_4	70

Through the operating conditions in Table 2- 3 we can see that phenols can react with alkenes under mild catalysis conditions. But when strong homogeneous acid catalysts are used, intramolecular rearrangement, disproportionation and transalkylation can still occur. Given sufficient reaction time the product distribution is affected by the thermodynamic equilibrium and equilibrium limited products are obtained.[34]

Ionic liquids at room temperature have received a great deal of attention during the past few years. They were proposed as alternative catalysts in biphasic catalysis. Ionic liquids are mainly mixtures of low melting salts, for example, pyridinium halides, imidazolium halides, the addition of $AlCl_3$ or other

Lewis acids to form the catalyst system. Alkylation with long chain olefins catalyzed by ionic liquids was also considered. The advantages of this catalyst system are that it can reduce corrosivity within the liquid alkylation system, and it makes product separation easier. However, there still are many difficulties and challenges to be overcome for commercial application of ionic liquid catalysts. The main technical hurdles include regeneration of the ionic liquid over extended time and instability of the system in the presence of water.[35,36]

In the early years, petrochemical industry benzene alkylations were usually catalyzed by $AlCl_3$ (for ethylbenzene), HF (for long chain alkyl-benzenes) and by ''solid phosphoric acids'' (for cumene) [37, 38, 39].

$AlCl_3$ may react with phenols to produce the aluminum complex $ArOAlCl_2$; the complex deactivates $AlCl_3$ and hence it reduces the productivity. The formation of deposits of $AlCl_3$ is another problem. Thus, even though HF and $AlCl_3$ are being used as catalysts, these catalysts are very corrosive and great effort is made for their substitution by solid catalysts (see Section 2.5.2).[18] Furthermore, final isolation of the product necessitates aqueous quenching and neutralization steps to remove the liquid acid, resulting in enormous quantities of hazardous waste.

2.5.2 Heterogeneous catalysts

Heterogeneous catalysts offer several inherent advantages compared to their homogeneous counterparts: product separation and catalyst reuse are easier; bifunctional phenomena involving in reactant activation between support and active phases; and process advantages through reactor operation in batch reactor versus continuous flow reactor.

However, to be economically viable, a suitable heterogeneous system must not only minimize the production of waste, but should also show activities and selectivities comparable or superior to the existing homogeneous catalysis.[40] The main limitations for application of solid acid catalysts include: the deactivation of the support materials, primarily because of pore-blockage resulting from isomerization of smaller olefinic molecules; unwanted shape selectivity especially with regards to branched hydrocarbons; difficulty in regeneration (only some catalysts) and higher operating temperatures, i.e. higher than needed in traditional homogenous liquid acid catalysts.

2.5.2.1 Solid phosphoric acid

Solid phosphoric acid catalyst was used in industry since the early 1930's. It was used for producing "polymer gasoline" from oligomerization of light olefins. Traditionally, the SPA was made by blending phosphoric acid with diatomaceous earth, known as kieselguhr. This mixture was then extruded and calcined at high temperature. This technology has not changed a lot since the 1930's. Subsequent studies focused mainly on the catalyst, including the

preparation method, the characterization of the silicon phosphate phase differences, crushing strength and other catalyst properties.[29,41] Aromatic alkylation over Solid phosphoric acid (SPA) follows an Eley-Rideal mechanism. It was shown that SPA inherently has a low multiple alkylation tendency, because of the steric hindrance of the bulky alkyl group. The alkyl group on an alkylated aromatic molecule creates a less-effective nucleophile than an unalkylated aromatic.[11]

Although SPA catalysts are widely used, they are being substituted progressively by zeolites and inorganic oxides because the latter are considered environmentally benign, easy to handle and to dispose of, thus implying less expensive process design.

2.5.2.2 Zeolites

The development of zeolites is a major accomplishment, for their considerable thermal and chemical stability.[3] Zeolite catalysts are suitable for the vapor-phase processes because of their high thermal stability. The stable property is needed for highly exothermic reactions and reactions conducted at high temperatures.

The reactivities as well as the product and isomer selectivities in microporous materials largely depend on the type, the number and the strength of the acid sites on the catalysts. They also depend on the geometry of the zeolite pores. In alkylation of phenol, monoalkylated product selectivity on

zeolites could be related to the average pore size of the catalysts (shape selectivity). Multiple alkylation was found with H-Beta (BEA), H-Mordenite (MOR), and H-ZSM-5 (MFI) catalysts. Both acid strength and catalyst pore size determined the chances that multiple alkylation happened.[11]

Recent years, different zeolites with different activity and selectivity were considered in the alkylation reaction process. Zeolites have been employed instead of the conventional aluminum chloride and phosphoric acid in the process of both ethylbenzene and cumene production. In the last few years, more than 50% of the cumene production processes use zeolite catalysts.[18,38]

ZSM-5 zeolite with smaller pore size is unsuitable for aromatic alkylation with propylene. Experimental results found in the literature show that the low activity is mainly caused by the low desorption of the reaction products from the narrows pores of this zeolite. [19]

Not all zeolites present problems with pore constraints. Large pore zeolites such Y-zeolite (FAU) and Mordenite catalysts have been proved as active and selective catalysts for the monoalkylation of benzene or toluene by linear olefins. Particularly in the case of Mordenite, the mesopores created by dealumination have a significant positive effect on the activity.[18]

Wide pore zeolites as Y-zeolite, beta-zeolite and mordenite show both good activity and selectivity in the monoalkylation reaction of benzene or toluene with linear 1-alkenes. The 2-phenyl isomer, for mordenite , reaches

values of more than 60%. Zeolites Y and beta demonstrate almost 100% conversion. [42]

However, zeolite catalysts also have certain weaknesses. H-Beta for example, displayed poor dependence of conversion on residence time and selectivity to the different product classes, compared to the behavior of the other catalysts studied. It showed prominent olefin skeletal isomerization and cracking activity, which resulted in the alkylated phenols containing more isomeric compounds than the alkylation products produced by any of the other catalysts. Furthermore, zeolites are known for their strong Brønsted acidity, and it is expected that this would make them more prone to poisoning by nitrogen bases present in coal liquids. [11]

2.5.2.3. Amorphous silica-alumina Catalysts

A solid mixture of SiO_2-Al_2O_3 contains acid sites stronger than those found in the pure oxides. Amorphous silica-aluminas were among the first solid acids used in the petrochemicals industry, and are employed widely in hydrocarbon cracking. The catalytic activity of amorphous silica-aluminas in reactions through carbonium ions is mostly because of the presence of Brønsted acid sites on their surface. Amorphous silica-aluminas provide acid sites and easy transport to the active sites, thus, they can be widely employed as cracking catalysts. The Brønsted and Lewis acid sites they possess are not as strong as that in zeolites. As a result, amorphous silica-alumina catalysts have been largely

superseded by zeolites in reactions which requires high acid strength or shape selectivity. But in the coal liquids where nitrogen compounds exist, mild acidity, on the contrary, can be an advantage.

It was investigated by Goodman and co-workers that amorphous silica-alumina catalysts have good selectivity over a wide range of temperature. They have a much larger temperature tolerance and are relatively stable for long reaction periods. Unlike zeolites, such as HZSM-5, both *gamma*-alumina and Siral-series amorphous silica-alumina catalysts were only reversibly poisoned by ammonia. [43,44]

In the early 1940's, the use of an amorphous silica-aluminas in alkylation of benzene with ethylene and propylene was employed.[44] The addition of silica to alumina was the main choice to optimize the acidity and support sites of the binary oxide.[45]

The model for the surface of the Siral-series amorphous silica-alumina catalysts with respect to the silica loading, has been proposed by Daniell et al. through FTIR and XPS analysis (figure 2- 3 was reprinted with permission).[44] The model assumes that all Siral particles are spherical in nature. A cross-section through each of these spheres is depicted. As the silica content increases, the surface composition of the catalysts change from just alumina to two separate oxide phases, then silica, alumina and a mixed aluminosilicate phase.

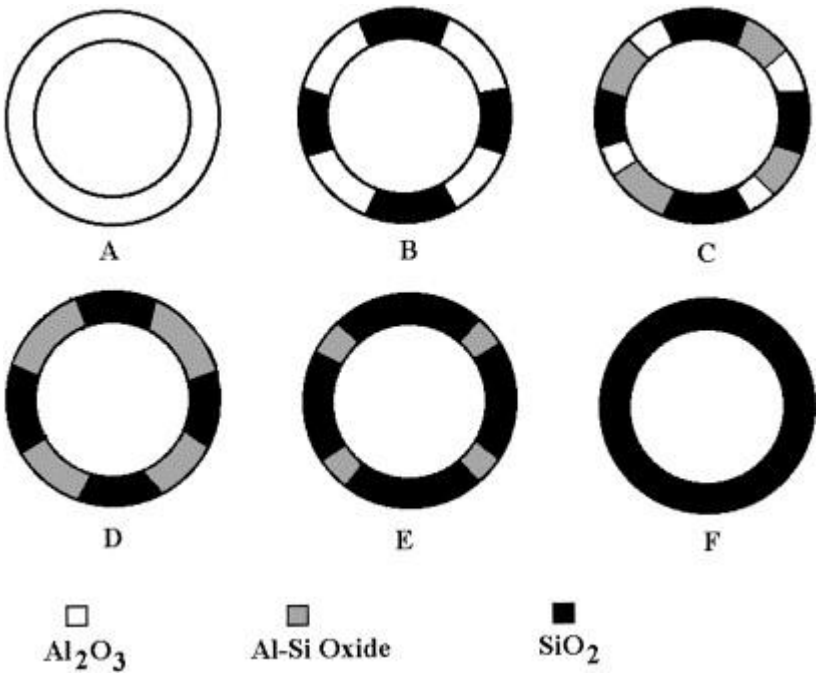

Figure 2- 3 Model Of the surface composition: PURAL SB (A), SIRALs 1.5–5 (B), SIRALs 10–20 (C), SIRALs 30–40 (D), SIRALs 60–80 (E) and SIRALs 90–100 (F).

2.5.2.4. Acidic resins

Acidic ion-exchange resins, such as Nafion resins or sulfonated polystyrenes, Amberlyst dry catalysts, are employed in liquid-phase processes. Amberlyst dry catalysts are especially designed for these applications; they can be dried to an optimal degree of moisture in order to ensure a high conversion rate and excellent selectivity. Their physical stability makes them suitable for stirred tank reactors and allows an efficient separation from the reactants.

Although acidic resins are capable of catalyzing aromatic alkylation, these catalysts are not industrially used for this purpose.

2.6 Catalyst Characterization Methods

2.6.1. Mercury Porosimetry

The term “porosimetry” is often used to define the measurements of pore size, surface area, volume, distribution, density, and other porosity-related characteristics of a material. We use mercury for the analysis of catalyst pore structure, because mercury does not wet most substances and will not penetrate pores spontaneously by capillary action. Mercury must be pushed into the pores by the application of external pressure. The required equilibrated pressure has an inversely proportional relationship with the size of the pores, greater pressures are required to force mercury into the small pores, while only slight pressure is necessary to intrude mercury into macropores.

Mercury porosimetry analysis is the progressive intrusion of mercury into a porous structure under stringently controlled pressures. From the pressure versus intrusion data, the porometer generates volume and size distributions using the Washburn equation. $P_L - P_G = 4\sigma\cos\theta / D_P$, where P_L is the pressure of liquid, D_p is the pore diameter, P_G is pressure of gas, σ stands for surface tension of liquid, θ is the contact angle of intrusion liquid. Clearly, the more accurate the pressure measurements, the more accurate the resulting pore size data.

The mercury porisometer operates by gradually increasing the externally applied pressure to force mercury into the pores of the sample. By measuring the volume of mercury that intrudes into the sample with each differential pressure change, we can know the volume of pores within a certain size range.

A mercury penetrometer is used to measure the volume of mercury that enters pores, it is a quartz glass tube, which is an insulator, and filled with mercury (a conductor) using low pressure. The sample is placed on the wider side of the tube, the stem of the tube is a capillary and works as a reservoir for the analytical volume of mercury. The tube is covered with metal (a conductor) when using high pressure analyze, these two conductor separated by glass, forming a coaxial capacitor. When pressure pushes Hg out of the stem and into the sample, the amount of mercury inside the capillary decreases, so does the capacitance, which is proportional to the volume of mercury leaving the stem with change in pressure.

In real coal liquids, which include bulky molecules, accessibility is important. Thus porosimeter can be used as a method to identify the larger pore size of the catalysts, in order to perform the reaction well. In my work Hg porosimetry was employed to determine the macro- and mesoporosity of different catalysts.

2.6.2 TPD (Temperature programmed desorption)

In 1925, the concept of "active centers" on catalytic surfaces was introduced by H.S. Taylor. It is generally accepted that catalytic reactions do take place on special groups of sites. Various techniques are used to obtain information on the active centers of catalysts, temperature programmed desorption is one of them.[46]

Temperature programmed desorption has been used to determine the total number of acid sites and their acid strengths. The sample is pretreated with a base, in our case ammonia. The temperature of the sample is then increased in order to desorb the ammonia, i.e. ammonia temperature programmed desorption (NH_3-TPD). The temperature at which the ammonia desorbs is an measure of the acid strength. A thermal conductivity detector (TCD) is used to collect the data. The detector senses thermal conductivity of the flow, in our case, the ammonia released from the sample, and compares it to the conductivity of the reference carrier gas (He). The signal difference between pure He and He with NH_3 is recorded by the detector as the temperature of the sample is increased.

Pyridine TPD has also been used to quantify acid sites, but the existence of steric limitations with the relatively large pyridine molecule is a problem. One drawback of NH_3 and pyridine TPD is that they do not differentiate between Lewis and Brønsted sites. Thus, FTIR is necessary to investigate the nature of the acid sites of the catalysts. In my work NH_3-TPD was employed only to determine the total concentration of the acid sites of various strengths.

2.6.3 Fourier Transform Infrared Spectroscopy (FTIR)

Fourier transform infrared spectroscopy (FTIR) is a technique that is used to obtain an infrared spectrum of absorption of a solid, liquid or gas. An FTIR spectrometer simultaneously collects spectral data in a wide spectral range. IR radiation refers broadly to that part of the electromagnetic spectrum between

the visible and microwave regions, to the chemist the portion between 4000 and 400 cm^{-1} is of greatest practical use. We can utilize FTIR spectra in conjunction with other spectral data in order to determine molecular structure.[47]

There is an interferometer in the FTIR. We send the infrared source energy through it and onto the sample. The light passes through a beamsplitter, which directs the light into two ways at right angles, one to the stationary mirror then goes back, one goes to a moving mirror, by movable the mirror the total path length varies versus that taken by the fixed mirror beam. The two beams recombine and pass through the sample. The path length difference creates an interferogram (intensity over time). The sample absorbs the different wavelengths characteristic of its spectrum, the intensity of the IR beam is collected by a detector. The signal is digitized and Fourier transformed by computer to convert it into an intensity vs frequency spectrum. Atmospheric components (CO_2, H_2O) appear in the spectrum and a background spectrum is usually run to substract the infrared absorption of these compounds from the spectrum we need.

Generally, the type and the strength of acidic sites of catalysts can be determined with the help of FTIR analyses using pyridine as probe molecule and by NH_3-TPD measurements. In my work FTIR spectra were collected of pyridine adsorbed catalysts at different temperature to determine the nature of the acid sites of different strengths.

2.6.4 X-ray Fluorescence (XRF)

When a primary X-ray excitation source from an X-ray tube or a radioactive source hits a sample, the X-ray can be absorbed by the atom, it also can be scattered through the material. The X-ray being absorbed by the atom by transferring all of its energy to an innermost electron is called the "photoelectric effect." During this process, when the primary X-ray has sufficient energy, electrons are expelled from the inner shells, creating vacancies that present an unstable condition for the atom. As the atom returns to its stable condition, electrons from the external shells are transferred to the internal shells, and give off a typical X-ray, its energy is the difference between the two binding energies of the corresponding shells.

Because each element has a unique set of energy levels, each element produces X-rays at a unique set of energies. This allows us to measure the elemental composition of a sample non-destructively. The process of emissions of characteristic X-rays is called "X-ray Fluorescence" (XRF). In most cases the K and L shells are involved in XRF detection. A typical X-ray spectrum from an irradiated sample shows multiple peaks of different intensities. The energy of the peaks provides identification of the elements in the sample and the intensity of the peak gives the relevant elemental concentration.

Chamber atmosphere is important for analysis using XRF. X-rays are absorbed and lose intensity. The solids or press pellets needs vacuum while Helium is used for liquids or powdered materials. A main disadvantage is that the

analyses are generally limited to elements heavier than fluorine. There are two ways for quantitative analysis of the sample, to create a standard curve as a reference for obtaining the element concentration of unknown sample, or the fundamental parameter method, which extrapolate the composition of the sample by its fluorescent X-ray intensity of each known element. Matrix interference also occurs when we are performing quantitative analysis, any element can absorb or scatter the fluorescence of our element of interest. The signal of one element may be enhanced or suppressed by another, thus, the values may be not precise because it is matrix-sensitive.

XRF analysis can determine the Si/Al ratio for silica-alumina catalysts. Thus, in my work the XRF technique was employed to measure the Si and Al content.[48]

2.6.5 Scanning Electron Microscope (SEM)

A focused beam of high-energy electrons was used to generate a variety of signals at the surface of solid samples when operating the scanning electron microscope (SEM). The signals from electron-sample interactions reveal information about the sample including external morphology (texture), surface topography, chemical composition, crystalline structure and also orientation of materials making up the sample. In most cases, data are collected over a selected area of the sample surface, and a 2-dimensional image is created that displays spatial variations in these properties.

SEM analysis is also a "non-destructive" investigation. X-rays generated by electron interactions do not lead to volume loss, so it is possible to analyze the same materials repeatedly. For the sample preparation, electrically insulating samples are coated with a thin layer of conducting material, usually carbon, gold, or some other metal or alloy. The choice of these materials for conductive coatings depends on what is required from the data: carbon is most desirable if elemental analysis is a priority, while metal coatings are most effective for high resolution electron imaging applications. Alternatively, electrically insulating samples can be examined without conductive coatings in an instrument capable of "low vacuum" operation.

In the SEM, an thermionic electron gun emits an electron beam. We usually use tungsten for electron emission due to its high melting point, low vapor pressure and low cost. The primary electron beam interacts with the sample, the electrons lose energy and the energy exchange between beam and the sample causes reflection of high-energy electrons. The emission of secondary electrons can be detected; the beam current adsorbed by the sample can be detected and create images of the distribution. The signals are amplified by various types of electronic amplifiers, showing as variations in brightness in the microscope. The resulting image displays a map of the intensity of the signal from the scanning area of the sample.

In my work, SEM was used to analyze the catalysts, to learn more about the structure of the catalysts and to support observations of other characterization techniques.

2.6.6 Thermal Gravimetric Analysis (TGA)

Thermal gravimetric analysis is a type of technique performed on samples that determines changes in weight related to a temperature program in a controlled atmosphere, normally in air or in an inert atmosphere, such as Helium or Argon. It is used to determine thermal stability and the fraction of volatile components of the sample. Such analysis relies on a high degree of precision in three measurements: weight, temperature, and temperature change. As many mass loss curves look similar, the mass loss curve may require transformation before results may be interpreted.

In addition to thermal gravimetric analysis, some instruments also investigate the thermal characteristics of substances, instead of studying weight changes. They also record the temperature difference between sample and reference, or record the heat flow difference into the sample and the reference, such as differential thermal analysis or differential scanning calorimetry.

In the TGA operation process, the maximum temperature is usually selected to ensure the sample weight is stable at the end of the experiment, all the chemical reactions and physical desorption are completed.

TGA is commonly used in research and testing to determine characteristics of materials such as polymers, to learn about the degradation temperatures, to figure out the level of inorganic and organic components in materials, and also to study the decomposition points of explosives, and solvent residues. It is also used in testing the adsorbed moisture content of materials, the hydration level, and for hydration study of the catalysts. This is important, since it was shown that water has a strong inhibiting effect on the activity of *gamma* alumina, while the effect over H-ZSM-5 is less significant.[44]

In my work, TGA was employed to study the hydration level of the alumina and Siral amorphous Si/Al catalysts and to determine the required calcination temperature of the catalysts.

References:

1 E. O. Rhodes, The chemical nature of coal tar. In Chemistry of coal utilization. Vol. II, H. H. Lowry Ed., Wiley: New York, 1945, pp. 1287-1370.

2 C. Karr Jr, Low-temperature tar. In Chemistry of coal utilization. Supplementary volume, H. H. Lowry Ed., Wiley: New York, 1963, pp. 539-579.

3 J. A. Cusumano, R. A. Dalla Betta and R. B. Levy, Catalysis in coal conversion, Academic Press: New York, 1978.

4 J. G. Speight, Synthetic fuels handbook. Properties, process, and performance, McGraw-Hill: New York, 2008.

5 S. Vasireddy, B. Morreale, A. Cugini, C. Song and J. J. Spivey, Clean liquid fuels from direct coal liquefaction: chemistry, catalysis, technological status and challenges, *Energy Environ. Sci.*, 2011, 4, 311-345.

6 M. Janardanarao, Cracking and Hydrogenation of Low-Temperature Coal Tars and Alkyl Phenols, *Ind. Eng. Chem. Prod. Res. Dev.,* 1982, 21, 375-390.

7 M. Sugano, R. Ikemizu and K. Mashimo, Effects of the oxidation pretreatment withhydrogen peroxide on the hydrogenolysis reactivity of coal liquefaction residue, *Fuel Processing Technology*, 2002, 77–78, 67–73.

8 K. Hirano, Outline of NEDOL coal liquefaction process development (pilot plant program), *Fuel processing Technology*, 2000, 62, 109–118.

9 J. Derosset, G. Tan, and J. G. Gatsis, Upgrading Primary Coal Liquids by Hydrotreatment, Refining of Synthetic Crudes, *Adv. Chem.*, 1979, 179, 109-119.

10 M.L.Gorbaty, Prominent frontiers of coal science: past, present and future, *Fuel*, 1994, 73, 1819–1828.

11 A. de Klerk and R. J. J. Nel, Phenol alkylation with 1-octene on solid acid catalysts, *Ind. Eng. Chem. Res.,* 2007, 46, 7066-7072.

12 Pollution Prevention Opportunities for PBT Chemicals—phenol; Office of Pollution Prevention, Ohio Environmental Protection Agency.2002, No.100

13 T. M. Sakuneka, R. J. J. Nel, and A. de Klerk, Benzene Reduction by Alkylation in a Solid Phosphoric Acid Catalyzed Olefin Oligomerization Process *, Ind. Eng. Chem. Res.,* 2008, 47, 7178–7183

14 D. L. King and A. de Klerk, Overview of feed-to-liquid (XTL) conversion, *ACS Symp. Ser.,* 2011, 1084, 1-24.

15 Y.T.Shah, et al. Oxygen, nitrogen, and sulfur removal reactions in donor solvent coal liquefaction, *Catal. Rev. Sci. Eng*., 1979, 20, 209-301.

16 Kirk-Othmer Encyclopedia of Chemical Technology, 2007, 203-231.

17 H. Morawetz, Phenolic Antioxidants for Paraffinic materials, *Ind. Eng. Chem.*, 1949, 41, 1442–1447.

18 Z. Daa, Z. Hana, P. Magnouxb and M. Guisnet, Liquid-phase alkylation of toluene with long-chain alkenes over HFAU and HBEA zeolites, *Appl. Catal. A: General*, 2001, 219, 45–52.

19 G. C. Laredo, J. Castillo and H. Armendariz-Herrera, Benzene reduction in gasoline by alkylation with olefins: Effect of the experimental conditions on the product selectivity, *Appl. Catal. A: General*, 2010, 384, 115–121.

20 M. Horňáček, P. Lovás, P. Hudec and A. Smiešková**,** Alkylation Of Toluene With 1-Decene In Liquid Phase Over Dealuminated Zeolite Y With Different Sodium Content, Ipc2011 ,*45th International Petroleum Conference*

21 M. De Wind, F.L. Plantenga and J.J.L. Heinerman, Upflow versus Downflow Testing of Hydrotreating Catalysts*, Appl. Catal.*, 1988, 43, 239-252.

22 P. Burchill, A. A. Herod, E.Pritchard, Estimation of basic nitrogen compounds in some coal liquefaction products, Journal of Chromatography A Volume 246, Issue 2, 17 September 1982, Pages 271–295

23 A. E. Hirschler, The effect of ammonia adsorption on the acidity of silica-alumina and alumina catalysts : The nature of the acid sites, *Journal of Catalysis,* Volume 6, Issue 1, 1966, 1–13

24 B. D. Adkins, D. R. Milburn, J. P. Goodman And B. H. Davis, Mechanism for Coking of Coal Liquefaction Catalysts Involving Basic Nitrogen Compounds, Sodium and Catalyst Acid Sites, *Applied Catalysis,* 44 (1988) 199-222

25 A. Nishijima, H.Shimada, Y.Yoshimura, T.Sato and N.Matsubayashi, Catalyst Deactivation 1987, Elsevier, 1987,39

26 E. Furimsky, Deactivation of molyhdate catalysts by nitrogen bases, Erdol und Kohle, 35 (1982) 455-459.

27 P.H.Holloway, Chemical studies of the Synthoil process : catalyst deactivation, Sandia National Labs. Report SAND78-0056,1978

28 Y.Yoshimura, H. Shimada. T.Sato, M.Kubota and A.Nishijima, Initial catalyst deactivation in the hydrotreatment of coal liquid over NiMo and CoMo-γ-Al_2O_3 catalysts, *Appl.Catal.,*29(1987)125

29 C. Perego, P. Pollesel, Advances in Aromatics Processing Using Zeolite Catalysts, *Advances in Nanoporous Materials*, Volume 1, 2010, 97–149

30 K.S.N. Reddy, B.S. Rao, V.P. Shiralkar, Alkylation of benzene with isopropanol over zeolite beta, *Applied Catalysis A: General* Volume 95, Issue 1, 1993, 53–63

31 K.S.N. Reddy, B.S. Rao, V.P. Shiralkar, Selective formation of cymenes over large pore zeolites, *Applied Catalysis A: General,* Volume 121, Issue 2, 1995, 191–201

32 G.C. Laredo, J. O. Marroquin , J. Castillo , P. Perez-Romo , J. Navarrete-Bolaños, Benzene reduction in gasoline by olefin alkylation: Effect of the catalyst on a C6-reformate heart-cut. *Applied Catalysis A: General* Volume 363, Issues 1–2, 2009, 19–26

33 C Perego, S Amarilli, A Carati, C Flego, G Pazzuconi, C Rizzo, G Bellussi, Mesoporous silica-aluminas as catalysts for the alkylation of aromatic hydrocarbons with olefins, *Microporous and Mesoporous Materials*, Volume 27, Issues 2–3, 1999, 345–354

34 L. Jie, Research progress on phenol alkylating catalyst, *Applied Chemical Industry,* 2004, 33(4).

35 C. Qiao, Y. Cai and Q. Guo, Benzene alkylation with long chain olefins catalyzed by ionic liquids: a review, *Front. Chem. Eng. China*, 2008, 2, 346–352.

36 J. A. Kocal, B.V. Vora, and T. Imai, Production of linear alkylbenzenes. *Appl. Catal. A,* 2001, 221, 295.

37 E.R. Lachter et al. Alkylation of toluene with aliphatic alcohols and 1-octene catalyzed by cation-exchange resins, *Reactive* & *Functional Polymers*, 2000, 44, 1 –7.

38 T. F. Degnan Jr, C. M. Smith and C. R. Venkat, Alkylation of aromatics with ethylene and propylene: recent developments in commercial processes. *Appl. Catal. A*, 2001, 221, 283.

39 C. Perego and P. Ingallina, Recent advances in the industrial alkylation of aromatics: new catalysts and new processes. *Catal. Today*, 2002, 73, 3.

40 K. Wilson and J. H. Clark, Solid acids and their use as environmentally friendly catalysts in organic synthesis**,** *Pure Appl. Chem.*, 2000, 72, 1313–1319.

41 . J.H. Coetzee et al. An improved solid phosphoric acid catalyst for alkene oligomerization in a Fischer–Tropsch refinery*, Appl. Catal. A: General*, 2006, 308, 204–209.

42 H. Michal, H. Pavol, S. Agáta and J. Tibor, Alkylation Of Benzene With Linear 1-Alkenes In Liquid Phase. Influence Of Zeolite Type And Chainlength Of 1-Alkenes On The Activity And Selectivity. 44th International Petroleum Conference, Bratislava, Slovak Republic, September 21-22, 2009.

43 M. Xu, J.H.Lunsford, D. W.Goodman and A. Bhattacharyya, Synthesis of Dimethyl Ether(DME) From Methanol Over Solid-acid Catalysts, *Appl. Catal. A: General*, 1997, 149, 289-301.

44 W. Daniell, U. Schubert, R. Glöckler, A. Meyer, K. Noweck and H. Knözinger, Enhanced surface acidity in mixed alumina-silicas: a low-temperature FTIR study, *Appl. Catal. A*, 2000, 196, 247-260.

45 J. Park, K. Nakano, Y.-K. Kim, J. Miyawaki, S.Yoon and I. Mochida, Characteristics on HDS over amorphous silica–alumina in single and dual catalytic bed system for gas oil, *Catal. Today*, 2011, 164, 100–106.

46 W. G. Frankenburg, Advances in Catalysis and Related Subjects, Academic Press, 1969, pp. 103-105

47 R. M. Silverstein and F. X. Webster, Spectrometric indetification of organic compounds, John Wiley & Sons, Inc. 6th edition 1998.

48 N. Hosseinpour, Y. Mortazavi, A. Bazyari and A.A. Khodadad, Synergetic Effects Of Y-Zeolite And Amorphous Silica-Alumina As Main FCC Catalyst Components On Tri Isopropylbenzene Cracking And Coke Formation, *Fuel Processing Technology*, 2009, 90, 171-179.

Chapter 3: Catalyst Characterization

3.1 Introduction

Normally, acid catalysis is not considered when a feed material contains basic compounds, because the basic compounds will act as catalyst poisons. The poisoning is due to the neutralization of the acid sites on the catalyst by the basic compounds in the feed through a typical acid-base reaction. But acid sites are only permanently deactivated if the acid site is so strong that the base cannot be thermally displaced.

There is consequently in theory a “sweet spot” where basic compounds will inhibit, but not poison acid catalysts. The challenge is in finding appropriate catalysts that have sufficient acid strength to perform useful catalysis, but that are not strong enough to be poisoned by strong bases at the operating conditions necessary for the conversion. In this chapter the focus will be on acid catalyst screening and characterization.

3.2 Materials

The range of Siral silica-alumina catalysts and the Pural range of alumina catalysts are especially interesting, because they are cheap, commercially available and provide a tuneable range of properties through silica:alumina ratio and hydration level. The inclusion of H-ZSM-5 (MFI zeolite) will give a point of contrast. We selected these catalysts for the catalyst screening and characterisation to find acid catalysts with appropriate acidity.

The alumina and amorphous silica-alumina catalyst types were commercially obtained from Sasol, Germany (former Condea GmbH): Pural BT (pure *eta*-alumina), Pural SB (pure *gamma*-alumina) and Siral series (silica-doped silica-alumina, with silica content varying from 1 to 40 wt% over the series, e.g. Siral 5 contains 5 wt% SiO_2). An MFI-zeolite (H-ZSM-5) was commercially obtained from Zeolyst International, USA (SiO_2/Al_2O_3 = 280, surface area = 400 m^2/g, and 0.05 wt% Na_2O). The zeolite was included in the study as a control, not because it was anticipated to perform well in this type of catalysis.

All of the catalysts were activated by heating in air at 550 °C for 6 hours before use. Pural BT and Pural SB were calcined at 550 °C for 6 hours to convert them into *eta*- or *gamma*-alumina respectively. The MFI-zeolite was supplied in its ammonia form and it was converted into the acidic form by calcining under flowing air at 550 °C for 6 hours.

3.3 Physical and chemical catalyst characterisation

For conversion of real coal liquids, the Hg intrusion based pore volume and surface area is a better measure than that the surface area by BET N_2 adsorption. With the Hg porosimeter the minimum pore size that could be measured was 6 nm. It was reported that the pore volume played an important role in the performance of catalysts during coal liquid hydrotreating. Catalysts with larger pores performed better. The best performance for hydrodenitrogenation and hydrodeoxygenates of coal liquids were found with catalysts having pores mainly in the 6-20 and 7-16 nm size ranges respectively.[1,2]

We used mercury porosimetry for catalyst pore volume and surface area. These analyses were conducted with a Quantachrome PoreMaster® Hg intrusion porosimeter. In order to also account for microporosity, the BET N_2 surface area was also important, which is given by the data sheet from Sasol Germany.

In order to learn more about the external morphology of the catalysts, we studied the catalysts by scanning electron microscopy (SEM). The SEM and Auger measurements were carried out using JAMP-9500F Auger microprobe (JEOL) at the Alberta Centre for Surface Engineering and Science, University of Alberta. The accelerating voltage used for SEM imaging was 5 kV. The samples were kept at a working distance of 22.4–24.6 mm.

The compositions of the catalysts were determined by energy dispersive X-ray fluorescence (XRF) analysis with a Bruker S2 Ranger, with a silicon drift detector. The X-ray source uses a Pd target. The analyses were performed at 10 kV with total count rate in the order of 20 000 counts per second; no filters or secondary targets were employed.

The surface area and pore volumes were determined for each catalyst and at each hydration state (level of calcination) (Table 3-1). There was good correlation with the BET surface area values previously reported for Pural SB (*gamma*-alumina) and the Siral-series of catalysts.[3]

Table3- 1 Catalyst Characterization Data

Catalyst	Intruded volume (cm^3/g) [a]	Porosimetry surface area (m^2/g) [a]	Intruded volume (cm^3/g) [b]	Porosimetry surface area (m^2/g) [b]	Intruded volume (cm^3/g) [c]	Porosimetry surface area (m^2/g) [c]	BET surface area (m^2/g) [c]
Siral1	0.31	89	0.40	143	0.63	226	263
Siral5	0.65	97	0.71	137	1.21	207	323
Siral10	0.72	105	0.79	157	0.99	199	391
Siral20	0.84	101	0.96	171	1.13	204	430
Siral30	1.10	104	1.37	181	1.40	200	483
Siral40	1.21	137	1.15	231	1.42	264	514
Pural SB	0.37	9	0.40	103	0.74	235	238
Pural BT	0.27	34	0.45	15	0.64	23	333
H-ZSM-5	0.51	5	-	-	0.58	12	400

[a] After activation at 150°C for 6 hours;
[b] After activation at 350C for 6 hours;
[c] After activation at 550°C for 6 hours;

The low macro- and mesoporosity of Pural BT (*eta*-alumina) and H-ZSM-5 indicated that it was unlikely that these two catalysts would have the accessibility needed to perform well with real coal liquids. This was anticipated in the case of the zeolite, which was included in the study as a control. The MFI zeolite structure has 0.51 × 0.55 and 0.53 × 0.56 nm pores,[4] and the intrusion volume and area that was found by porosimetry is due to the matrix, and not due to the zeolite crystals. The low macro- and mesopore surface area of the *eta*-alumina compared to the *gamma*-alumina was not anticipated.

In Table 3-1, it shows that hydration, which is related to calcination temperature, affects the catalyst surface area, with higher activation temperature, the surface area increases. More macro and meso-porosity developed in the catalysts when changing the hydration level.

Siral5(150°C calcined 6h)

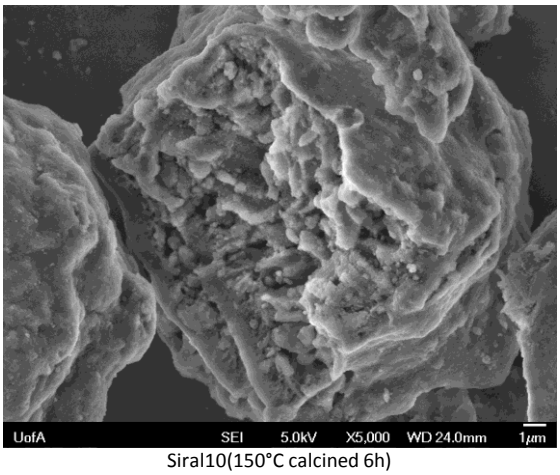

Siral10(150°C calcined 6h)

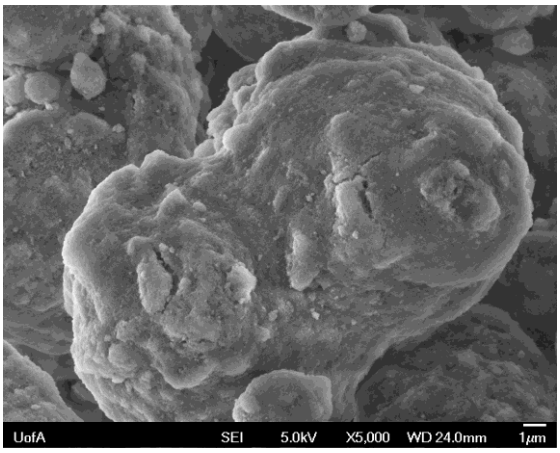

Siral40(150°C calcined 6h)

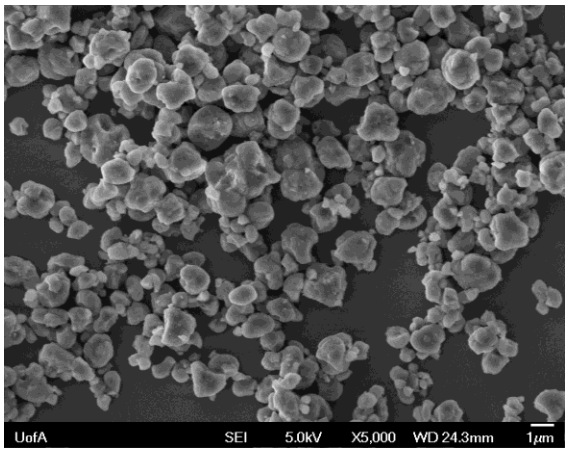

H-ZSM-5(550°C calcined 6h)

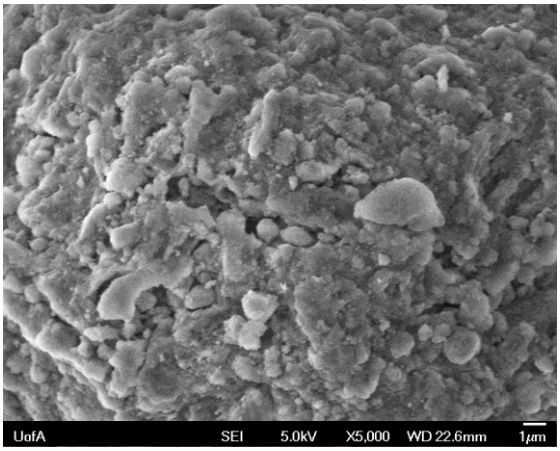

Siral 30(150°C calcined 6h)

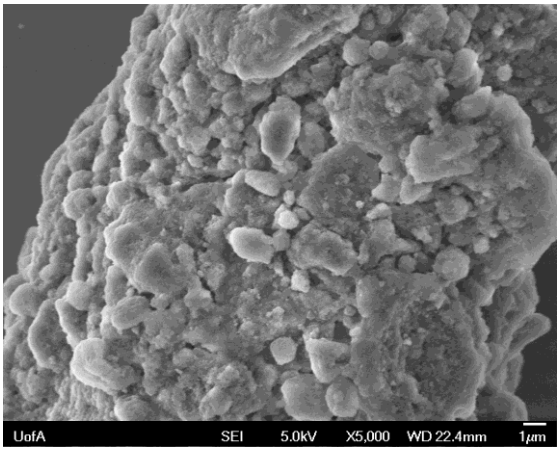

Siral30(550°C calcined 6h)

Figure3- 1 Scanning electron microscopy images of the samples

From the SEM (fig 3-1) we can find that a) there are certain amounts of macropores on the surface of siral catalysts and compared to H-ZSM-5 it is more obvious that siral have more larger pores than the zeolite; b) we can't see any

obvious differences between catalysts before or after calcination at 550 °C, it seems that the only difference might be the changes in meso- or micropores, which can't be seen here. These results match the data of porosimeters. (Fig 3-2 shows the pore size distribution of Siral 5, the rest can be found in appendix I Figure I-1)

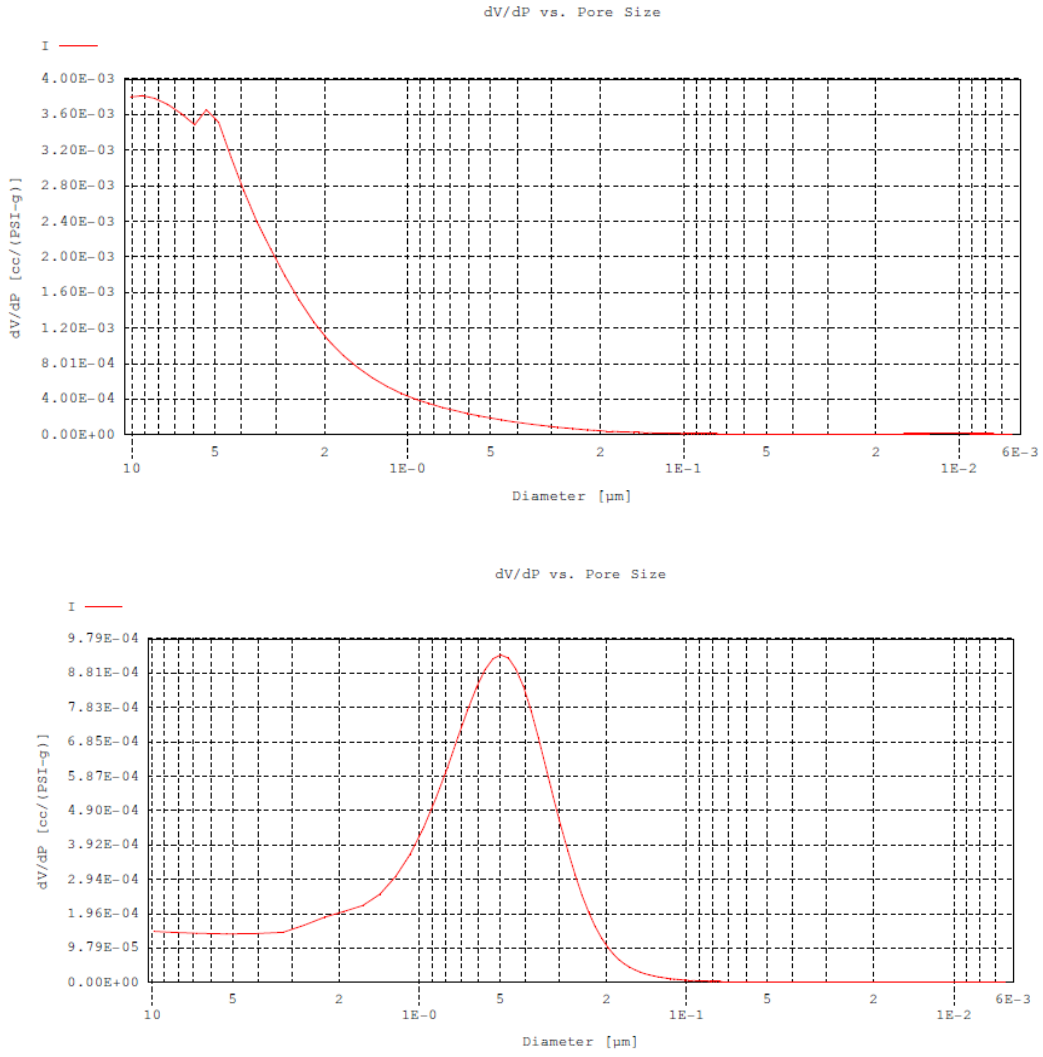

Figure3- 2 Poresize Distribution: Siral 5 (150°C calcined 6h); H-ZSM-5 (550°C calcined 6h);

The silica (SiO_2) and alumina (Al_2O_3) content of the catalysts (Table 3-2) were determined by X-ray fluorescence analysis. The results are considered only semi-quantitative and the reported values differ somewhat from the compositions reported by the catalyst suppliers. Nevertheless, it was confirmed that the catalysts consisted mainly of silica and alumina. The catalysts contained less than 0.5 wt% in total of Na, Mg, P, Ca and Ti oxides (Fig 3-3, Fig I- 2).

Table3- 2 Compounds Distribution in Catalysts

Catalyst	Al_2O_3 Wt%	SiO_2 Wt%
Siral1	98.3	1.6
Siral5	96.4	3.5
Siral10	91.9	8.1
Siral20	84.2	15.8
Siral30	76.7	23.2
Siral40	68.1	31.9
Pural SB	98.4	0.9
Pural BT	98.7	1.2
H-ZSM-5	0.6	99.4

When the calcined catalysts (350°C and 550°C) were analysed by XRF, the compositions stayed similar, which means that the elements still remain in the same quantities in the catalysts with different hydration level. There was no detectable dealumination.

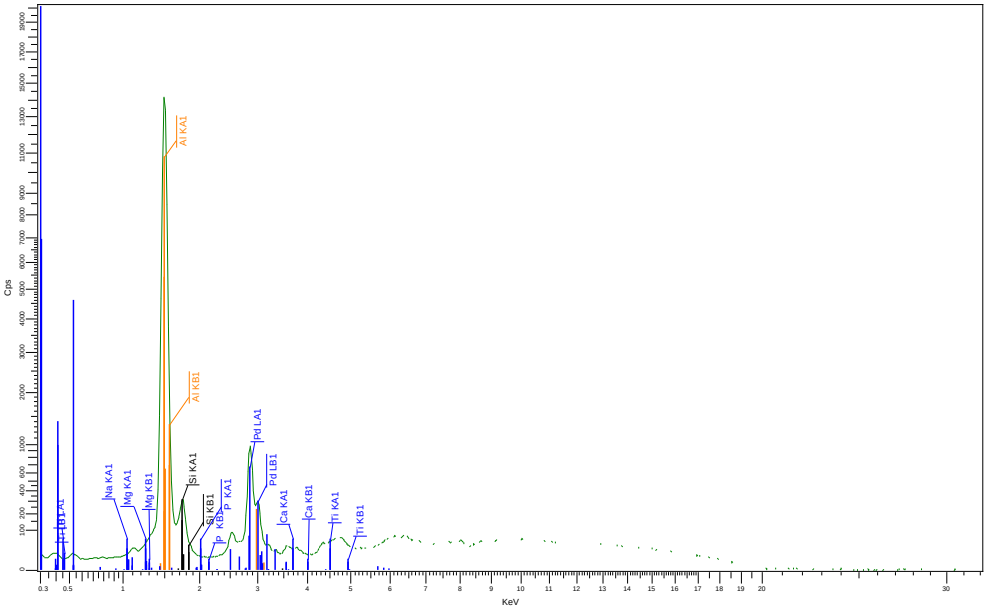

Figure3- 3 XRF for the representative catalysts Siral 1(150°C calcined 6h)

3.4 Catalyst Acid Site Concentration and Strength

The ability of a catalyst to perform acid catalysis in the presence of nitrogen-bases requires specific acid site characteristics, as was outlined in the introduction. The characterisation of the catalysts in terms of their acid site concentration and strength was therefore central to the study.

Total acid concentration and acid strength of the catalysts were determined by ammonia temperature programmed desorption (NH_3-TPD). The NH_3-TPD analysis was performed using a Quantachrome ChemBET TPR/TPD Chemisorption Flow Analyzer equipped with a thermal conductivity detector (TCD). For each analysis about 60 mg of catalyst was pretreated under flowing helium (50 ml/min) at 550 °C for 6 hours and then cooled down to room temperature. Ammonia (NH_3) adsorption was then performed at room

temperature by exposing the catalyst to an NH_3 flow of 70 ml/min for 1 hour. After the removal of physisorbed NH_3 by keeping the sample in He flow for 100 minutes, the TPD experiments were carried out. The sample was heated from room temperature to 650 °C at 15 °C/min under a He flow of 50 ml/min. We also performed the same experiments at different heating rates, to see if the heating rates have anything to do with the results.

The nature of the acid sites was determined by Fourier transform infrared (FTIR) analysis. Spectra were collected on an ABB MB3000 FTIR with a Pike DiffusIR attachment. The DiffusIR has an environmental chamber that is temperature controlled and can heat up to 500 °C. The analytical procedure was as follows. Catalyst (2 mg) was pressed into a ceramic cup, the catalysts were pretreated at 550°C. The catalyst was then exposed to flowing He saturated with pyridine vapour for 1 hour, followed by purging with clean He flow for about 1 hour. Purging with clean He also removed physisorbed pyridine from the surface, leaving only the stronger chemisorbed species. This cleaning process could be followed by FTIR and was continued until no further changes were observed. The analysis of the catalyst with adsorbed pyridine started at ambient temperature and the ceramic cup was heated at a rate of 10 °C/min under He flow from 25 to 500 °C. We used a gas washing bottle for bringing the pyridine vapor into the chamber (Fig 3-4). The temperature was held constant during spectral acquisition. Spectra were

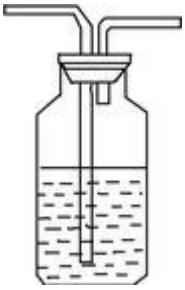

Figure 3-4

recorded at 50 °C intervals at a resolution of 16 cm^{-1} as the average of 120 scans.

The acid site concentration and strength were determined by ammonia temperature programmed desorption (Figure 3-5). The total volume of ammonia desorbed, represented by the area under each curve in Figure 3-5, equals the total acid site concentration. The temperature at which the desorption takes place, relates to the strength of the acid site. The stronger the acid site, the stronger ammonia is bound and the higher the temperature that is required to desorb the ammonia from the acid site.

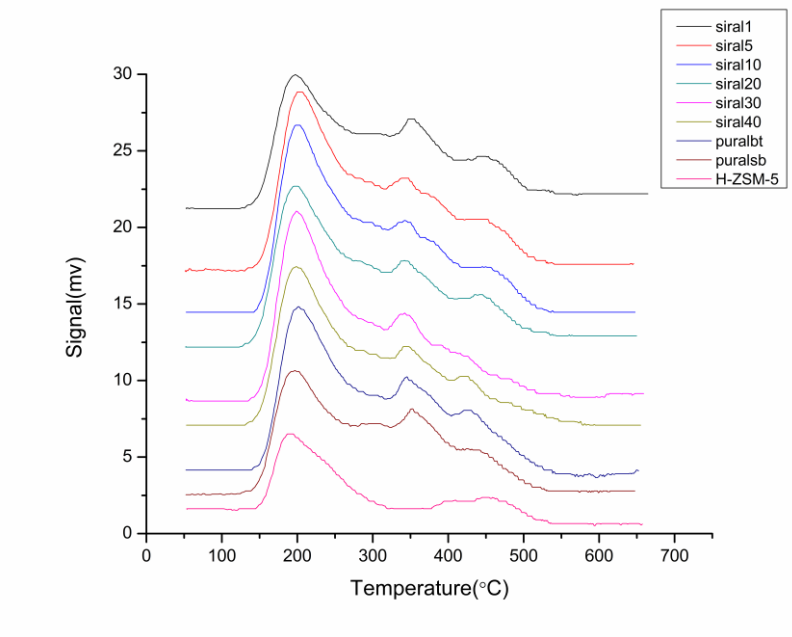

Figure3- 5 Acid site concentration and acid strength distribution determined by NH_3-TPD

Although there is a continuum of acid strengths, most catalysts displayed three desorption peaks, which represent weak, medium and strong acid sites (Table 3-3). The integrated areas of the overlapping features in the TPD spectra

were calculated by means of the TPRWin peak-analysis software, employing a Lognormal function to fit the experimental peak shapes which was automatically chosen to be curve-fitting method. (Fig3-6)

It was known from previous work on the alkylation of phenol with 1-octene,[5] that the performance of Siral 30 and 40 was better than over more alumina-rich Siral catalysts, such as Siral 5 and 10. Yet, there is overlap in the concentration of weak acid sites on these catalysts (Table 3-3). The contribution of weak acid sites to alkylation is therefore small.

Medium strength acid sites are likely to be the most useful for acid catalysis in the presence of nitrogen-bases. Even though some of the medium strength acid sites may be deactivated, at least some of these acid sites will just be inhibited.

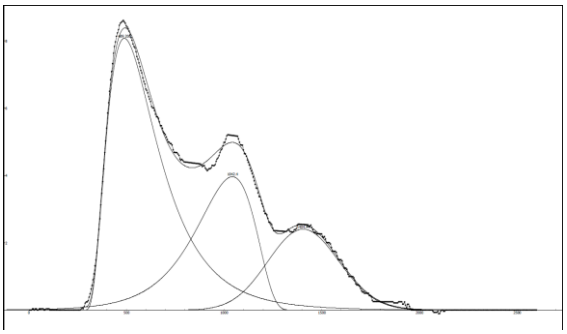

Siral1

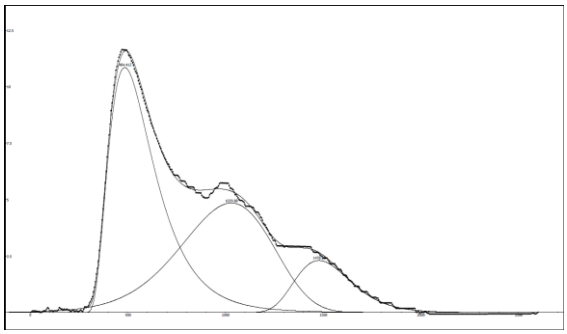

Siral5

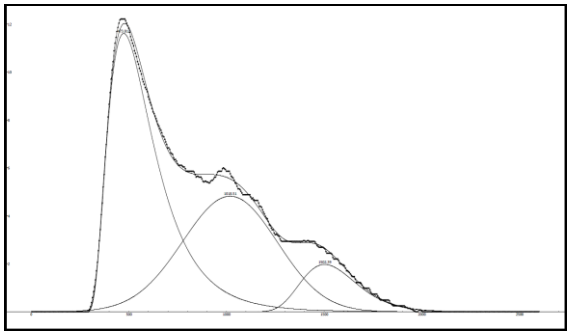

Siral10

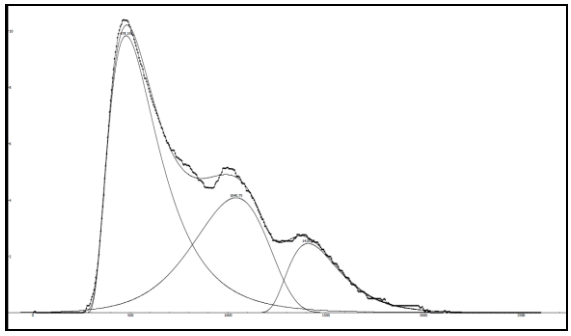

Siral20

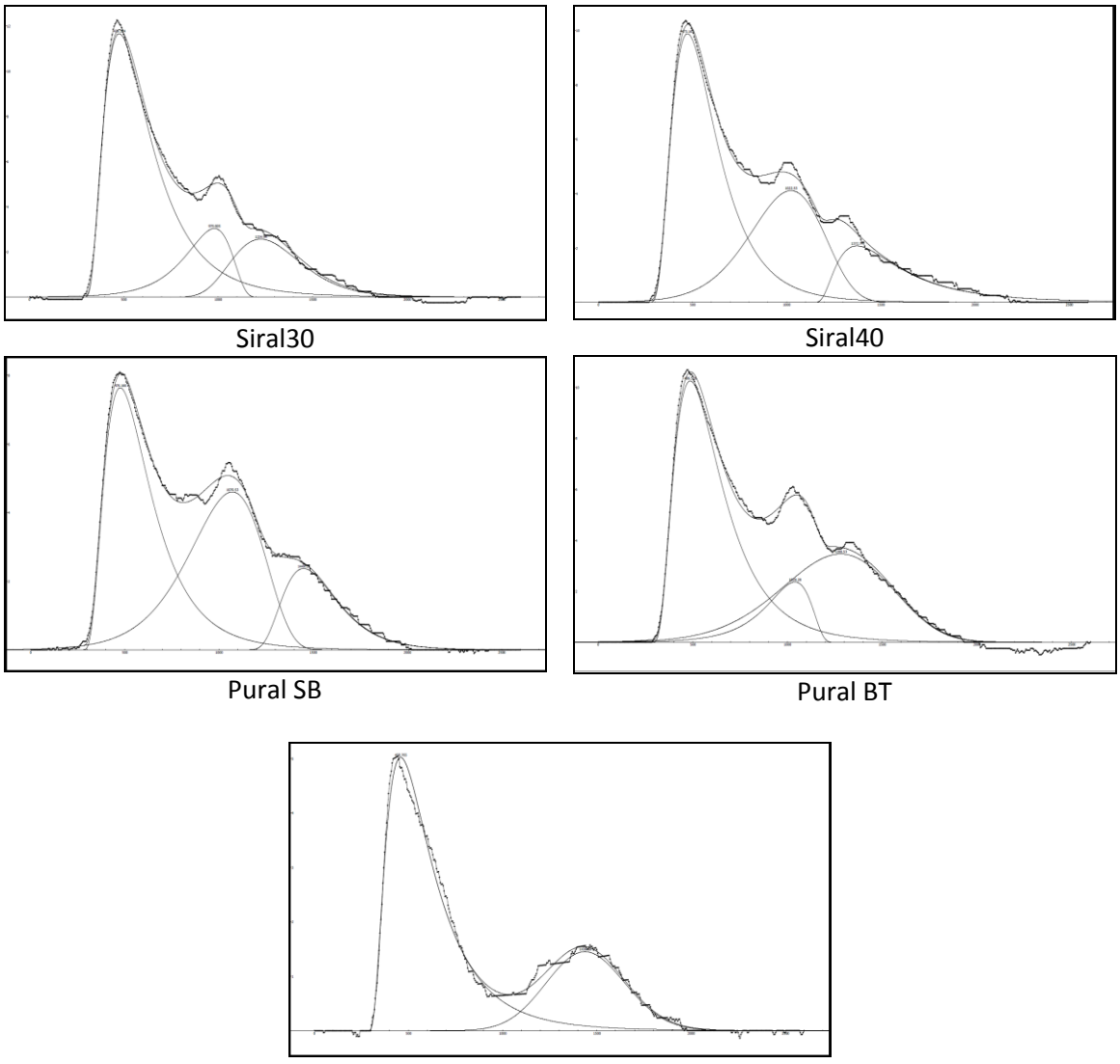

Figure 3-6 Peak Fitting of the Catalysts (Siral 1-40, Pural SB, Pural BT and H-ZSM-5)

The strong acid sites will contribute to aromatic alkylation in the absence of nitrogen-bases only. Strong acid sites will bind basic compounds strongly and in the presence of pyridine, the strong acid sites will be completely deactivated. The reaction between strong acid sites and nitrogen bases is not reversible at

typical alkylation temperatures; the peak NH_3 desorption temperature for the strong acid sites is >400 °C (Table 3-3).

Table3-3 Acid Site Concentration and Acid Strength Distribution Determined by Ammonia Temperature Programmed Desorption

Catalyst	Acid site concentration (μmol/g)				Peak NH_3 desorption temperature (°C)		
	Total	Weak	Medium	Strong	Weak	Medium	Strong
Siral 1	703	368	205	130	196	351	444
Siral 5	818	394	326	98	203	346	455
Siral 10	938	493	353	92	203	354	466
Siral 20	808	453	246	109	199	350	448
Siral 30	1127	452	489	186	200	333	461
Siral 40	820	480	170	170	201	348	413
Pural SB	719	337	124	258	197	351	414
Pural BT	810	428	86	296	204	347	413
ZSM-5	386	296	0	90	197	-	454

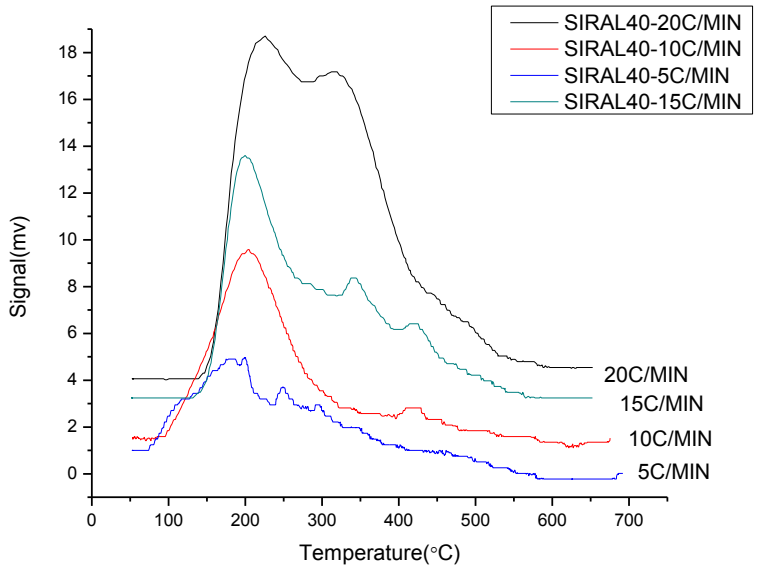

Figure3-7 Ammonia TPD Curves of Siral 40 at Different Heating Rates

We chose Siral 40, which has stronger acidity, to investigate the heating rate influence on the experiments. The sample was heated to 650°C using four different heating rates (Fig 3-7). As expected, the TPD peaks for every sample shifted to lower values as heating rates decreased, while it almost maintained the same order of acid strength at each rate.[6] The peaks are better separated at the heating rate of 15 °C/min. When the rate is too high, the peaks are overlapping more, (Fig 3-8) as we found when performing a range of NH_3-TPD experiments at 20 °C/min for more catalysts (Siral1-40 and Pural SB, Pural BT). When the heating rate is too low the major peaks of the desorption cannot be clearly recognized.

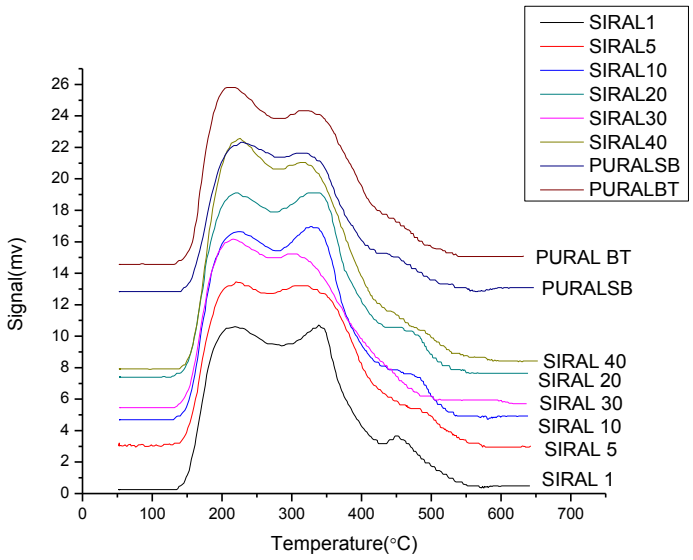

Figure3- 8 Acid Site Concentration and Acid Strength Distribution Determined by NH_3-TPD (Heating Rate at 20°C/min)

As shown in the figure, more overlapping occurred between weak acid cites and medium acid sites, and for some catalysts the strong acid cites were not clear, compared with curves at heating rate of 15 °C/min.

Low temperature rate is beneficial for separating the peaks related to different active sites. Since it also affects the TCD sensitivity, we should avoid possible phenomena of re-adsorption, otherwise the resulting peaks will be too large. The temperature ramping rates of 15 °C/min ensured that no significant re-adsorption took place, but at 5 °C/min, undesired peaks were enlarged, making the results imprecise; no specific peak was observed.[7]

Silica-alumina materials posses both Lewis and Brønsted acid sites. Lewis acid sites are electron pair acceptors, whereas Brønsted acid sites are H^+-donors. The nature of the acid sites can be probed by FTIR analysis of pyridine treated catalysts.[8] The infrared absorption at around 1450 cm^{-1} is characteristic of the coordinative adsorption of pyridine on Lewis acid sites. The infrared absorption band at around 1540 cm^{-1} is characteristic of the pyridinium ion formed on Brønsted acid sites. Both acid sites contribute to the infrared absorption at 1490 cm^{-1}.

The FTIR spectra of the pyridine treated catalysts at 25 °C are shown in Figure 3-9 and reflects the overall Lewis to Brønsted acid ratio (L:B ratio) of the catalysts. The sharper increase in the high Al_2O_3 range is mainly due to weak sites which are revealed by a pyridine band at around 1600 cm^{-1} while pyridine coordinated with strong Lewis sites gives a band at 1620 cm^{-1}.[9]

Although the overall L:B ratio of the catalysts at 25 °C is of interest from a materials perspective, it does not reflect the nature of the acid sites in relation to their acid strength. The L:B ratio of acid sites in a specific strength range can be obtained from the difference in the FTIR spectra of pyridine saturated catalysts collected at different temperatures (Figure 3-10).

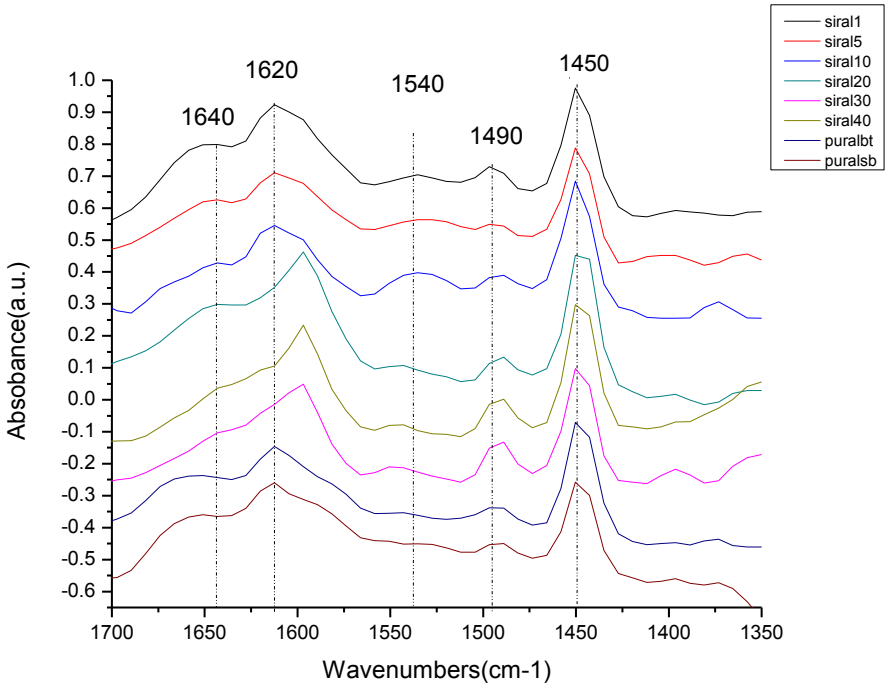

Figure 3-9 FTIR Spectra in the 1700 To 1350 cm-1 Region of Pyridine Treated Catalysts

The decrease in absorbance at 1450, 1490 and 1540 cm^{-1} with increase in temperature correlates to the change in Lewis and Brønsted acid site concentration within the strength range indicated by pyridine desorption. Thus one can calculate the nature and the concentration of the weak, medium and strong Lewis and Brønsted acid sites from Table 3-3 in combination with the temperature dependent L:B ratios obtained from FTIR (e.g. Figure 3-10). In this

way the concentration of weak, medium and strong Lewis and Brønsted acid sites were calculated for the catalysts of interest (Table 3-4).

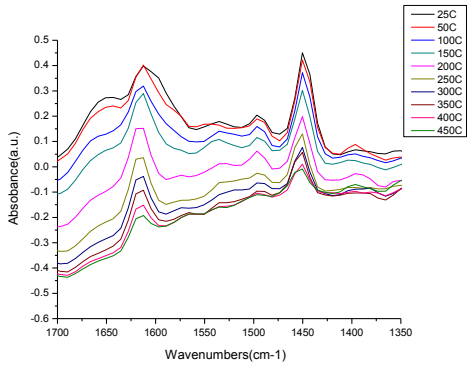

Siral1 (550°C calcined 6h)

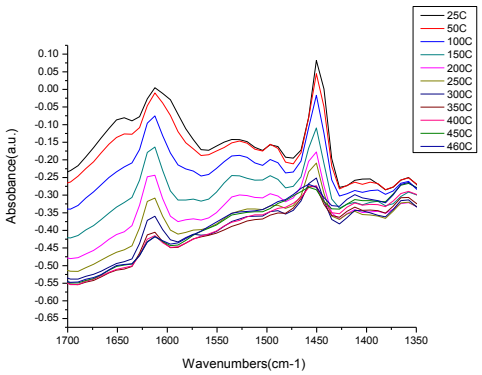

Siral5 (550°C calcined 6h)

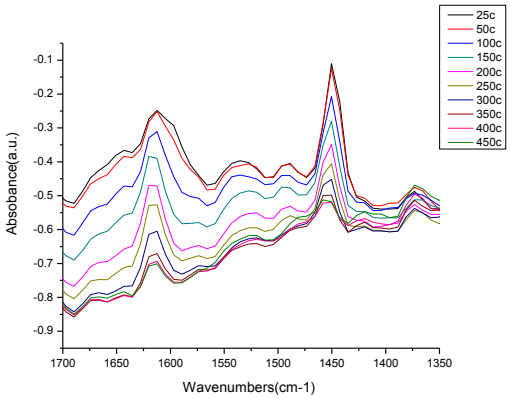

Siral10 (550°C calcined 6h)

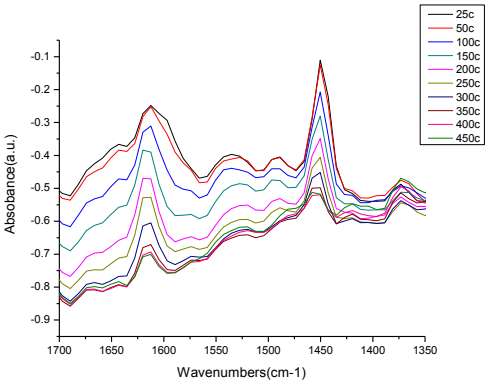

Siral20 (550°C calcined 6h)

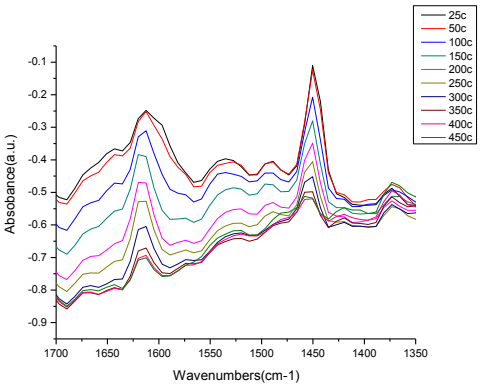

Siral30 (550°C calcined 6h)

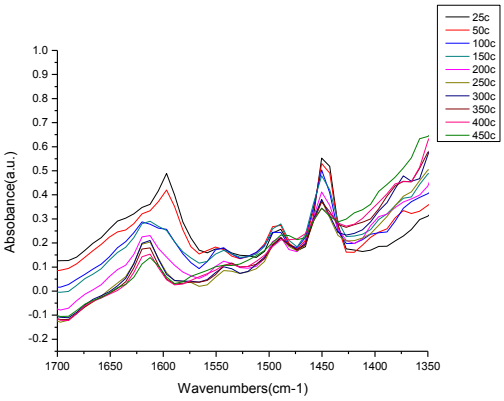

Siral40 (550°C calcined 6h)

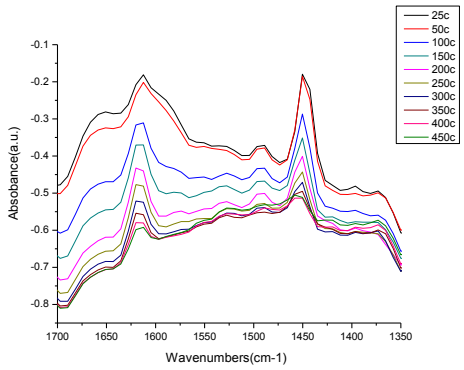

Pural SB (550°C calcined 6h)

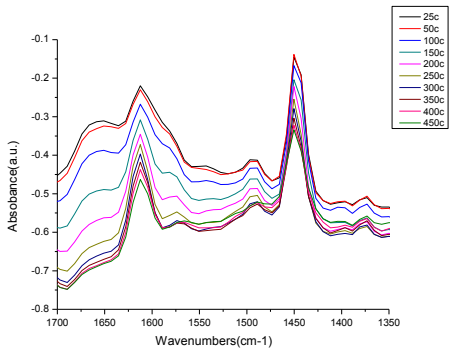

Pural BT (550°C calcined 6h)

Figure 3-10 Temperature dependent FTIR spectra of pyridine treated Catalysts

The calculation procedure is based on different assumptions and approximations that affect the quantitative outcome:

(a) As a first approximation the boundary between weak and medium acid sites was taken at 300 °C, and between medium and strong acid sites at 400 °C. Thus, the FTIR spectra of pyridine treated catalysts collected at 400 °C would reflect only strong acidity, whereas the FTIR spectra collected at 300 °C would reflect medium and strong acidity.

(b) The acid concentration for each type of acid site strength determined by NH_3-TPD was directly related to the pyridine-based temperature dependent Lewis and Brønsted acid determination using FTIR. Pyridine is a slightly weaker base than ammonia, which potentially introduces bias in L:B ratio if there is a significant change in L:B ratio between weak, medium and strong acid sites.

(c) It was assumed that the optical path length for the FTIR analyses were constant and care was taken to ensure this.

(d) A key challenge was to assign absorption coefficients to the FTIR absorptions, so that the concentration of each type of acid site could be determined.[8] The quantification of acid site concentration was based on the infrared absorptions at 1450 and 1490 cm^{-1}, using *gamma*-alumina as a standard for Lewis acid sites. The Brønsted acid site concentration was calculated by difference using the infrared absorption at 1490 cm^{-1}, rather than the absorption at 1540 cm^{-1}, since it was better defined (Appendix II).

Table3-4 Lewis to Bronsted acid ratio determined by FTIR analysis of pyridine treated catalysts and the calculated concentration of acid sites of each type

Catalyst	Lewis:Brønsted acid ratio			Weak acid sites (μmol/g)		Medium acid sites (μmol/g)		Strong acid sites (μmol/g)	
	25 °C	300 °C	400 °C	Lewis	Brønsted	Lewis	Brønsted	Lewis	Brønsted
Siral 1	5.9	11.6	7.3	293	75	194	11	114	16
Siral 5	8.1	5.9	4.4	366	28	283	43	80	18
Siral 10	14.6	11.6	3.3	468	25	339	14	71	21
Siral 20	4.9	5.3	2.6	372	81	220	26	79	30
Siral 30	3.1	2.7	3.3	360	92	350	139	143	43
Siral 40	3.8	2.2	2.4	415	65	114	56	120	50

For the most part the calculated L:B ratio (Table 3-4) was in the 3-6 range, as suggested by Basila and Kantner based on the characterisation of commercial silica-alumina catalysts with 12-25 % alumina.[10] Notable exceptions are found in the Siral 1 to 10 catalysts, which are more alumina-rich. The higher L:B ratio is therefore not surprising, since pure alumina has high Lewis acidity. The characterisation of Siral series catalysts by Knözinger and co-workers,[3] unfortunately did not include quantification of the L:B ratio.

3.5 Catalyst hydration

When dealing with real coal liquids, hydration will become an important consideration. The acidity and L:B ratio of silica-alumina catalysts depend on the level of catalyst hydration.[9] It will also be important to quantify and characterize the nature of weak acidity as a function of hydration level, since hydration affects acid strength[9] and product selectivity. Coal liquids naturally contain oxygenates and will therefore affect the hydration level. We used TGA to obtain a profile of mass loss due to dehydration with temperature, and also FTIR to get a better picture of the relationship with bonds changing and hydration.

The nature of the acid sites related with hydration was determined also by Fourier transform infrared (FTIR) analysis. Spectra were collected on an ABB MB3000 FTIR with a Pike DiffusIR attachment, the procedure was the same as before, the catalysts were pretreated at three different temperatures (150°C, 350°C, 550°C) for the hydration investigation. The analysis of catalysts without being treated by pyridine was tested using a Pike diamond ATR attachment on another ABB MB3000 FTIR; these catalysts were pretreated at 150°C and 550°C.

The mass loss of the water in the catalysts was investigated by TGA. We conducted the experiments using a TGA from TA Instruments, SDT-Q600. Before actual sample runs, the TGA should be temperature calibrated. Typical test conditions are: Sample size: 9-13 mg. Initial temperature was ambient, heated up to 100°C, and maintained for 5 minutes and then heated up to 600°C at

10°C/min under nitrogen flow. Since a variation in moisture content among samples will affect results, test specimens should be dry and handled only with gloves or tweezers. In addition, sample size and surface area should be kept relatively constant. The sample is loaded into a clean, tared, platinum sample pan in the TGA module. It is then heated at the selected heating rates, eight samples were tested. After all experiments were completed, the stored data files were then analyzed using TGA Analysis Software.

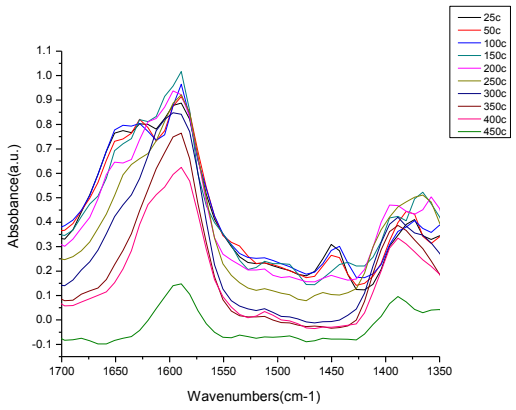

Siral 1

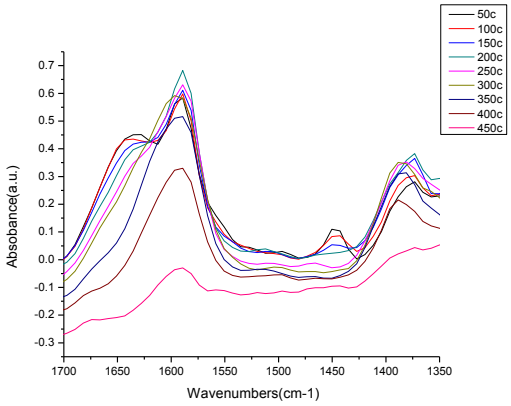

Siral 5

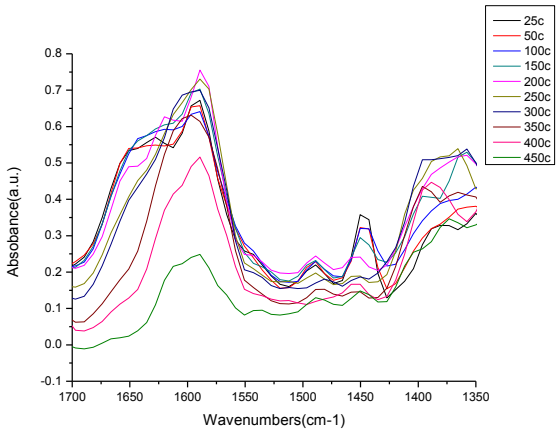

Siral 10

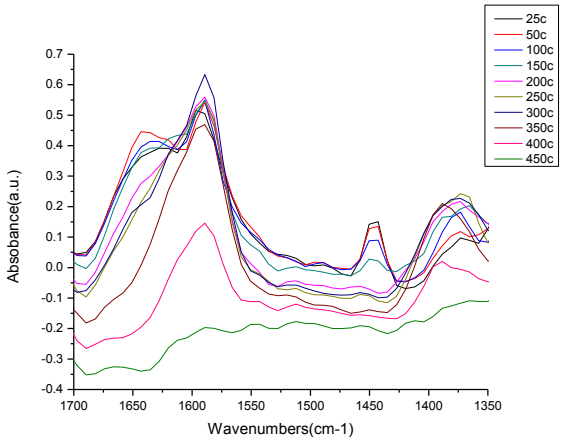

Siral20

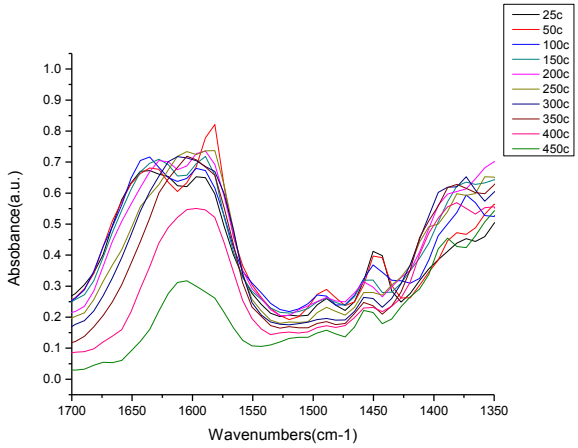

Siral30

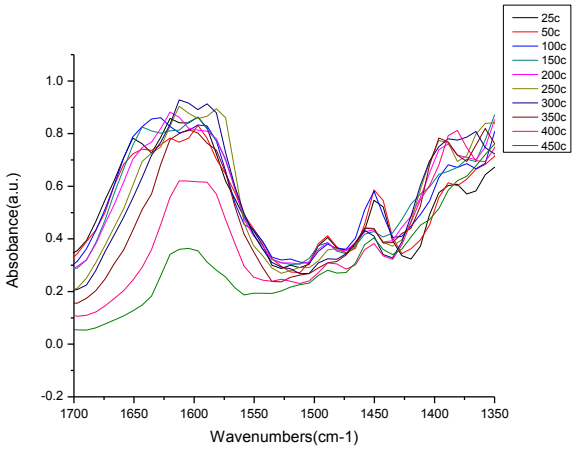

Siral40

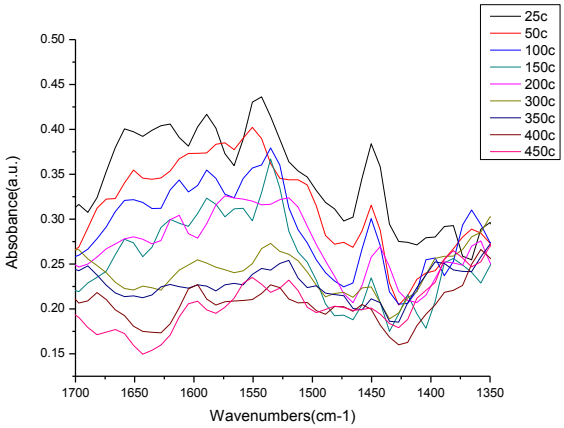

Pural SB

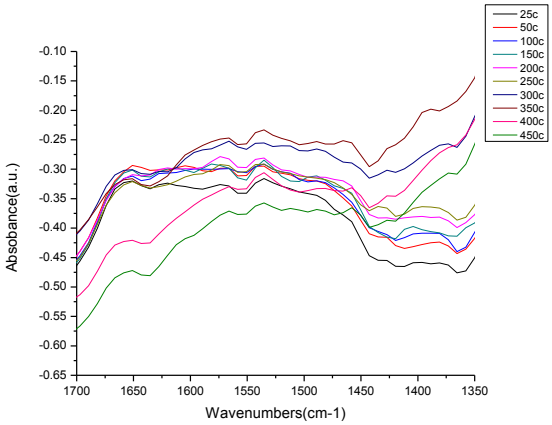

Pural BT

Figure 3-11 Temperature dependent FTIR spectra of pyridine treated catalysts (150°C calcined 6h)

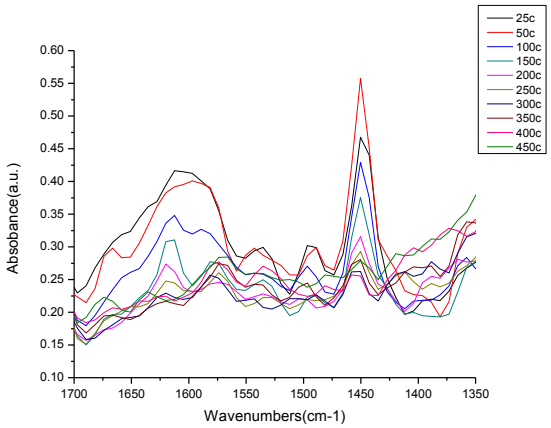

Siral1

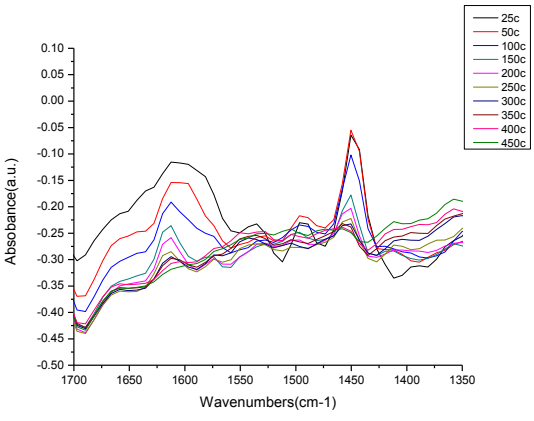

Siral5

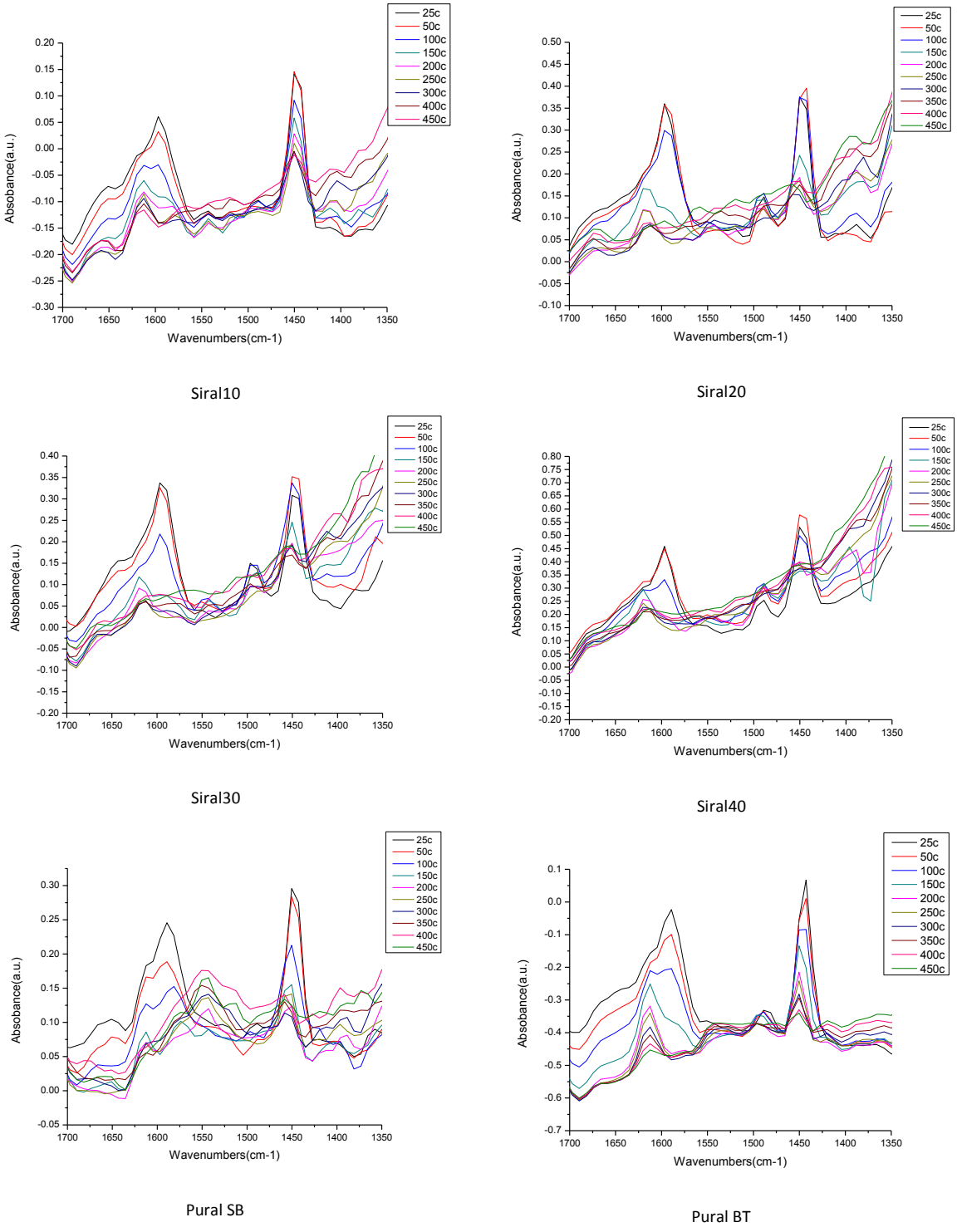

Figure 3-12 Temperature dependent FTIR spectra of pyridine treated catalysts(350°C calcined 6h)

When catalysts were calcined at different temperatures, certain differences are observed in the spectrum. From the FTIR spectrum, the specific acid peaks of catalysts with calcination at 350°C is obviously neater than the ones with calcination at 150°C, even though not as sharp as the typical peaks of catalysts being calcined at 550°C. (Fig.3-11, Fig.3-12) This can be illustrated more clearly by the difference in Lewis acidity observed at different hydration levels (Fig. 3-13).

Catalytic conversion is very dependent on the level and nature of surface hydration of the catalysts. Any water in the feed may act as catalyst modifier, which poisons, inhibits or activates the catalysts depending on the reaction. The pretreatment is very important. The temperature history and water content of the catalysts containing alumina affect the surface chemistry of the acid sites, water was present as adsorbed water and as chemically incorporated water.

The surface of the alumina in the catalysts is gradually transformed by the progressive dehydration, the initially adjacent hydroxyl groups' infrared absorption was at 3200-3600 cm^{-1}, Isolated hydroxyl groups go towards a maximum as the surface is increasingly dehydrated, and the amount of coordinative unsaturated Al Lewis acid sites increases, thus the activity increases. As the dehydration increases, the activity passes through a maximum, because of the loss of the surface area is a competing effect that affect increasing activity.[11, 12]

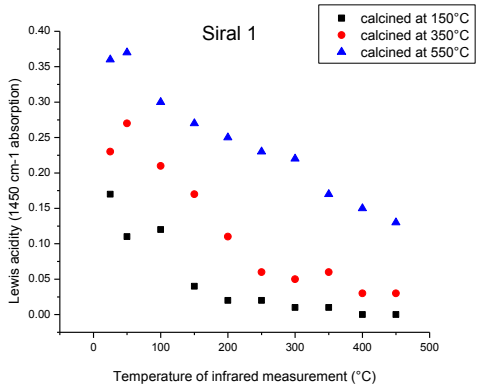
Siral 1
calcined at 150°C
calcined at 350°C
calcined at 550°C
Lewis acidity (1450 cm-1 absorption)
Temperature of infrared measurement (°C)

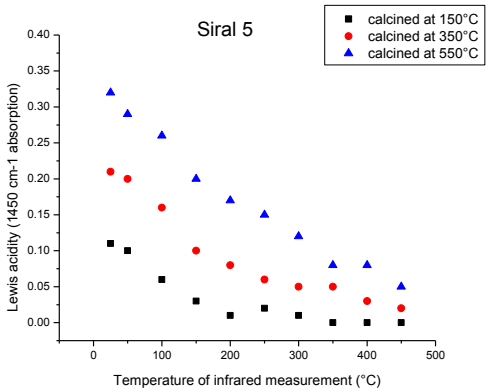
Siral 5
calcined at 150°C
calcined at 350°C
calcined at 550°C
Lewis acidity (1450 cm-1 absorption)
Temperature of infrared measurement (°C)

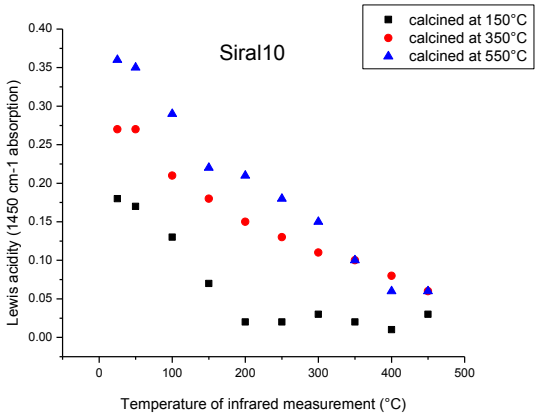
Siral10
calcined at 150°C
calcined at 350°C
calcined at 550°C
Lewis acidity (1450 cm-1 absorption)
Temperature of infrared measurement (°C)

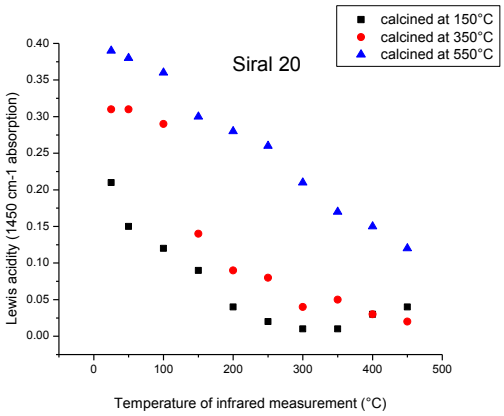
Siral 20
calcined at 150°C
calcined at 350°C
calcined at 550°C
Lewis acidity (1450 cm-1 absorption)
Temperature of infrared measurement (°C)

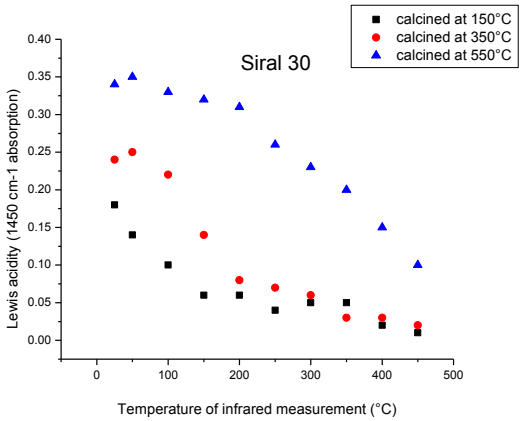
Siral 30
calcined at 150°C
calcined at 350°C
calcined at 550°C
Lewis acidity (1450 cm-1 absorption)
Temperature of infrared measurement (°C)

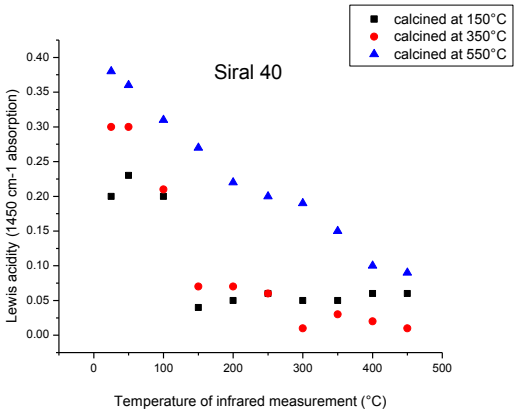
Siral 40
calcined at 150°C
calcined at 350°C
calcined at 550°C
Lewis acidity (1450 cm-1 absorption)
Temperature of infrared measurement (°C)

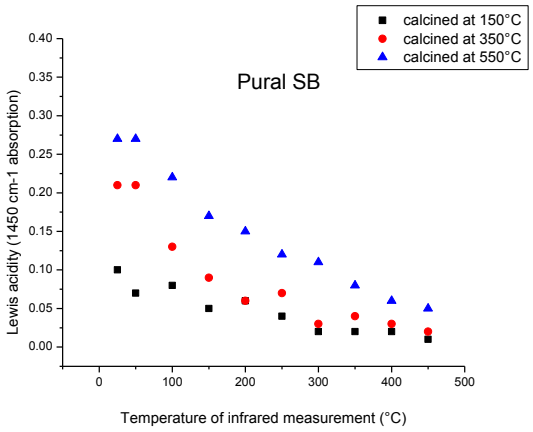

Figure 3-13 Effect of hydration on Lewis acid content, illustrated by Siral 1-40 and Pural SB infrared absorption at 1450 cm^{-1}

Compared with other catalysts, Pural BT (*eta*-alumina after it has been calcined) is different. For pural BT, when calcined at 150 °C, there are almost no acid sites (Fig. 3-11), more acid cites occurred in catalysts calcined at 350°C (Fig. 3-12).

It is illustrated by the many conflicting reports in literature that the catalytic behaviour of alumina is complex, alumina preparation and pretreatment can influence the catalysis pathways. Porous aluminas of catalytic interest exist in different forms, the *eta* and *gamma* modifications are the most common ones. *Eta*-alumina is formed by the thermal decomposition of bayerite, while *gamma*-alumina is from boehmite, it was known that both the structure and the texture such as surface area, pore size of them are of great differences.[13]

It is reported by Maciver and co-workers that the water content of *gamma*-alumina is much greater than that of *eta*-alumina, the extra water in

gamma-alumina was believed be consist of molecular water tightly adsorbed on the surface of the alumina. Thus it can be seen from the TGA curves in Fig 3-14, most of the catalyst were reaching constant slow additional water loss at higher temperature than Pural BT.

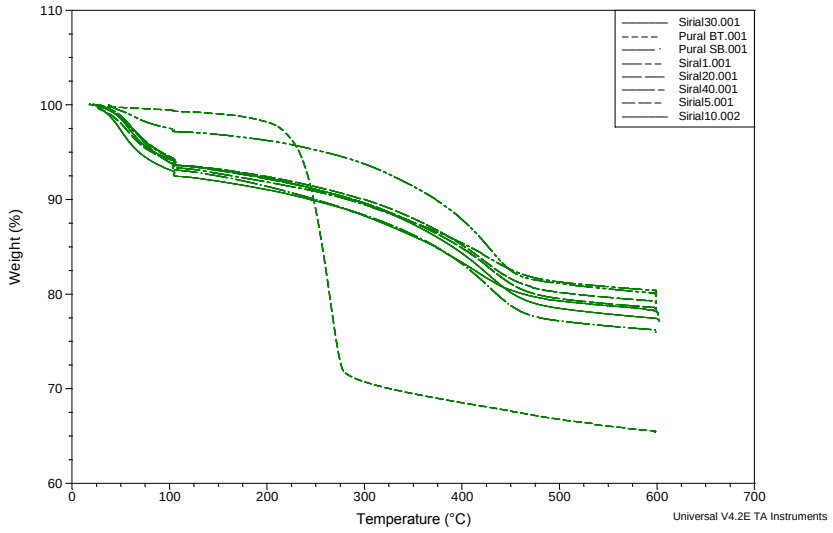

Figure 3-14 TGA for Non-calcined Siral 1-40,and pural SB, pural BT

The seperated TGA results are shown in Fig 3-15. The physically absorbed water lost is from 25°C to 100°C, and the tightly bound chemical water, i.e. loss of structural water in the main layer of the structure, is from 100°C until around 500°C, except Pural BT, which is until around 300°C.

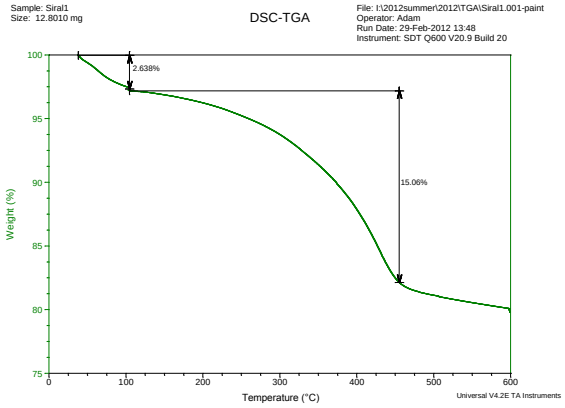
Sample: Sirial1
Size: 12.8010 mg
DSC-TGA
File: I:\2012summer\2012\TGA\Sirial1.001-paint
Operator: Adam
Run Date: 29-Feb-2012 13:48
Instrument: SDT Q600 V20.9 Build 20
2.638%
15.06%
Weight (%)
Temperature (°C)
Universal V4.2E TA Instruments

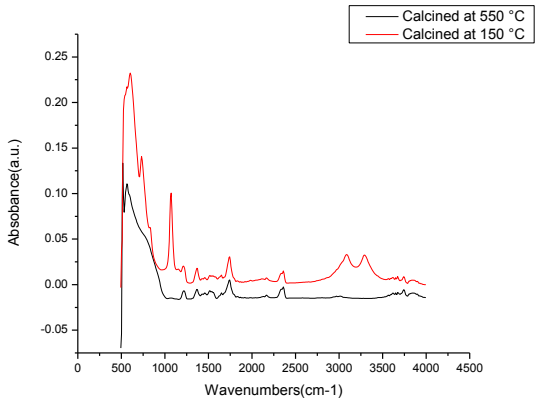
Calcined at 550 °C
Calcined at 150 °C
Absobance(a.u.)
Wavenumbers(cm-1)

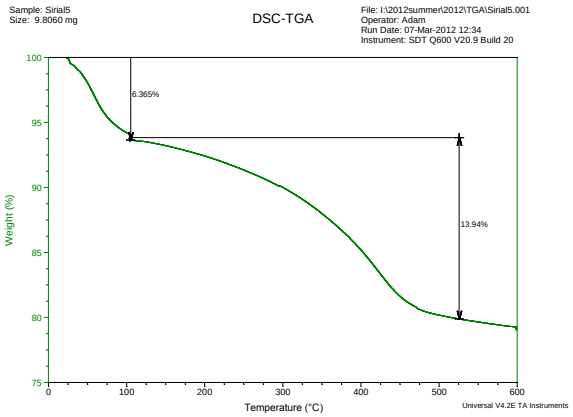
Sample: Sirial5
Size: 9.8060 mg
DSC-TGA
File: I:\2012summer\2012\TGA\Sirial5.001
Operator: Adam
Run Date: 07-Mar-2012 12:34
Instrument: SDT Q600 V20.9 Build 20
6.365%
13.94%
Weight (%)
Temperature (°C)
Universal V4.2E TA Instruments

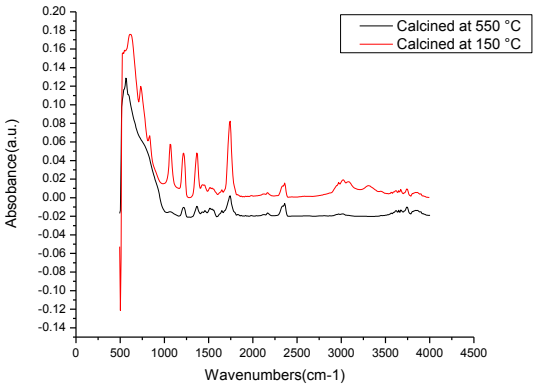
Calcined at 550 °C
Calcined at 150 °C
Absobance(a.u.)
Wavenumbers(cm-1)

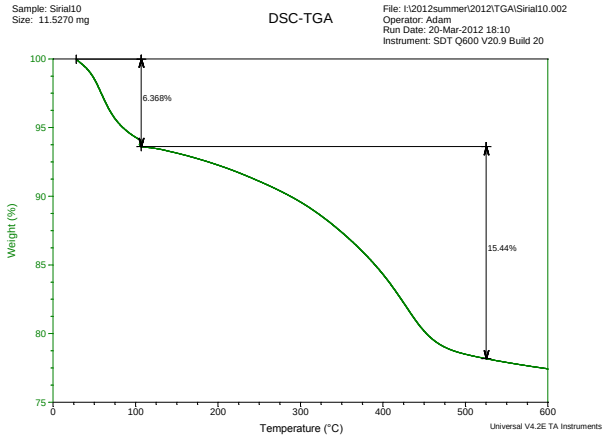
Sample: Sirial10
Size: 11.5270 mg
DSC-TGA
File: I:\2012summer\2012\TGA\Sirial10.002
Operator: Adam
Run Date: 20-Mar-2012 18:10
Instrument: SDT Q600 V20.9 Build 20
6.368%
15.44%
Weight (%)
Temperature (°C)
Universal V4.2E TA Instruments

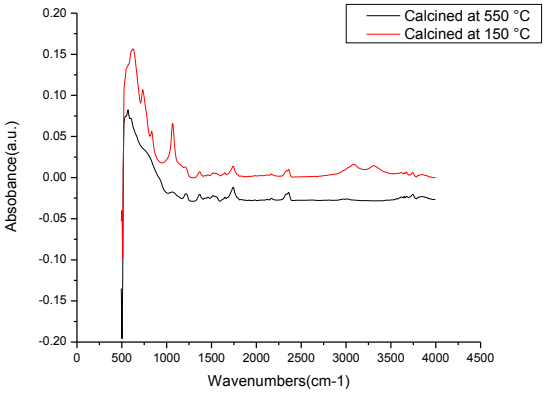
Calcined at 550 °C
Calcined at 150 °C
Absobance(a.u.)
Wavenumbers(cm-1)

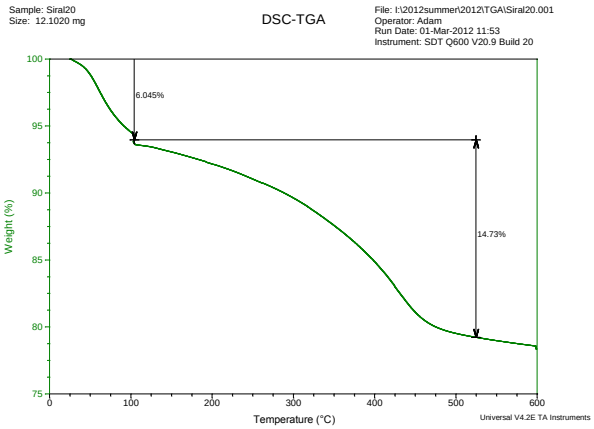
Sample: Siral20
Size: 12.1020 mg
DSC-TGA
File: I:\2012summer\2012\TGA\Siral20.001
Operator: Adam
Run Date: 01-Mar-2012 11:53
Instrument: SDT Q600 V20.9 Build 20
6.045%
14.73%
Weight (%)
Temperature (°C)
Universal V4.2E TA Instruments

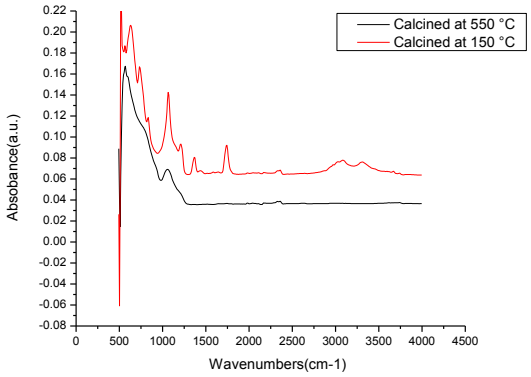
Calcined at 550 °C
Calcined at 150 °C
Absobance(a.u.)
Wavenumbers(cm-1)

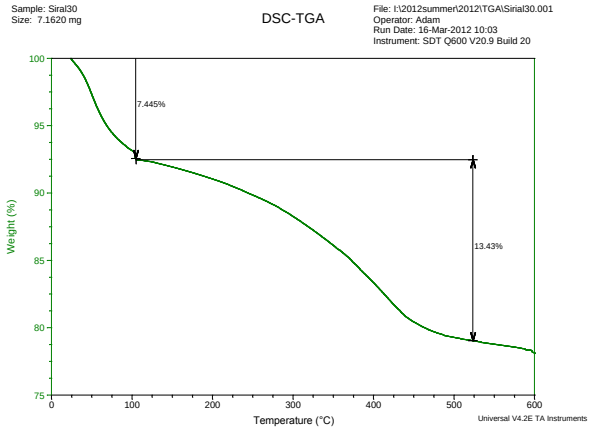
Sample: Siral30
Size: 7.1620 mg
DSC-TGA
File: I:\2012summer\2012\TGA\Sirial30.001
Operator: Adam
Run Date: 16-Mar-2012 10:03
Instrument: SDT Q600 V20.9 Build 20
7.445%
13.43%
Weight (%)
Temperature (°C)
Universal V4.2E TA Instruments

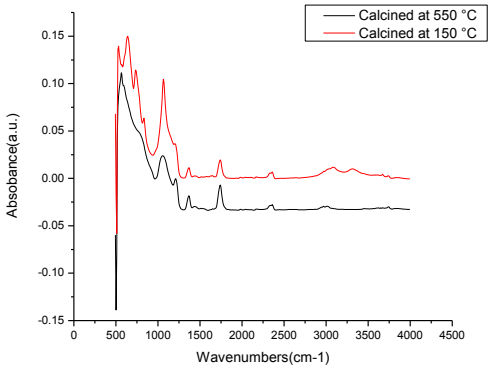
Calcined at 550 °C
Calcined at 150 °C
Absobance(a.u.)
Wavenumbers(cm-1)

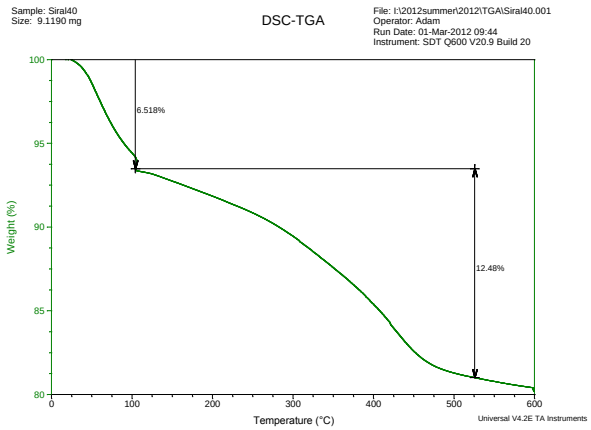
Sample: Siral40
Size: 9.1190 mg
DSC-TGA
File: I:\2012summer\2012\TGA\Siral40.001
Operator: Adam
Run Date: 01-Mar-2012 09:44
Instrument: SDT Q600 V20.9 Build 20
6.518%
12.48%
Weight (%)
Temperature (°C)
Universal V4.2E TA Instruments

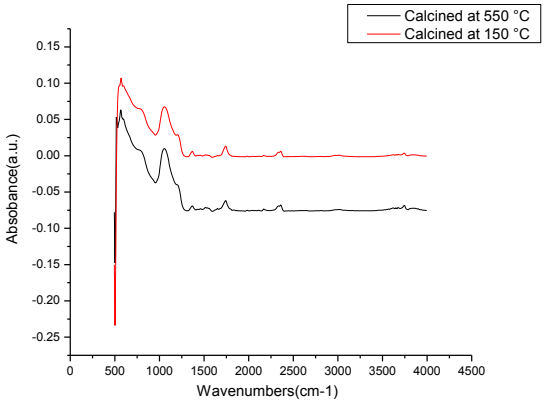
Calcined at 550 °C
Calcined at 150 °C
Absobance(a.u.)
Wavenumbers(cm-1)

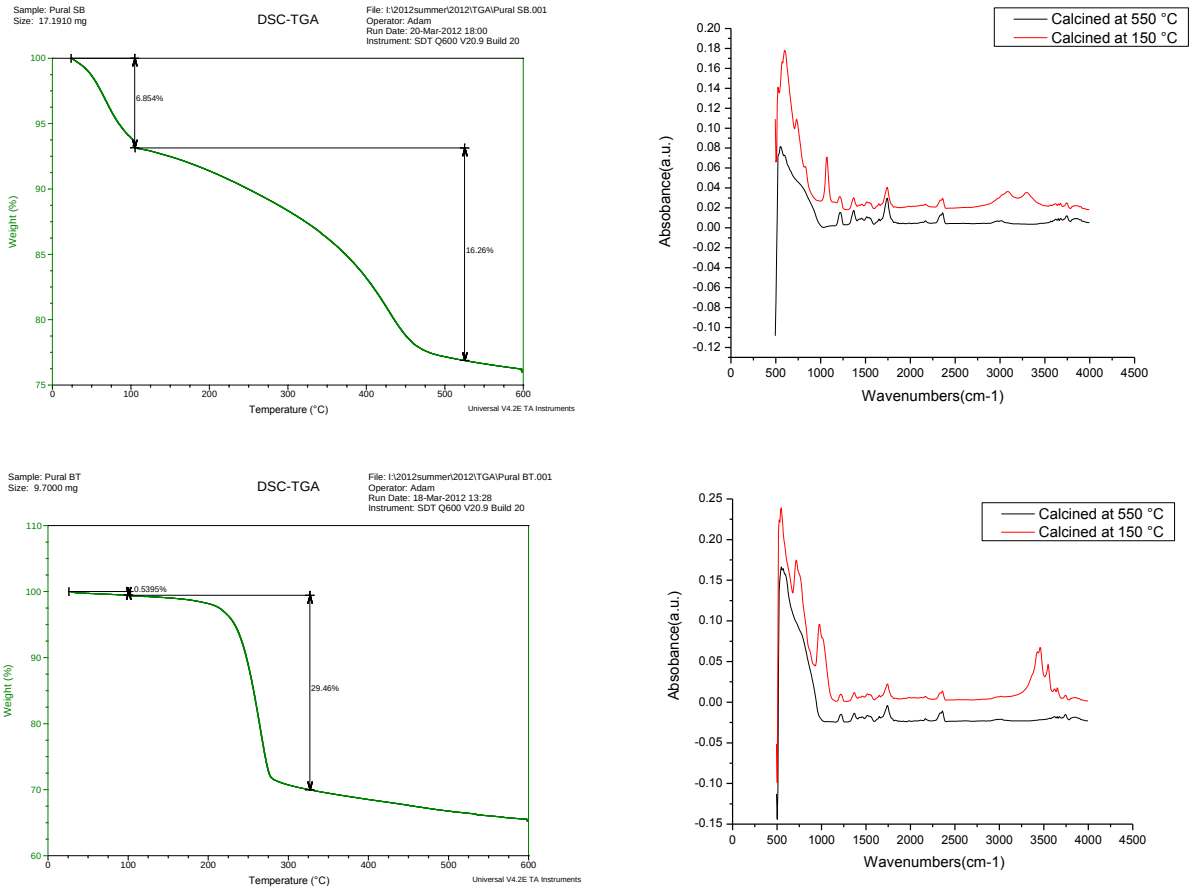

Figure 3-15 TGA for Non-calcined Siral 1-40,and pural SB, pural BT ; FTIR spectrum for the same catalysts calcined at different temperatures

In order to learn more about the connection between hydration and activity of the catalysts, we also tested the catalysts calcined at 150°C (removed physically absorbed water) and catalysts calcined at 550°C using FTIR without the presence of pyridine, the wavenumbers from around 500 to 1500 cm^{-1} are the fundamental silicon-oxygen vibrations. For samples calcined at 150°C, IR bands near 3300 and 1650 cm^{-1} were observed, in accordance with spectroscopic data on silica gel, these were attributed to the stretching and bending frequencies of

molecular water adsorbed on the alumina surface,[8] although the actual wavenumbers will vary slightly due to the effects of the rest of the molecule. From the FTIR figures we can find that compared to the uncalcined catalysts, the absorbed light in the 3600 to 3400 cm^{-1} region, which is the O-H stretching functional group disappeared in the spectra of the calcined catalysts. When comparing them with TGA results (Fig 3-15), the observations are corroborated. In TGA analyses we can see that from 500°C there are little additional mass loss of tight bound chemical water; we chose a calcination temperature in the middle of 500°C to 600°C. Thus it was decided to employ a calcination temperature of 550°C, which can decrease the influence of the water in the catalysts, and control the level of hydration at a constant value.

The nature of the catalysts are important variables, controlling catalyst activity and selectivity. This we explored in the alkylation reaction chapter.

References

1 R. L. McCormick, J. A. King, T. R. King, H. W. Haynes Jr, Influence of support on the performance of coal liquid hydrotreating catalysts, *Ind. Eng. Chem. Res.*, 1989, *28*, 940-947.

2 D. O. Leckel, Hydrodeoxygenation of heavy oils derived from low-temperature coal gasification over NiW catalysts - effect of pore structure, *Energy Fuels*, 2008, *22*, 231-236.

3 W. Daniell, U. Schubert, R. Glöckler, A. Meyer, K. Noweck and H. Knözinger, Enhanced surface acidity in mixed alumina-silicas: a low-temperature FTIR study, *Appl. Catal. A*, 2000, *196*, 247-260.

4 C. Baerlocher, W. M. Meier and D. H. Olson, *Atlas of zeolite framework types*, 5ed, Elsevier: Amsterdam, 2001, pp. 184-185.

5 A. de Klerk and R. J. J. Nel, Phenol alkylation with 1-octene on solid acid catalysts, *Ind. Eng. Chem. Res.* 2007, *46*, 7066-7072.

6 A. S.M. Junaid, M. Rahman, H. Yin, W. C. McCaffrey and S. M. Kuznicki Natural zeolites for oilsands bitumen cracking: Structure and acidity, *Microporous and Mesoporous Materials*, 2011, *144*, 148–157.

7 M. Fadoni and L. Lucarelli, Temperature programmed desorption, reduction, oxidation and flow chemisorption for the characterisation of heterogeneous catalysts. Theoretical aspects, instrumentation and applications, *Studies in Surface Science and Catalysis*, 1999, *120A*, 177–225.

8 M. L. Hair, Infrared spectroscopy in surface chemistry, Marcel Dekker: New York, 1967.

9 P. O. Scokart, F. D. Declerck, R. E. Sempels and P. G. Rouxhet, Evolution of the acidic properties of silica-alumina gels as a function of chemical composition: Infrared approach, *J. Chem. Soc. Faraday Trans. I*, 1977, *73*, 359-371.

10 M. R. Basila and T. R. Kantner, The nature of acidic sites on silica-alumina. A revaluation of the relative absorption coefficients of chemisorbed pyridine, *J. Phys. Chem.* 1966, *70*, 1681-1682.

11 A. de Klerk, Key catalyst types for the efficient refining of Fischer–Tropsch syncrude: alumina and phosphoric acid, *Catalysis*, 2011, *23*, 1–49.

12 D. S. Maciver, W. H. Wilmot and J. M. Bridges, Catalytic Aluminas II. Catalytic Properties of *Eta* and *Gamma* Alumina*, J. Catal.,* 1964, *3*, 502-511.

13 D. S. Maciver, H. H. Tobin and R. T. Barth, Catalytic Aluminas I. Surface Chemistry of *Eta* and *Gamma* Alumina, *J. Catal.*, 1963, *2*, 485-497.

Chapter 4
Aromatic alkylation temperature window explored by synthesizing and testing of alkylation compounds

4.1 Introduction

The main acid catalyzed reaction of interest in coal liquids is aromatic alkylation and there exists a limited operating window where alkylation takes place at significant rate and dealkylation is not yet significant.

The aromatic alkylation reaction is acid catalyzed (including self-catalyzed in the case of phenol), but the aromatic dealkylation reaction can be both acid catalysed and due to thermal decomposition (free radical mechanism). The upper temperature limit of the catalysis is therefore set either by thermal stability of the product, or by the acid strength of the catalyst. If it is the former, it will simplify our analysis, but if it is the latter we will have to study the effect of N-base deactivation too. Catalytic cracking in the model system can be due to the very strong acid sites that will be deactivated in a coal liquid. In such cases one would have to determine whether the upper temperature threshold is set by catalytic cracking in the presence of N-bases too, or whether it then reverts to the thermal cracking limit.

The main classes of aromatic alkylation compounds of interest to study are:

(a) C-alkylated phenols

(b) O-alkylated phenols

(c) Alkylated benzenes

From the NH_3-TPD of the catalysts, the weaker acid sites of the silica-alumina catalysts desorbed ammonia in the range 150-250°C, with peak desorption around 196-204°C (Table 4-1). In order to avoid poisoning, the operating temperature should be sufficient to allow base desorption from at least the weaker acid sites. Alkylation must therefore be conducted at higher temperature, typically >205 °C.

Table4- 1[a] Acid site concentration and acid strength distribution determined by ammonia temperature programmed desorption

Catalyst	Acid site concentration (μmol/g)				Peak NH_3 desorption temperature (°C)		
	Total	Weak	Medium	Strong	Weak	Medium	Strong
Siral 1	703	368	205	130	196	351	444
Siral 5	818	394	326	98	203	346	455
Siral 10	938	493	353	92	203	354	466
Siral 20	808	453	246	109	199	350	448
Siral 30	1127	452	489	186	200	333	461
Siral 40	820	480	170	170	201	348	413
Pural SB	719	337	124	258	197	351	414
Pural BT	810	428	86	296	204	347	413
H-ZSM-5	386	296	0	90	197	-	454

a. For convenience, the acid site characterisation data previously given in Table 3-3 is repeated here as Table 4-1.

The upper temperature threshold for each representative compound is expected to be determined without catalyst (thermal decomposition) and with each catalyst (catalytic decomposition) using high pressure DSC. The temperature range of interest is likely 250-350 °C. We are aiming to find out the upper limit temperature of the catalytic alkylation reaction.， Thus we have to synthesize the products that are the same as the model reaction products, using two basic chemistry reactions: Friedel-Crafts alkylation for alkylphenol and alkylbenzene,

and Williamson Ether Synthesis for phenol ether.

4.2 Experimental

4.2.1 Materials

The phenol (99+%), Toluene, Benzene, 1-hexene (97%), Aluminum chloride (99.9% trace metals basis), 1-Chlorohexane (99%), 1,6-Dichlorohexane, Sodium phenoxide trihydrate (99%), 1-Bromohexane (98%), Calcium Chloride (≥93.0%, anhydrous) were commercially obtained from Sigma-Aldrich and used without further purification.

4.2.2 Synthetic procedure

Friedel-Crafts (F-C) alkylation and Williamson synthesis are the two ways to synthesis aromatic alkylation compounds. Friedel-Crafts alkylation were performed in a 25 ml flask, 4.31 ml phenol and 0.4 g aluminum chloride were put in the flask first. Then 6.72ml 1-chlorohexane or 7.11ml 1,6-dichlorohexane (which was used for getting heavier alkylated compounds) was added dropwise into the flask while keeping the flask in an ice bath. Toluene alkylation and benzene alkylation were also performed using F-C alkylation methods, using 5.22ml toluene and 7ml benzene.

Williamson synthesis was conducted to prepare the phenyl ethers. Sodium phenoxide trihydrate 2.16 g and 2 ml phenol was combined in a 25ml flask kept in an ice bath. To this mixture 1-bromohexane 5.62 ml was dropwise added and allowed to stand at room temperature for 5 min (until no more

exothermic reaction occurs).

Both F-C alkylation and Williamson ether synthesis were then gently refluxed for 3 hours using a stirring bar and condenser. The product was washed with water in separating funnel, shaked and the upper organic layer was collected. The organic product was dried with 0.3 g $CaCl_2$ (anhydrous). The mixture was filtered to remove the $CaCl_2$, and the final products were obtained using rotavap distillation at 2 kPa (absolute) and the bath temperature was 70 °C.

4.2.3 Analyses

The products from lab scale alkylation experiments were analysed by GC to confirm successful synthesis of the alkylbenzene, alkyltoluene, alkylphenol and phenol ether. GC analysis was performed using an Agilent 7890 gas chromatograph with flame ionization detector (GC-FID). The peak areas from the GC-FID chromatograms were related to product mass by employing appropriate FID response factors. The parameters are showed in the Table 4-2.

Table 4-2 Gas Chromatograph Instrumental Parameters

Inlet Temperature	250°C
Inlet Pressure	45PSI
Oven Program	
Initial Temperature	40 °C
Hold Time	5 minutes
Ramp	4 °C/min up to 120 °C, then at 20 °C/min to 300 °C
Hold Time	5 minutes
Column	50 m long, 200 mm ID, film thickness of 0.5 mm HP-PONA
Carrier Gas	Helium
Carrier Flow	30ml/min

The reaction products were then analysed by Mettler Toledo STAR System HP-DSC 1 at the pressure of 8 MPa. This pressure was sufficient to suppress

endothermic volatilization during the thermal investigation. To ensure the integrity of data gathered on any analytical instrument, periodic calibrations should be performed. We used Indium (In) as calibration standard, ran through its melting point. The peak temperature and peak areas were then determined and programmed into the instrument.

The following procedure was adopted after the calibration. Certain weights (around 10 mg) of the samples were prepared in matched aluminium containers (40ul) and placed in the sample holders while the reference was placed in another holder, both of the crucibles were covered with lids, the lid has a small hole in it. The hole is required to equilibrate the test chamber pressure with the sample pressure, or in case it releases gas and blows up, because of the high internal pressure. They were put in a high pressure container, and then we increased the pressure gradually to 8MPa under N_2, and heated it up to certain temperature. The heat flow was compared to that of an empty container over a temperature range of 25°C to 500° (scan speed; 10°C/ min). And the representative products were tested using a Pike diamond attenuated total reflectance (ATR) attachment on an ABB MB3000 FTIR.

4.3 Reaction chemistry

4.3.1 Friedel-Crafts Alkylation

Friedel and Craft demonstrated that benzene would react with alkyl halides in the presence of a Lewis acid (e.g. $AlCl_3$) to produce alkyl benzenes. This reaction became known as Friedel-Crafts alkylation (Equation 4.1). [1]

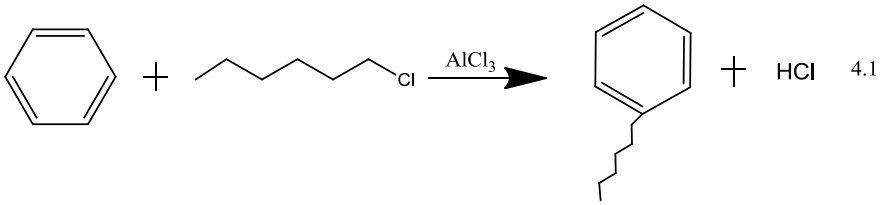

4.1

The 1-chlorohexane for example, reacts with the Lewis acid to generate the hexyl carbocation (Equation 4.2).

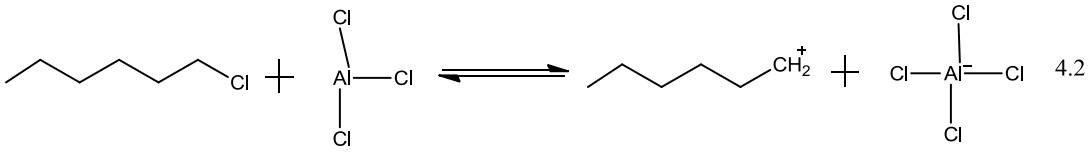

4.2

The hexyl carbocation acts as the electrophile, and forms a *sigma* complex (Equation 4.3).

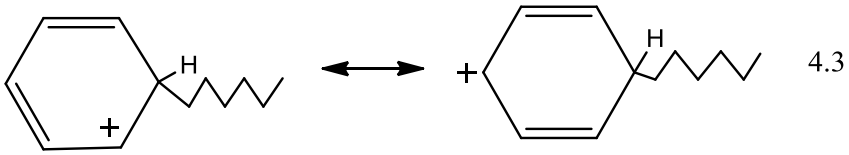

4.3

This is followed by loss of a proton, giving hexyl benzene as the product. The Lewis acid catalyst is regenerated in the last step. Friedal-Crafts reactions work with a variety of alkyl halides, and so is a very versatile reaction.

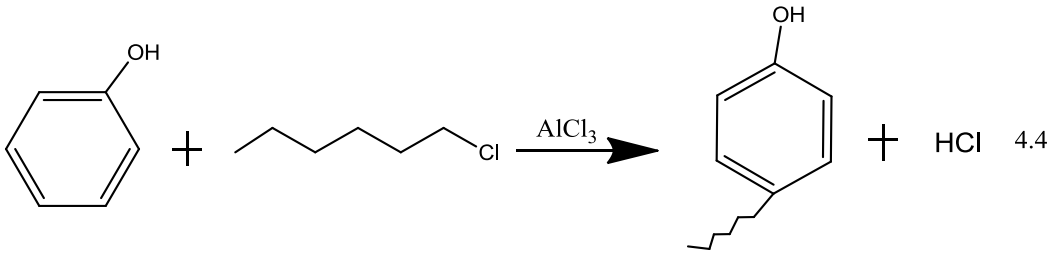

4.4

Friedel-Crafts alkylation is one of the most common methods for the alkylation of phenols. Phenol (so are benzene and toluene) can be alkylated by alkyl halides (Equation 4.4), also by alkenes.

The specific procedure employed by us in the batch and flow reactor studies (Chapters 5 and 6) used an alkene as the alkylating agent in the presence of an acid catalyst. The reaction steps are shown in Equation 4.6. The alkene and catalyst interact to form a carbocation and counter ion (1), which interacts with phenol to form a *pi*-complex (2). This complex is combined by the overlap of the filled *pi*-orbital of the aromatic ring with the empty orbital of the carbocation.[2] The *pi*-complex can rearrange to the *sigma*-complex (3). Loss of R_1 (the alkyl group) from complex (3) results in no reaction, while loss of H^+ results in the alkylation of phenol. The driving force for the formation of (2) can be viewed as the result of electrostatic interaction, an electron deficient species being attracted to an electron rich species.[3]

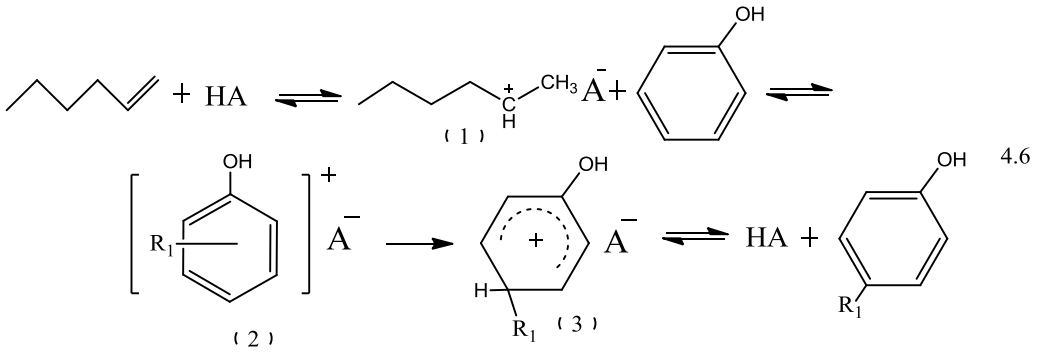

4.6

During the alkylation, side reactions, such as dimerization, oligomerization and cracking may occur. Typically, alkene–alkene reactions compete with phenol–alkene reactions at the synthesis conditions.

4.3.2 Williamson Ether Synthesis

There are many different ways to synthesize ethers. Williamson ether synthesis is the easiest and perhaps the fastest way to create ether products. In a related reaction, alkyl halides undergo nucleophilic displacement by phenoxides. The alkyl halide cannot be used to react with the alcohol directly. However, phenoxides can be used to replace the alcohol, while maintaining the alkyl halide. Since phenols are weakly acidic, they readily react with a strong base like sodium hydroxide to form phenoxide ions (Equation 4.7). The phenoxide ion will then substitute the -X group in the alkyl halide, forming the ether with an aryl group attached to it in a reaction with an S_N2 (Nucleophilic Substitution) mechanism (Equation 4.8).

$$C_6H_5OH + OH^- \rightarrow C_6H_5\text{-}O^- + H_2O \qquad 4.7$$

$$C_6H_5\text{-}O^- + R\text{-}X \rightarrow C_6H_5OR + X^- \qquad 4.8$$

4.4 Results and Discussions

We use GC for analyzing the products of the synthesis (Fig III-1). Some of the main products properties are listed in Appendix III. From the chromatograms

we can figure out the following:

a) We performed the GC analysis of the synthesized compounds at the same conditions and oven program as analyzing the samples from the batch reactor study (Chapter 5). So, we use the synthesizing results to compare with of GC retention times of unknown batch reactor products. We also compared the product identification results from GC-MS when doing batch reactor alkylation reactions (Figure 5-3); the retention times of the main products, alkylphenols are similar. From 27 to 33 min are the mono-alkylated phenols, longer retention time shows the multi-alkylated phenol products. For the alkylbenzenes, similar retention times were also found.

b) The reaction times during synthesis were not long enough. The conversions were not totally completed and thus we still had reactants in the mixtures. We used rotovap for the separation, using different temperatures and pressures depending on the boiling point of reactants, trying to remove the reactants from the products. Most of the reactants were removed, but we still observed some reactants in the chromatograms, especially 1,6-dichlorohexane.

We used high pressure DSC trying to investigate the upper temperature limit set by thermal decomposition of the representative compounds. If the normal boiling point is reached before decomposition, the product will evaporate and it was therefore not possible to employ conventional DSC. The situation can

be improved by suppressing evaporation using HP-DSC at elevated pressure.

The thermal decomposition temperatures from HP-DSC are shown in Table 4-3.[4,5] The reaction to form alkylphenols and alkylbenzenes are exothermic and decomposition should be endothermic. There are more than one peak in some of the figures (Figure III-2), these may due to the impurities in the products, and also 'analytic artifacts' due to inadequate pressure stability. Any non-steady state gas movement is detected as an energy change, thereby creating an 'analytical artifact'.

Table 4-3 Onset of Decomposition Temperatures of the Alkylation Products by HP-DSC

Alkylation products	Phenol ether	Alkylphenol	Alkylbenzene (1-chlorohexane)
Temperature(°C)	200	200	150
Alkylation products	Alkylbenzene (1,6-Dichlorohexane)	Alkyltoluene (1-chlorohexane)	Alkyltoluene (1,6-Dichlorohexane)
Temperature(°C)	160	390	360

We performed DSC of alkylbenzene (benzene reacted with 1,6-dichlorohexane) with catalysts as well (Fig III-3), aiming to get a better idea of catalytic decomposition. The onset of decomposition temperature of the samples with catalysts inside increased compared to samples without catalysts. As the silica ratio increased, an increase in the onset of decomposition can be observed.

We also performed the DSC in a reversible way (Fig III-4), that is, we heated up to certain temperatures (260 °C, 330°C) and then cooled down then heated up (330°C) again, in order to learn about the thermal history effects of the samples and to identify reversible phase changes. Calorigrams give changes in

energy and using the DSC in this way helped to interpret the calorigrams.

To better understand the nature of the products and how the products were affected by temperature, we used FTIR to identify the chemical bonds of the products and also in the samples after treatment by HP-DSC. We use phenol ether as the illustrative sample to explain the process that was followed for all the samples.

The FTIR spectrum of the phenol ether, which we synthesized, was compared with the phenol ether treated at 260 °C and 330 °C in the HP-DSC (Figure 4- 1).

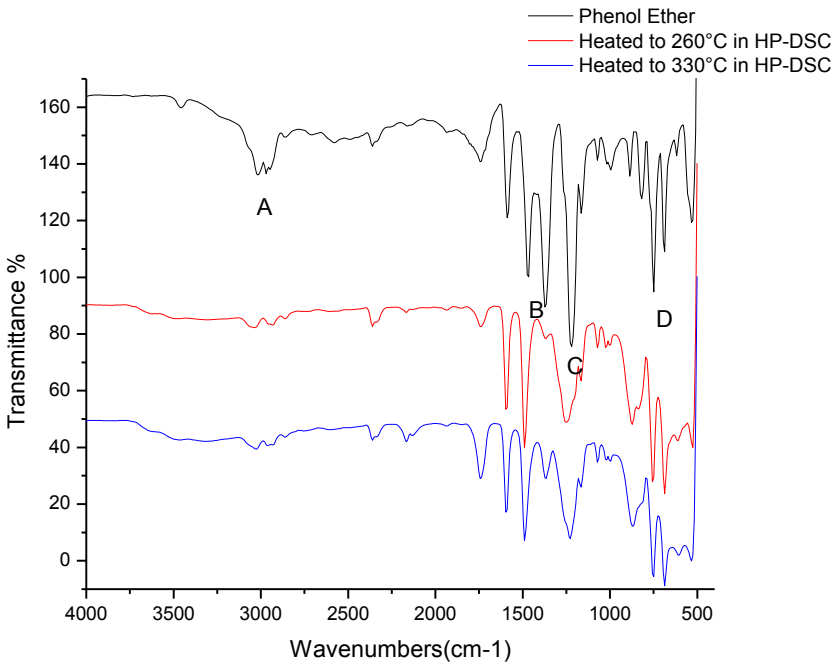

Figure 4- 1 FTIR Spectra of Phenol Ether Products

In the FTIR spectrum of hexyl phenol ether (Figure 4-1), the peaks we can identify are given. A, should be the aromatic and aliphatic C-H stretch, 3000,

2950 cm^{-1}. Peaks in the B area, 1600, 1500, 1450 cm^{-1}, are the ring C=C stretch. C, is the special asymmetric C-O-C stretch at 1250 cm^{-1}, which means that hexyl phenol ether was successfully produced by our synthesis. D shows the out-of-plane C-H bend, 780, 754 cm^{-1}, also out-of-plane ring C=C bend, 692 cm^{-1}.[6] Compared with the high pressure DSC treated phenol ether, the peak 1250cm^{-1} relative to peak 1500cm^{-1} in the spectrum of original phenyl ethers is more prominent.

Aromatic ether absorb around 1250 and 1040 cm^{-1}, both of the peaks can be apparently observed in all of the IR spectra. This suggests that phenyl ethers were present in the compounds at all temperatures. However, the relative changes in the adsorption just above 1250 cm^{-1} and just below 1250 cm^{-1}(sample heated to 260°C) suggest that we still have some free phenol in the original sample, which became less as we heated to 260°C, and then at 330°C some decomposition started occurring, releasing phenol again. Thus in the batch reactor, we could operate at above 260°C, since no thermal decomposition will occur.

But the decomposition temperatures of the synthesis products determined by HP-DSC were not clear, both alkylation and decomposition reactions complicated interpretation. It was therefore decided that it is better to run the reaction with catalysts at different temperatures in the batch reactor, and use Chapter 4's results only as a point of reference to find the best temperature to perform the alkylation reaction.

References:

1. L. G. Wade, Jr., *Reactions of Aromatic Compounds,* Organic Chemistry, 5th Edition, Prentice-Hall, Upper Saddle River, NJ, 2003.
2. J. March, *Advanced Organic Chemistry Reactions, Mechanisms, and Structure*, 3rd., John Wiley & Sons, Inc., New York, 1985, p. 448.
3. J. F. Lorenc, G. Lambeth, W. Scheffer, Alkylphenols, *Kirk-Othmer Encyclopedia of Chemical Technology, 4th ed. (John Wiley and Sons, New York*), Volume 2, 113-143 (1992).
4. J. Coret and A. Chamel, Effect of some ethoxylated alkylphenols and ethoxylated alcohols on the transfer of [^{14}C] chlorotoluron across isolated plant cuticles, *Weed Research*, 1994, Volume 34,445-451
5. E. W. Kendall, B. R. Trethewey, Jr., Thermal Analysis of the Polymerization of Phenol Formaldehyde Resins*, Wilsonart International, Inc.*
6. R. M. Silverstein, F. X. Webster, Spectrometric identification of organic compounds 6th ed., *John Wiley & Sons, Inc.* 1998, 91-111.

Chapter 5 Batch reactor catalytic alkylation of Phenol and 1-hexene

When we characterized the catalysts (Chapter 3), we needed to identify some catalysts with mild acidity. The temperature chosen for our alkylation reaction needed to be in within the operating temperature window for aromatic alkylation (Chapter 4). We knew that a higher temperature would be better for thermal desorption of nitrogen bases and that it should likely be within the base desorption temperature range of medium strength acid sites. Thus, we operated the alkylation reaction at several temperatures ranging from 220, 250, 315 to 350 °C, in order to pick out a suitable temperature for the reaction.

When we tried toluene alkylation at 350°C and acid catalyzed cracking occurred, resulting in an increase in lighter than C_6 alkenes and corresponding phenol alkylation products (Appendix IV GC results). This was not a problem at 315 °C, which was selected as our preferred alkylation temperature for the investigation.

To demonstrate that the acid catalysed alkylation of aromatics can be performed in the presence of nitrogen bases, we performed experiments with phenol and 1-hexene and then added some pyridine to the mixture. The contribution of autocatalysed phenol alkylation to overall conversion was also determined.

5.1 Experimental

5.1.1 Materials

The phenol (99+%), 1-hexene (97%) and pyridine (99+%) were commercially obtained from Sigma-Aldrich and used without further purification. The alumina and amorphous silica-alumina catalyst types were the same as characterized in Chapter 3, which were commercially obtained from Sasol, Germany (former Condea GmbH).

5.1.2 Experiment and procedure

The conversion of phenol and 1-hexene, without and with the addition of pyridine, were investigated using batch reactors. All experiments were repeated at least once to confirm the results.

The batch reactor experiments employed 15ml stainless steel microreactors. For each experiment, the reactor was loaded with 5.2 g phenol, 4.3 g 1-hexene and 0.5 g catalyst. The molar ratio of phenol to 1-hexene is 1:1, and the mass ratio of feed to catalyst was 19:1. The reactor was put in a constant temperature fluidized sand bath for one hour, i.e. equivalent to performing flow reactor experiments at a weight hourly space velocity (WHSV) of 19 h^{-1}. Reactions were performed at temperatures of 220, 250, 315, and 350 °C under autogenous pressure. The autocatalysed conversion of phenol and 1-hexene was also investigated by experiments containing only the reaction mixture, but without a catalyst. This was necessary to determine the contribution of self-catalyzed (autocatalytic) alkylation of phenol.

The effect of pyridine on catalyst performance was determined by pretreating the catalysts with pyridine, as well as pretreating the catalysts with pyridine and adding 0.05 % pyridine (6 mg) to the reaction mixture.

5.1.3 Analyses

The reaction products from the batch reactor experiments were identified using an Agilent 7890 GC with 5975C mass selective detector (GC-MS). The products were quantified by analysis with an Agilent 7890 gas chromatograph with flame ionization detector (GC-FID). The peak areas from the GC-FID chromatograms were related to product mass by employing appropriate FID response factors. A 50 m long, 200 mm ID, film thickness of 0.5 mm HP-PONA column was employed for product separation. The temperature program started at 40 °C, with a hold of time of 5 minutes, whereafter the temperature was increased by 4 °C/min up to 120 °C, and then at 20 °C/min to 300 °C and holding for 5 minutes.

5.1.4 Calculations

In order to propose the optimal catalyst for aromatic alkylation, conversion and catalytic selectivity should be calculated and compared. In the batch reactor experiments, conversion and selectivity are reported on a mass basis, as FID detector is a mass-sensitive analyzer that responds to the number of carbon atoms entering per unit of time. And the calculation is as follows:

$$\text{Conversion} = (A_f - A_r)/A_f \times 100\%$$

A_f stands for total GC area of phenol in the feed, A_r stands for the GC area

for phenol after reation.

Selectivity to product i is S_i, can be determined as,

$$S_i = A_i / A_t \times 100\%$$

Product i's area is A_i, A_t is the sum of all the products areas. Some bias was introduced, because the area derived composition was not corrected with FID response factors for each compound.

5.2 Result and discussions

5.2.1 Non-catalytic phenol alkylation

Blank runs without catalyst were performed to determine whether the reactor or phenol aided conversion in any way.

Phenol is a weak acid ($K_a = 1 \times 10^{-10}$) and some double bond isomerisation was anticipated in the blank runs. This was indeed found and in the absence of a catalyst 1-hexene double bond isomerisation took place.

Of more interest was the autocatalysed alkylation of phenol. It was reported that phenol is capable of alkylation with various alkenes even in the absence of a catalyst,[1] this was indeed found. It was established that there is a baseline non-catalytic conversion of phenol both in the absence and in the presence of added pyridine (Table 5-1).

Table 5- 1 Phenol alkylation with 1-hexene in the absence of a catalyst for 1 hour in the temperature range 220-315 °C and at autogenous pressure

Temperature (°C)	Phenol conversion (wt %)	
	without pyridine	with pyridine
220	0.5	0.1
250	1.3	0.3
315	3.4	1.7
350	6.5	3.7

Pertinent observations from literature and from our experimental work are:

(a) Phenol alkylation is apparently not catalysed by stainless steel, with little difference in phenol alkylation observed when conducted in either 304 stainless steel or in glass lined vessels.[1]

(b) Reaction temperature plays a role (Table 5- 1) , but as the temperature is increased there is an equilibrium limitation on the autocatalysed conversion. The reversibility of the reaction was established at 330 °C where dealkylation of alkylphenol was observed.[1]

(c) The rate of conversion is strongly dependent on the phenol concentration, with a second to sixth order dependence on phenol.[1, 2] There was a very strong dilution effect, with pentane dilution drastically reducing the alkylation rate.[1] A proportional decrease in phenol alkylation rate was also reported with dioxane dilution.[2] The reported strong influence of phenol concentration on uncatalyzed phenol conversion was not observed in our work.

(d) Phenol could be alkylated by linear and branched alkenes. The rate and conversion was determined mainly by steric factors. About 50 % phenol conversion was observed during autocatalysed phenol alkylation with ethene at 330 °C for 3 hours.[1]

(e) Autocatalysed phenol alkylation has a high selectivity for the *ortho*-C-alkylated product.[1,4]

(f) There is spectroscopic evidence for the hydrogen bonding of alkenes to phenol. In the presence of alkenes the 3610 cm^{-1} infrared absorption of the unbonded phenol O–H decreases with an increase in the bonded phenol O–H infrared absorption at 3550-3510 cm^{-1}; the wavenumber decreases with increasing basicity of the alkene.[5]

These results and observations are consistent with a six-membered ring as transition state that is assisted (stabilised) by additional phenol molecules in the mixture (Figure 5-1).

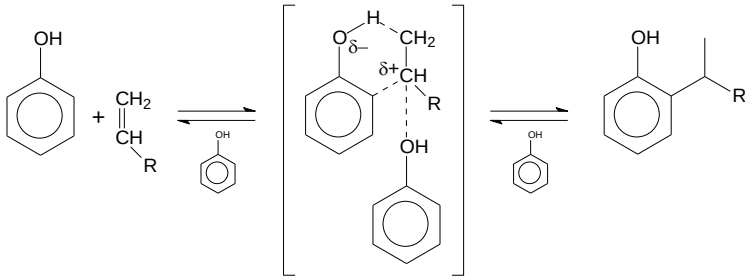

Figure5- 1 Transition state for autocatalysed phenol alkylation by 1-hexene

When pyridine is added to the phenol containing solution, the acid-base reaction between pyridine and phenol will convert a fraction of the phenol to the

corresponding acid-base pair. In poorly solvating solutions this can lead to clustering of phenol-pyridine acid-base pairs,[6] but such behaviour was not anticipated in our work. The addition of 0.05% pyridine reduced autocatalysed phenol alkylation and the conversion was significantly higher for the solution without pyridine than the solution with pyridine added (Table 5-1).

5.2.2 Catalytic phenol alkylation

The temperature range within which phenol alkylation takes place at a reasonable rate was established by performing experiments in the temperature range 220-350 °C. At 350 °C acid catalysed cracking became significant, resulting in an increase in lighter than C_6 alkenes and corresponding phenol alkylation products. In order to avoid the complication presented by cracking, it was decided to conduct the evaluation at 315 °C.

Phenol alkylation with 1-hexene without and with pyridine was conducted over Siral 5-40 catalysts (Table 5-2). In the first series of experiments the baseline conversion was established with clan catalysts and just phenol and 1-hexene in the feed. In the second series of experiments the catalysts were exposed to pyridine beforehand, but the feed mixture contained only phenol and 1-hexene. The third series of experiments exposed the catalysts pyridine beforehand in addition to including pyridine in the feed mixture.

Table5- 2 Phenol alkylation with 1-hexene, with and without pyridine over Siral 5-40 catalysts at 315 °C, autogenous pressure and an equivalent WHSV of 19 h^{-1}

Description	Phenol conversion (wt %)				
	Siral 5	Siral 10	Siral 20	Siral 30	Siral 40
Clean catalyst, clean feed	13	17	31	24	26
Pyridine treated catalyst, clean feed	11	11	10	16	5
Pyridine treated catalyst and pyridine in feed	10	9	10	12	3

The contribution of autocatalytic phenol conversion complicates the analysis of the catalytic contribution to overall phenol. However, some general observations can be made:

(a) Baseline phenol conversion (clean catalyst and clean feed) resulted in no obvious correlation with physical or acidic catalyst properties. The most active catalyst was Siral20, which was unexpected from the catalyst characterisation that was performed. If Siral20 result is disregarded, the conversion over the other catalysts correlated best with strong Brønsted acidity. This does not imply that other acid site types do not contribute to phenol conversion, only that with a clean feed the dominant alkylation pathway is by strong Brønsted acid catalysed alkylation.

(b) When the catalysts are exposed to pyridine, the strong acid sites are poisoned. As anticipated, conversion of a clean feed over pyridine treated catalysts depends mainly on medium strength acid sites. A better correlation was found between phenol conversion and the total concentration of medium acid sites than for either Lewis or Brønsted acid sites individually. Although the contribution of weak acid sites cannot be ruled out, the precipitous drop in

conversion over Siral 40 in the presence of pyridine suggests that the contribution of weak acid sites is likely to be small.

(c) The additional inhibiting effect of adding pyridine to the feed indicated that the adsorption and desorption of pyridine is sensitive to the concentration in the bulk medium. It also indicated that within the broad classification of acid strength there is a sub-structure. For example, the conversion over Siral 5-20 was much less affected in relative terms than that over Siral 30-40. This reflects the stronger acidity of Siral 30 and 40 reported before,[7] i.e. pyridine related inhibition is stronger.

(d) One aspect that was not investigated, but pointed out by Dr. S. Bergens, is the possibility that phenol may interact with Lewis acid sites to create additional Brønsted acidity.

5.2.3 Product selectivity

Identification of specific alkylphenol isomers was complicated by hexene isomerisation, which increased the number of isomers present in the product. Nevertheless, it was possible to identify the main product classes based on the electron impact mass spectra of the products.

In a previous study on phenol alkylation with 1-octene on solid acid catalysts, the alkylation of phenol by olefins over solid acid catalysts results in the formation of both O-alkylated and C-alkylated products.[8]

The mass spectra of O-alkylated phenols (phenyl ethers), *ortho*-C-alkylated phenols and *meta*-/*para*-C-alkylated phenols are quite distinct. The O-

alkylated phenols have a distinctive ion at 94 m/z.[9] The fragmentation of the C-alkylated phenols depends on the alkylation position, with *ortho*-C-alkylated phenols having a distinctive ion at 107 m/z, while *meta*-/*para*-C-alkylated phenols have a distinctive ion at 121 m/z.[10] It is therefore possible to use mass spectrometry to distinguish between most of the isomers, but not between the *meta*- and *para*-C-alkylated phenols. The electron impact fragmentation of the O-alkylated phenols, *ortho*-C-alkylated phenols and *meta*/*para*-C-alkylated phenols are different (Figure 5- 2).[11]

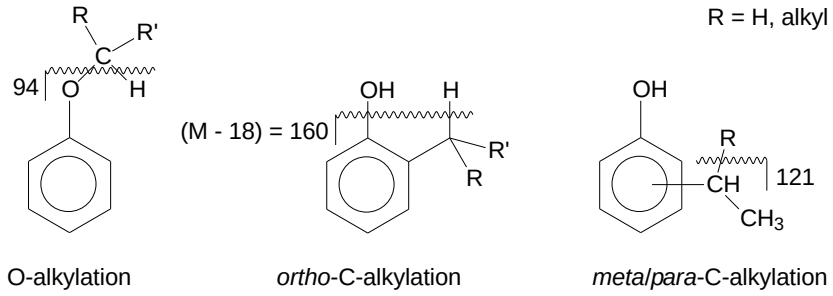

Figure5- 2 Electron impact fragmentation of different phenol isomers

The chromatograms obtained by phenol alkylation were overlaid (Figure 5-3). The O-alkylated phenols had a shorter residence time. Isomerisation to form *ortho*-, *meta*- and *para*-substituated C-alkylated phenols readily occurs (even in the absence of a catalyst).[12] It was not possible to distinguish between the *meta*- and *para*-isomers. The *ortho*-isomers were the most abundant isomers. The retention times of the various alkyl phenols are listed in Table 5-3.

The presence of pyridine caused a meaningful change in the product selectivity obtained during catalytic phenol alkylation (Table 5-4). Most

noticeable was suppression of multiple alkylation and decrease in *meta*/*para*-C-alkylation selectivity when pyridine was added.

The selectivity data was not collected at constant conversion and a direct comparison is not possible. It was reported that the initial product selectivity during phenol alkylation with 1-octene at 200 °C over Siral 5-40 catalysts was exclusively to produce O-alkylated and *meta*/*para*-C-alkylated products.[13] As conversion increased the *ortho*-C-alkylation selectivity increased mostly at the expense of O-alkylation selectivity. The present study was conducted at higher temperature (315 vs 200 °C) and the results suggest that there is an increase in *meta*/*para*-C-alkylation at the expense of *ortho*-C-alkylation selectivity with increase in phenol conversion. The observed selectivity change is therefore likely due to the change in conversion rather than a change in the inherent selectivity of the catalysts in the presence of pyridine.

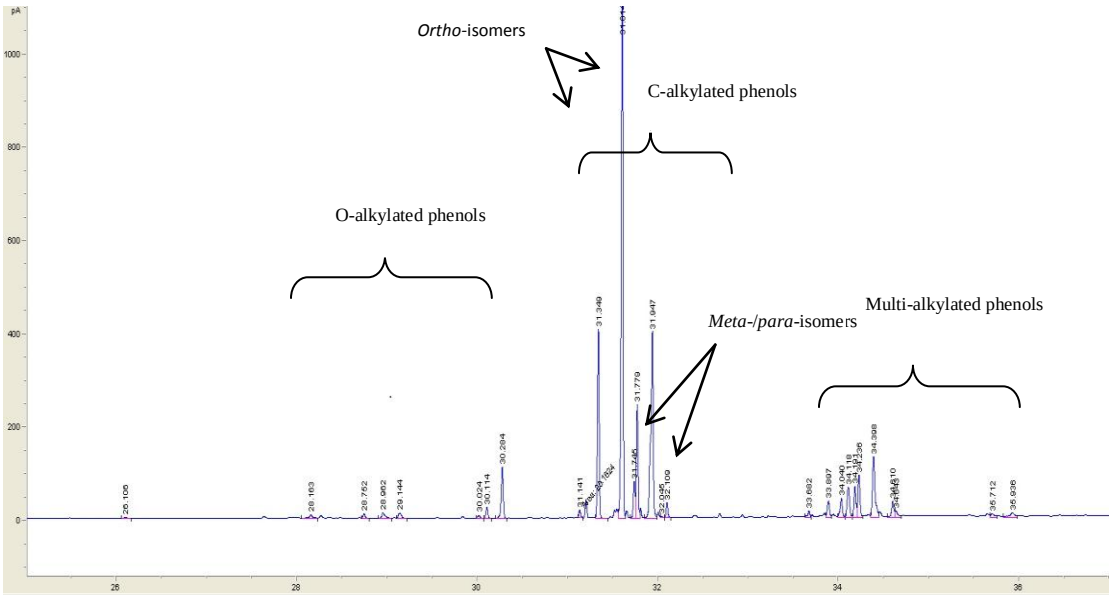

Figure5- 3 Chromatograms showing the alkylated products from phenol alkylation with 1-hexene on siral 30

Table5- 3 Separation of the products from the acid catalysed alkylation of phenol with 1-hexene by siral30

Retention time(min)	Area	Assignment
28.163	17	O-alkylation (phenyl ether)
28.752	14.5	O-alkylation (phenyl ether)
28.962	27.5	O-alkylation (phenyl ether)
29.144	25.3	O-alkylation (phenyl ether)
30.114	33.2	O-alkylation (phenyl ether)
30.284	171.7	O-alkylation (phenyl ether)
31.141	20.2	*ortho*-C-alkylation (o-hexylphenol)
31.349	526.3	*ortho*-C-alkylation (o-hexylphenol)
31.614	1735.9	*ortho*-C-alkylation (o-hexylphenol)
31.745	100.8	*meta*/*para*-C-alkylation (m/p-hexylphenol)
31.779	330.7	*meta*/*para*-C-alkylation (m/p-hexylphenol)
31.947	735.1	*ortho*-C-alkylation (o-hexylphenol)
32.045	5.5	*meta*/*para*-C-alkylation (m/p-hexylphenol)
32.109	42.9	*meta*/*para*-C-alkylation (m/p-hexylphenol)
33.682	26.3	Multi-alkylated phenols
33.897	62.7	Multi-alkylated phenols
34.040	73.4	Multi-alkylated phenols
34.118	123.8	Multi-alkylated phenols
34.191	103.7	Multi-alkylated phenols
34.236	144.1	Multi-alkylated phenols
34.396	263.4	Multi-alkylated phenols
34.610	63.2	Multi-alkylated phenols

Table 5- 4 Product selectivity and conversion during phenol alkylation with 1-hexene, with and without pyridine over Siral 5-40 catalysts at 315 °C, autogenous pressure and an equivalent WHSV of 19 h^{-1}

Description	Selectivity to different alkylphenol species (wt %)					
	No catalyst	Siral 5	Siral 10	Siral 20	Siral 30	Siral 40
Clean catalyst, clean feed						
Conversion	3	13	17	31	24	26
O-alkylation	4	3	5	4	4	6
ortho-C-alkylation	86	75	75	45	45	49
meta/*para*-C-alkylation	8	9	7	32	26	42
multiple alkylation	2	13	13	18	25	2
Pyridine treated catalyst, clean feed						
Conversion	-	11	11	10	16	5
O-alkylation	-	5	4	3	6	4
ortho-C-alkylation	-	85	83	71	79	80
meta/*para*-C-alkylation	-	4	6	14	8	10
multiple alkylation	-	6	6	13	8	7
Pyridine treated catalyst and pyridine in feed						
Conversion	2	10	9	10	12	3
O-alkylation	11	8	10	4	5	5
ortho-C-alkylation	85	81	80	79	80	82
meta/*para*-C-alkylation	1	4	6	8	8	9
multiple alkylation	3	7	4	9	6	3

Although other studies can be cited that obtained high *ortho*-C-alkylation selectivity over silica-alumina catalysts,[14-16] there are also studies reporting high *para*-C-selectivity. No clear and consistent explanation could be found in literature and the alkylation selectivity seems to be influenced by the extent of conversion, operating conditions and catalyst properties, i.e. just about everything. Our work highlighted no specific relationship between selectivity and acid strength or alumina content of the catalyst beyond that which is caused by a change in conversion.

Table 5- 5 Product selectivity and conversion calculated on catalyst surface area basis during phenol alkylation with 1-hexene, with and without pyridine over Siral 5-40 catalysts at 315 °C, autogenous pressure and an equivalent WHSV of 19 h^{-1}

Description	Selectivity to different alkylphenol species/surface area (wt%/m2/g)				
	Siral 5	Siral 10	Siral 20	Siral 30	Siral 40
Clean catalyst, clean feed					
Conversion	0.06	0.09	0.15	0.12	0.10
O-alkylation	0.01	0.03	0.02	0.02	0.02
ortho-C-alkylation	0.36	0.38	0.22	0.23	0.19
meta/*para*-C-alkylation	0.04	0.04	0.16	0.13	0.16
multiple alkylation	0.06	0.07	0.09	0.13	0.01
Pyridine treated catalyst, clean feed					
Conversion	0.05	0.06	0.05	0.08	0.02
O-alkylation	0.02	0.02	0.01	0.03	0.02
ortho-C-alkylation	0.41	0.42	0.35	0.40	0.30
meta/*para*-C-alkylation	0.02	0.03	0.07	0.04	0.04
multiple alkylation	0.03	0.03	0.06	0.04	0.03
Pyridine treated catalyst and pyridine in feed					
Conversion	0.05	0.05	0.05	0.06	0.01
O-alkylation	0.04	0.05	0.02	0.03	0.02
ortho-C-alkylation	0.39	0.40	0.39	0.40	0.31
meta/*para*-C-alkylation	0.02	0.03	0.04	0.04	0.03
multiple alkylation	0.03	0.02	0.04	0.03	0.01

Table 5- 6 Product selectivity and conversion calculated based on catalyst acid site concentration during phenol alkylation with 1-hexene, with and without pyridine over Siral 5-40 catalysts at 315 °C, autogenous pressure and an equivalent WHSV of 19 h^{-1}

Description	Selectivity to different alkylphenol species/acid sites (wt%/µmol/g)				
	Siral 5	Siral 10	Siral 20	Siral 30	Siral 40
Clean catalyst, clean feed					
Conversion	0.016	0.018	0.038	0.021	0.032
O-alkylation	0.004	0.005	0.005	0.004	0.007
ortho-C-alkylation	0.092	0.080	0.056	0.040	0.060
meta/*para*-C-alkylation	0.011	0.007	0.040	0.023	0.051
multiple alkylation	0.016	0.014	0.022	0.022	0.002
Pyridine treated catalyst, clean feed					
Conversion	0.013	0.012	0.012	0.014	0.006
O-alkylation	0.006	0.004	0.004	0.005	0.005

ortho-C-alkylation	0.104	0.088	0.088	0.070	0.098
meta/*para*-C-alkylation	0.005	0.006	0.017	0.007	0.012
multiple alkylation	0.007	0.006	0.016	0.007	0.009
Pyridine treated catalyst and pyridine in feed					
Conversion	0.012	0.010	0.012	0.011	0.004
O-alkylation	0.010	0.011	0.005	0.004	0.006
ortho-C-alkylation	0.099	0.085	0.098	0.071	0.100
meta/*para*-C-alkylation	0.005	0.006	0.010	0.007	0.011
multiple alkylation	0.009	0.004	0.011	0.005	0.004

To better understand the relationship of conversion and selectivity of the reaction with catalysts, we also normalized our conversion and selectivity results with catalysts characterization results, such as surface area and total acidity. Through the data in Table 5-5 and Table 5-6, we found that the conversion per surface area and acid cites remain similar as the conversion without normalization, so were the selectivity.

Literature suggests that either an increase in conversion, or an increase in temperature, results in an increase in *ortho*-C-alkylation.[14,15,17] An increase in *ortho*-C-alkylation selectivity was reported for the conversion of phenol with 1-octene over H-Beta (BEA) zeolite at 100 °C as the conversion of phenol increased.[17] It was also found that *ortho*-C-alkylation selectivity over BEA increased as the temperature was increased from 100 to 200 °C.[17]

Based purely on conversion, the observed increase in *ortho*-C-alkylation selectivity when pyridine was added could not be explained. It is not just a conversion-related effect. It is more likely due to the conversion and the nature of the acid sites involved in alkylation. Poisoning of BEA by potassium exchange

resulted in a decrease in phenol alkylation conversion at constant temperature, but an increase in *ortho*-C-alkylation selectivity.[17] Deprotonation of an industrial silica-alumina catalyst likewise resulted in a decrease in phenol alkylation conversion at constant temperature, but an increase in *ortho*-C-alkylation selectivity.[15]

Our results and the observations from literature suggest that the C-alkylation isomer distribution is also influenced by the nature of the acid sites. Similar conversion over different catalysts yielded different isomer distributions.

References

1 E. A. Goldsmith, M. J. Schlatter and W. G Toland, Uncatalyzed thermal *ortho*-alkylation of phenols, *J. Org. Chem.,* 1958, 23, 1871-1876.

2 H. Hart and J. H. Simons, The kinetics and mechanism of the uncatalyzed alkylation of phenol, *J. Am. Chem. Soc*., 1949, 71, 345-352.

3 H. Hart, F. A. Cassis and J. J. Bordeaux, Inhibition of phenol alkylations by ethers. Kinetic evidence for phenol-ether complexes, *J. Am. Chem. Soc.,* 1954, 76, 1639-1641.

4 T. Sato, G. Sekiguchi, T. Adschiri and K. Arai, *Ortho*-selective alkylation of phenol with 2-propanol without catalyst in supercritical water, *Ind. Eng. Chem. Res.,* 2002, 41, 3064-3070.

5 R. West, Hydrogen bonding of phenols to olefins, *J. Am. Chem. Soc.,* 1959, 81, 1614-1617.

6 A. Wakisaka, Y. Yamamoto, Y. Akiyama, H. Takeo, F. Mizukami and K. Sakaguchi, Solvation-controlled clustering of a phenol-pyridine acid-base pair, *J. Chem. Soc. Faraday Trans.*, 1996, 92, 3339-3346.

7 W. Daniell, U. Schubert, R. Glöckler, A. Meyer, K. Noweck and H. Knözinger, Enhanced surface acidity in mixed alumina-silicas: a low-temperature FTIR study, *Appl. Catal. A*, 2000, 196, 247-260.

8 Q. Ma, D. Chakraborty, F. Faglioni, R.P. Muller, W.A. Goddard, T. Harris, C. Campbell and Y. Tang, Alkylation of Phenol: A mechanistic view, *J. Phys. Chem. A*, 2006, 110, 2246.

9 D. Harnish and J.L. Holmes, Ion-radical complexes in the gas phase: Structure and mechanism in the fragmentation of ionized alkyl phenyl ethers, *J. Am. Chem. Soc.,* 1991, 113, 9729.

10 F.W. McLafferty and F. Tureček, Interpretation of mass spectra, 4th ed; University Science Books: Mill Valley, CA, 1993

11 Y. Xia and A. de Klerk, Refining of coal liquids: Phenol alkylation by 1-hexene as model reaction, *Prepr. Pap.-Am. Chem. Soc., Div. Fuel Chem.,* 2012, 57(1), 553-554.

12 S. Natelson, Rearrangement of alkyl phenyl ethers on heating at moderate temperatures. Synthesis of tertiary amyl, tertiary butyl and diisobutyl phenols. *J. Am. Chem. Soc.,* 1934, 56, 1583.

13 A. de Klerk and R. J. J. Nel, Phenol alkylation with 1-octene on solid acid catalysts, *Ind. Eng. Chem. Res.*, 2007, 46, 7066-7072.

14 L. A. Potolovskii, N. M. Kukui, A. R.Lipshtein, G. G. Kotova and V. N. Vasil'eva, Alkylation of phenol with oct-1-ene with an aluminosilicate catalyst, *Petrol. Chem. USSR*, 1972, 12(2), 87-90.

15 I. T. Golubchenko, P. N. Galich, V. I. Khranovskaya and V. G. Motornyi, Alkylation of phenol by n-decene-1 on deprotonized aluminosilicates, *Petrol. Chem. USSR*, 1988, 28(3), 192-196.

16 K. G. Bhattacharyya, A. K. Talukdar, P. Das and S. Sivasanker, Al-MCM-41 catalysed alkylation of phenol with methanol*, J. Mol. Catal. A*, 2003, 197, 255-262.

17 S. Wagholikar, S. Mayadevi, S. Sivasankan, Liquid phase alkylation of phenol with 1-octene over large pore zeolites, Appl. Catal. A, 2006, 309, 106-114.

Chapter 6 Aromatic Alkylation in Continuous Fixed Bed Catalytic Reactor

To better prove that the catalysed alkylation of aromatics can be performed in the presence of nitrogen bases, we employed the same alkene and aromatics for alkylation, added some nitrogen bases to the mixture, but performed the evaluation in a continuous flow reactor instead of a batch reactor. This was necessary to demonstrate that the encouraging results obtained during the batch reactor alkylation (Chapter 5) was not due to an equilibration with a finite amount of nitrogen base, i.e. there could be sacrificial consumption of the base during batch experiments. In a flow system the base is continuously replenished and the contribution of sacrificial base consumption is eliminated. Once the flow system reaches steady state operation, only the effect of dynamic inhibition by the nitrogen base will be observed.

6.1 Experimental

6.1.1 Materials

Alumina and amorphous silica-alumina catalysts, Siral 30 and Siral 40, were employed. These catalyst types were the same as characterized in Chapter 3, and were commercially obtained from Sasol, Germany (former Condea GmbH). The phenol (99+%), 1-hexene (97%) and pyridine (99+%) were commercially obtained from Sigma-Aldrich and used without further purification. N_2 (purity 99.998%) were purchased from Praxair.

6.1.2 Experimental procedure and equipment

The catalysts were pretreated by calcination at 550°C for 6 hours. The reaction was carried out in a packed bed reactor instead of a constant-volume batch reactor as described in Chapter 5.

The continuous fixed bed catalytic reactor experiments were conducted in a stainless steel reactor with internal diameter of 1cm. A reactor setup schematic is shown in Figure 6- 1.

The lines up- and downstream from the reactor were heated to 60°C to preheat reactants and avoid solidification of the feed and product (phenol has a melting point of 43 °C). The whole system was maintain at a temperature sufficient to keep phenol liquid. The catalysts were diluted with 400 mesh (38μm) carborundum. The ratio of catalyst to carborundum was 1:1. The average particle size of the catalyst was 50 μm as given by Sasol. The catalyst bed volume is 5ml, and the catalyst weight is 0.5g. The catalyst packing in the reactor is shown in figure 6-2.

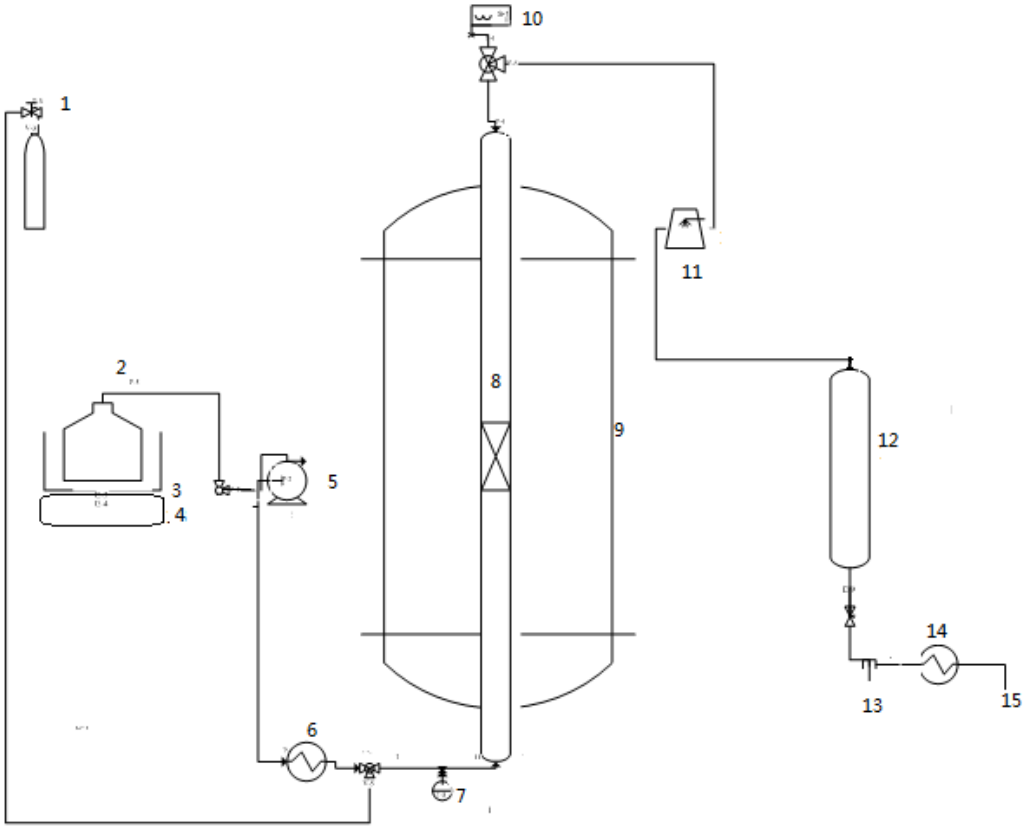

Fig 6- 1 Flow Reactor Design

1. N_2 Cylinder
2. Mixture Feed
3. Heating Plate
4. Balance
5. Seri I Pump
6. Heater 1
7. Pressure Indicator
8. Stainless Steel Reactor
9. Furnace
10. Thermocouple
11. Heater 2
12. Product-Collecting Container
13. Heavier Products Collection
14. Cooling Water
15. Lighter Products Collection

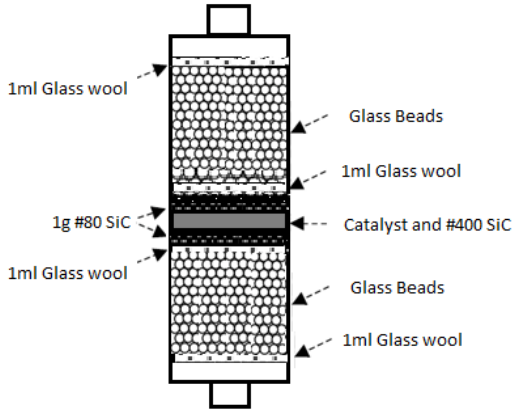

Fig 6- 2 Catalyst packing

Our model compounds, phenol and 1-hexene, were mixed in a container and were pumped into the reactor through a SERI I pump at a flow rate of 0.15ml/min. The flow reactor experiments were conducted at a weight hourly space velocity (WHSV) of 17 h^{-1}. The mixture is pumped from the bottom to the top of the reactor (i.e. upflow mode of operation). The catalytic reactions were carried out at an internal temperature of 315°C and atmospheric pressure.

Before starting the experiment, the bed was fully wetted by passing the mixture feed at slightly higher rate, then, the flow rate was adjusted to the desired values. Nitrogen was used to purge the inside of the reactor and was also employed for leak testing.

It took approximately two hours to attain steady state. The attainment of steady state was determined by measuring the flow rate using the balance under the feed container. The mass balance was also checked by measuring the feed and the outlet.

We ran the system continuously. Once the flow rate was steady, we gradually added increasing amounts of pyridine into the mixture. When the pyridine content of the feed was 0.25%, the extent of permanent deactivation was assessed. We heated up the reactor to 450 °C and then went back to 315°C, repeating the reactor with clean feed and then we added pyridine again.

The product was collected every 1h. Reaction products were confirmed by GC-MS and then quantified by GC-FID. The calculation is same as the methods for the batch reactor results. Each reaction was repeated at least twice to confirm the results. The analytical procedures were similar to that reported in Chapter 5.

6.2 Results and Discussion

Catalyst performance for phenol alkylation was evaluated without and with pyridine addition (figure 6- 3).

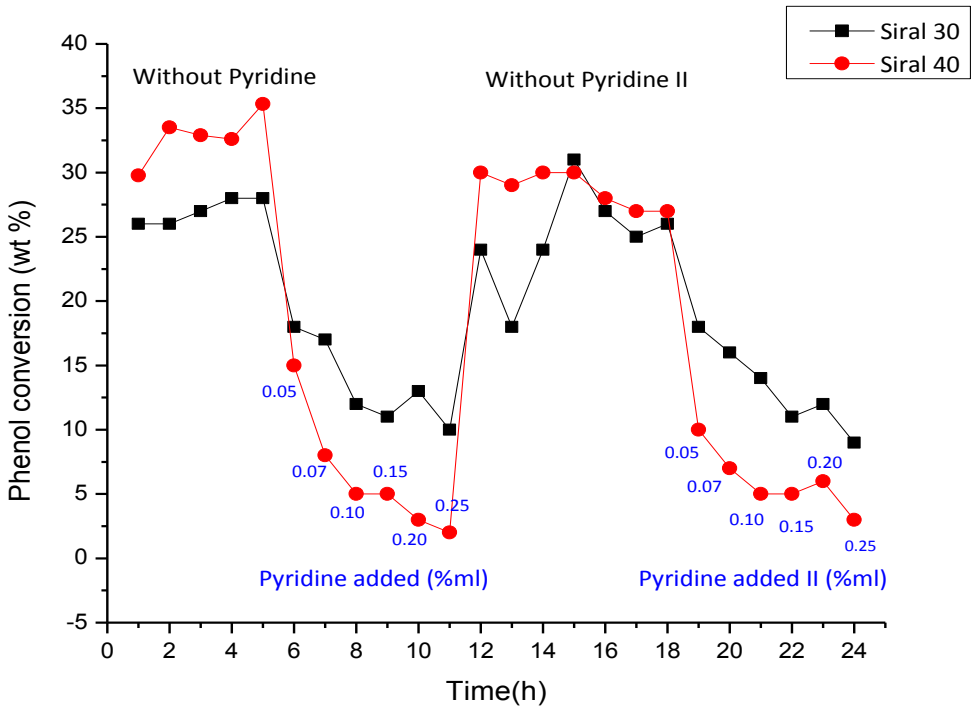

Fig. 6-3 Phenol conversion comparison of Siral30 and Siral40 with and without pyridine

From figure 6- 3 we can find that the conversion of Siral 40 is better than Siral 30 without pyridine for the first run. When we added 0.05% pyridine, the conversion dropped sharply for Siral 40, and it deactivated more when we added more pyridine. The Siral 30 catalyst also exhibited decreased conversion with the nitrogen base inside the feed, but not as much as Siral 40.

When we tested the products after the catalyst was heated up inside the reactor to 450 °C before reducing the temperature to 315 °C again, the conversion recovered for both catalysts. This suggested that the catalysts were mainly inhibited by the nitrogen base, but not completely poisoned. The conversion data in Table 6-1 were normalized to surface area and acid cites

distribution of Siral30 and Siral40. It shows that Siral30 performed slightly better in clean feed when the results are expressed on a surface area basis. Conversion per µmol acid cites per gram catalysts yielded the same trend with conversion without normalization.

Table 6- 1. Phenol alkylation with 1-hexene, with and without pyridine over Siral 30 and Siral40 catalysts at 315 °C, atmosphere pressure and an equivalent WHSV of 17 h^{-1}

Pyridine	Conversion on surface area basis(wt%/m^2/g)		conversion on acid cites basis (wt%/µmol/g)		Time(h)
%	Siral30	Siral40	Siral30	Siral40	
0	0.13	0.11	0.023	0.037	1
0	0.13	0.13	0.023	0.041	2
0	0.14	0.13	0.024	0.040	3
0	0.14	0.13	0.025	0.040	4
0	0.14	0.13	0.025	0.043	5
0.05	0.09	0.06	0.016	0.018	6
0.07	0.09	0.03	0.015	0.010	7
0.1	0.06	0.02	0.011	0.006	8
0.15	0.06	0.02	0.010	0.006	9
0.2	0.07	0.01	0.012	0.004	10
0.25	0.05	0.01	0.009	0.002	11
Heating up then return to 315°C					
0	0.12	0.11	0.021	0.037	12
0	0.09	0.11	0.016	0.035	13
0	0.12	0.11	0.021	0.037	14
0	0.16	0.11	0.028	0.037	15
0	0.14	0.11	0.024	0.034	16
0	0.13	0.10	0.022	0.033	17
0	0.13	0.10	0.023	0.033	18
0.05	0.09	0.04	0.016	0.012	19
0.07	0.08	0.03	0.014	0.009	20
0.1	0.07	0.02	0.012	0.006	21
0.15	0.06	0.02	0.010	0.006	22
0.2	0.06	0.02	0.011	0.007	23
0.25	0.05	0.01	0.008	0.004	24

In the feed, poisoning is the loss of activity because of the strong chemisorption of impurities on the active sites. Usually, there is a distinction between poisons and inhibitors.[1] Strong and irreversible interaction with the active sites are generally described as poisons, whereas inhibitors are usually weaker and reversibly absorb on the catalyst surface. The action of inhibitors could be called an intermediate between very strong poisoning and the normal competition among the molecules for an active site.

It is believed that nitrogen containing compounds inhibit the catalytic reactions because basic nitrogen blocks the acid sites. For our catalysed aromatic alkylation, the competitive adsorption of the basic compound pyridine onto an acid catalyst is an example of inhibition. The competitive inhibitor, which is the pyridine molecule here, occupied the catalytic site (acid site), due to its accessibility to the catalysts and the base-acid interaction. By occupying the active sites, the inhibitors block a reaction path and thus prevent alkylphenol production on that site while the pyridine is adsorbed. In this way it slows down the reaction.

As we added more pyridine, because of the competitive adsorption between our feed and the nitrogen containing compound, the performance become poorer. Yet, the catalyst remained active for phenol alkylation, suggesting that adsorption on some of the acid sites was reversible at reaction conditions. However, due to the general reversibility of the acid-base reaction

we can regenerate the catalysts. Heating up to a higher temperature helped us to eliminate some the inhibitors on the acid sites and the conversion recovered.

It is learned that for poisoning, a change in selectivity occurs, which means the most active sites, as related to the acid strength, is a factor in being poisoned. The most active sites will be poisoned first, which may lead to various relationships between the catalyst activity and quantities of poison sites.[2] It should be noted though that the strong acid sites that were poisoned at the operating temperature could be regenerated and the poisoning was not permanent.

We can see that the Siral 40 deactivated more sharply. It may due to its higher concentration of strong acid sites.

References:

1. J. Haber, J.H. Block and B. Delmon, Manual Of Methods And Procedures For Catalyst Characterization, *Pure Appl. Chem*., 1995, 67(8)(9), 1257.
2. P Forzatti and L. Lietti, Catalyst deactivation, *Catalysis Today*, 1999, 52, 165-181.

Chapter 7 Conclusions

Our main purpose of the research was to find appropriate catalysts that can conduct acid catalysis in the presence of nitrogen bases for the aromatic alkylation. Some key points which can be highlighted from the study are as follows:

a) Our interest is in the direct application of acid catalysis to unhydroprocessed coal liquids. In Chapter 2 it was pointed out that the main class of nitrogen bases in coal liquids are the aniline, pyridine and quinoline families, which are bases of medium strength. By selecting a catalyst with adequate medium strength acidity, it was postulated that at alkylation temperature the pyridine will only inhibit acid catalysed phenol alkylation.

b) Through a series of catalyst characterization studies in Chapter 3, we learned that amorphous silica-alumina catalysts in the Siral series (Siral 1 to 40) and gamma-alumina has good accessibility for bulky coal liquids. A combined study involving total acid concentration (from NH_3-TPD) and the Lewis:Brønsted acid ratio (from FTIR) indicated that Siral30 has considerably higher medium strength Lewis and Brønsted acid sites than the other catalysts investigated. It was postulated that this would be the best catalyst for acid catalysed phenol alkylation in the presence of nitrogen bases.

c) A high Lewis:Brønsted acid ratio was observed in the Siral1 to Siral10 catalysts. This may due to the high amount of alumina (>90 %) in these catalysts, which has high Lewis acidity. It was anticipated that these catalysts would be close in behavior to pure alumina.

d) Hydration is an important variable to consider, since it affects the catalytic activity and selectivity. This was demonstrated by our catalyst characterization studies of the catalysts pretreated at different calcination temperatures.

e) The rate of acid catalysed aromatic alkylation increased with temperature. There is a threshold temperature at which acid catalysed cracking becomes significant as a competing reaction with alkylation. Model alkyl aromatic and alkyl phenyl ether compounds were prepared to study decomposition (Chapter 4). The results from this study were unfortunately inconclusive.

f) The base desorption from weaker acid sites, as determined in Chapter 2, indicated that phenol alkylation must be performed preferably at a temperature higher than 205 °C. Selective alkylation was possible at high rate at 315 °C.

g) Phenol alkylation with alkenes can proceed in the absence of a catalyst. In Chapter 5 it was found that the contribution of uncatalysed phenol

alkylation increases with temperature. At 315°C uncatalysed phenol conversion was 3%. The main product is the *ortho*-C-alkylated phenol. Uncatalysed phenol alkylation is inhibited by pyridine, with phenol conversion decreasing by half on the addition of 0.05 wt% pyridine.

h) In Chapter 5 phenol alkylation was performed with 1-hexene over selected catalysts in micro batch reactors. It was found that catalysed phenol alkylation displayed high *ortho*-C-alkylation selectivity at lower conversion, with an increase in *meta*/*para*-C-alkylation selectivity observed at higher conversion. There was no clear relationship between high *ortho*-C-alkylation selectivity and acid strength, or the alumina content of the catalysts. However, the selectivity could not be explained just in terms of conversion.

i) A 24% phenol conversion was obtained with clean feed over Siral30 at 315 °C and an equivalent weight hourly space velocity of 19 h^{-1}. At the same conditions 12% phenol conversion was obtained after the catalyst was treated with pyridine and 0.05% pyridine was added to the feed. It demonstrated phenol alkylation could be performed in the presence of pyridine.

j) In batch reactors the amount of nitrogen base is inherently limited and to confirm that it was truly inhibition and not partial poisoning, the tests were repeated in a continuous flow reactor. In Chapter 6, the catalytic

phenol alkylation performed in the continuous fix bed reactor confirmed that Siral30 sustained alkylation conversion of phenol, while pyridine was continuously added.

k) During flow reactor experiments catalyst activity could be completely restored by *in situ* heating of the catalysts to 450 °C and resuming alkylation with clean feed at the original test conditions. It indicated that the catalysts were mainly inhibited by the nitrogen bases and not permanently poisoned.

l) It was found that better conversion in the presence of different levels of pyridine inhibition was obtained with Siral30, while the highest conversion with clean feed was obtained by Siral40. These observations can be generalized. Phenol alkylation in the absence of nitrogen bases was best correlated to the concentration of strong Brønsted acid sites. The best phenol alkylation performance in the presence of pyridine was achieved by the catalyst with the highest combined medium strength Lewis and Brønsted acid site concentration.

Appendix I

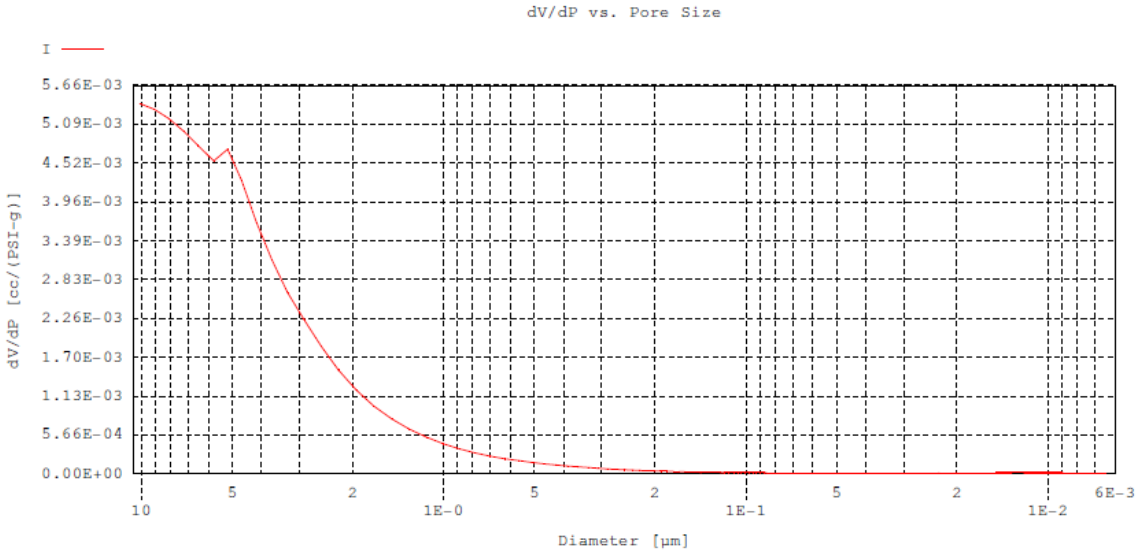
dV/dP vs. Pore Size
I
5.66E-03
5.09E-03
4.52E-03
3.96E-03
3.39E-03
2.83E-03
2.26E-03
1.70E-03
1.13E-03
5.66E-04
0.00E+00
dV/dP [cc/(PSI-g)]
10
5
2
1E-0
5
2
1E-1
5
2
1E-2
6E-3
Diameter [µm]

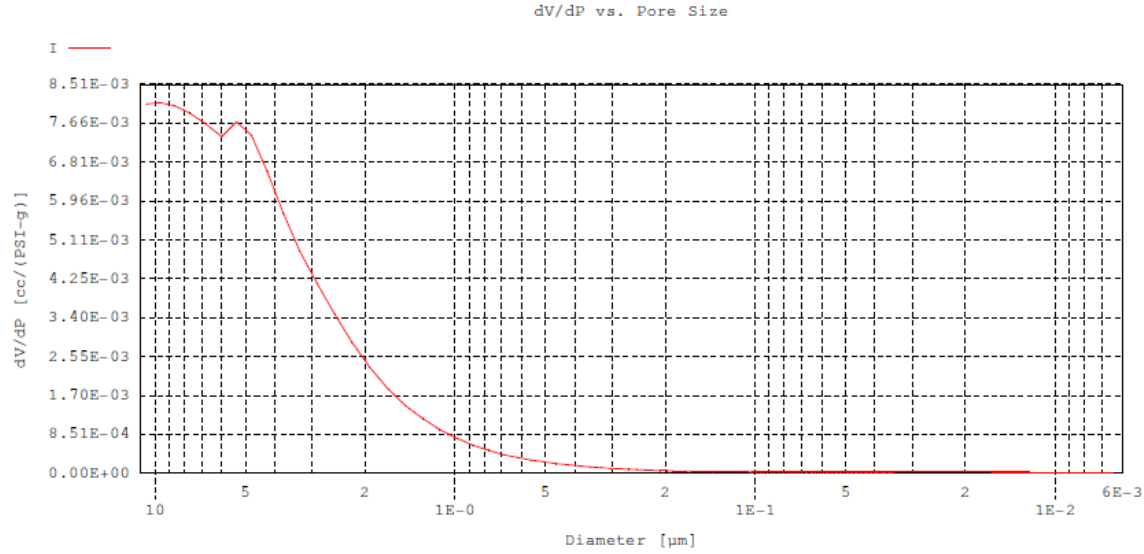
dV/dP vs. Pore Size
I
8.51E-03
7.66E-03
6.81E-03
5.96E-03
5.11E-03
4.25E-03
3.40E-03
2.55E-03
1.70E-03
8.51E-04
0.00E+00
dV/dP [cc/(PSI-g)]
10
5
2
1E-0
5
2
1E-1
5
2
1E-2
6E-3
Diameter [µm]

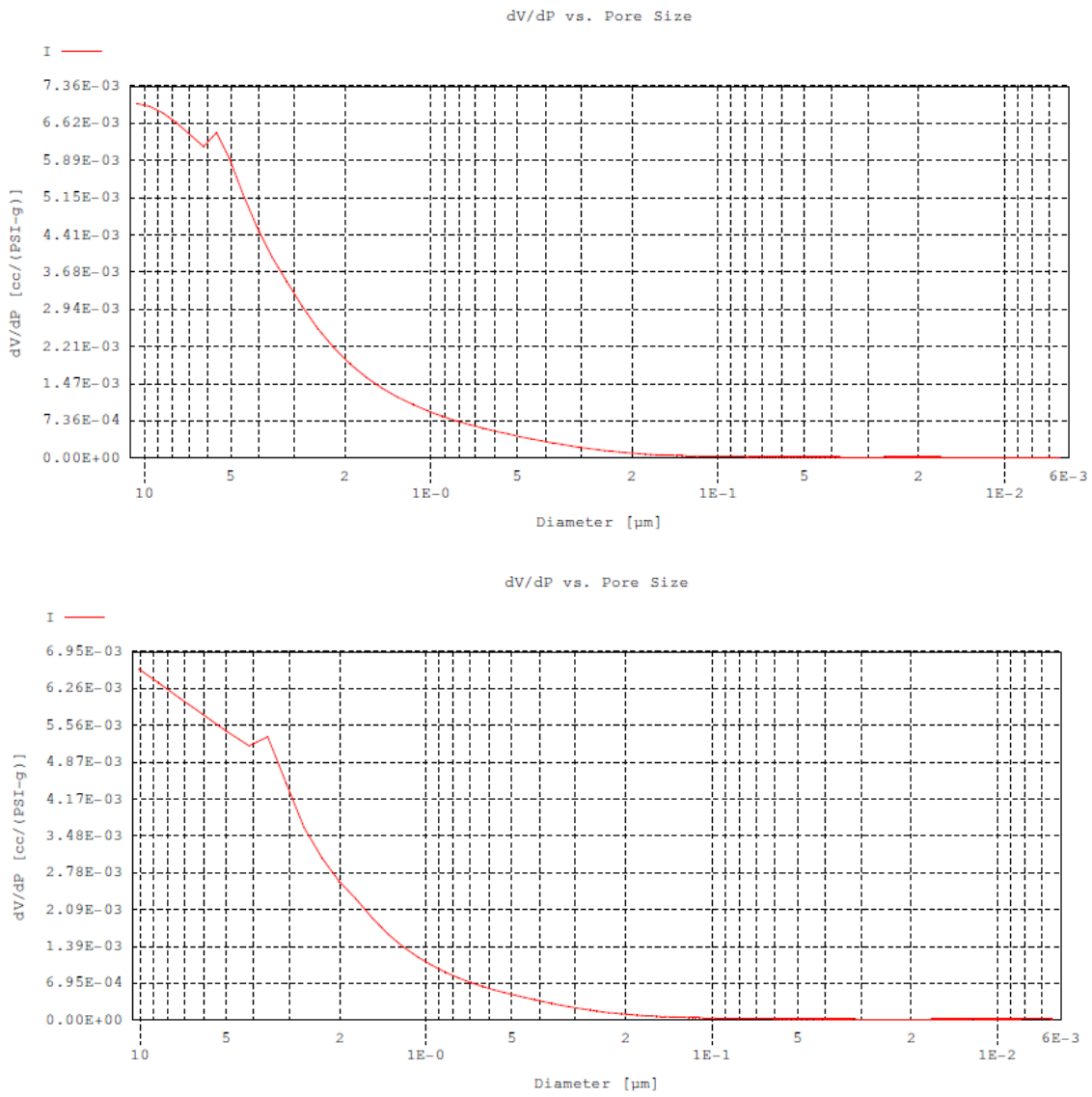

Figure I- 1 Pore size distribution: Siral 10 (150°C calcined 6h); Siral40 (150°C calcined 6h); Siral30 (150°C calcined 6h); Siral30 (550°C calcined 6h)

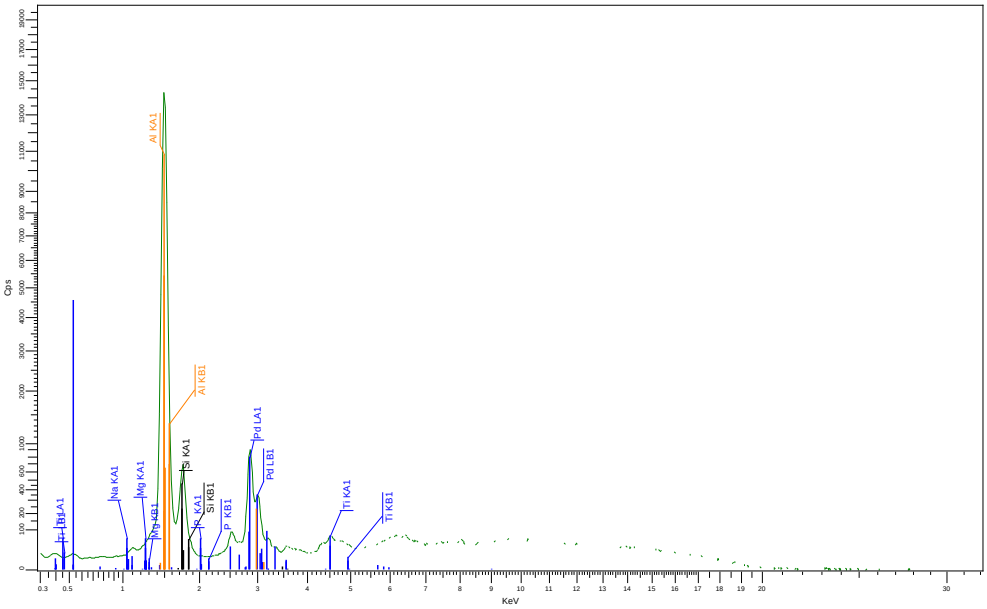
Cps
KeV
Al KA1
Al KB1
Si KA1
Pd LA1
Pd LB1
Na KA1
Mg KA1
Mg KB1
Si KB1
P KB1
Ti KA1
Ti KB1

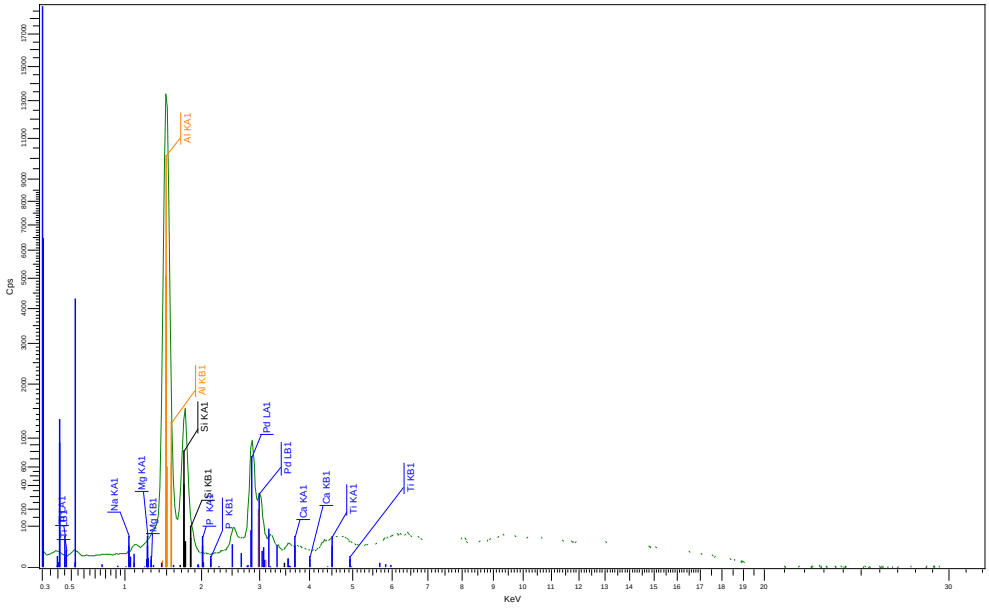
Cps
KeV
Al KA1
Al KB1
Si KA1
Pd LA1
Pd LB1
Na KA1
Mg KA1
Mg KB1
Si KB1
P KB1
Ca KA1
Ca KB1
Ti KA1
Ti KB1

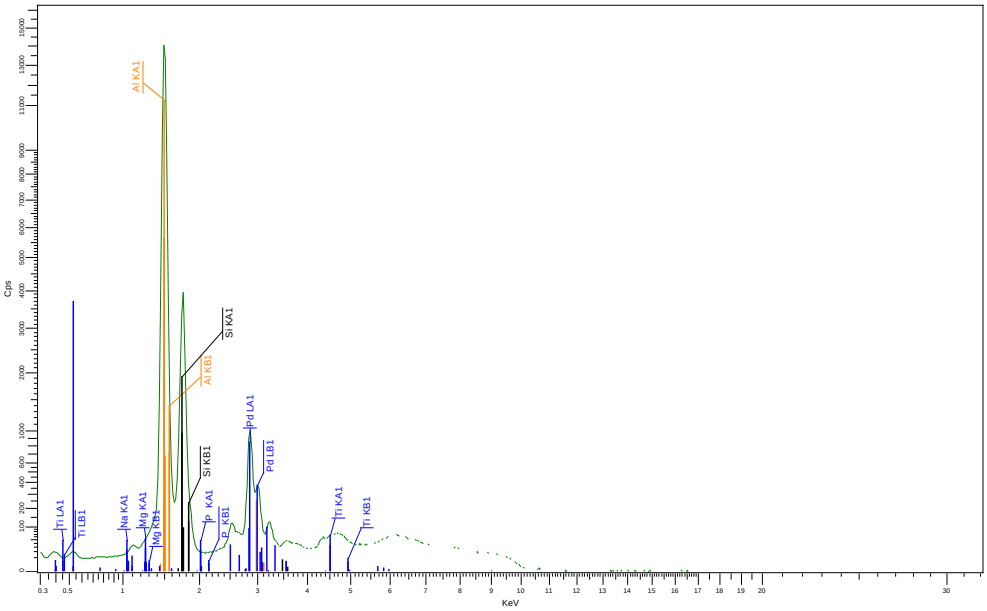
Cps
KeV
Al KA1
Si KA1
Al KB1
Si KB1
Pd LA1
Pd LB1
Ti LA1
Ti LB1
Na KA1
Mg KA1
Mg KB1
P KA1
P KB1
Ti KA1
Ti KB1

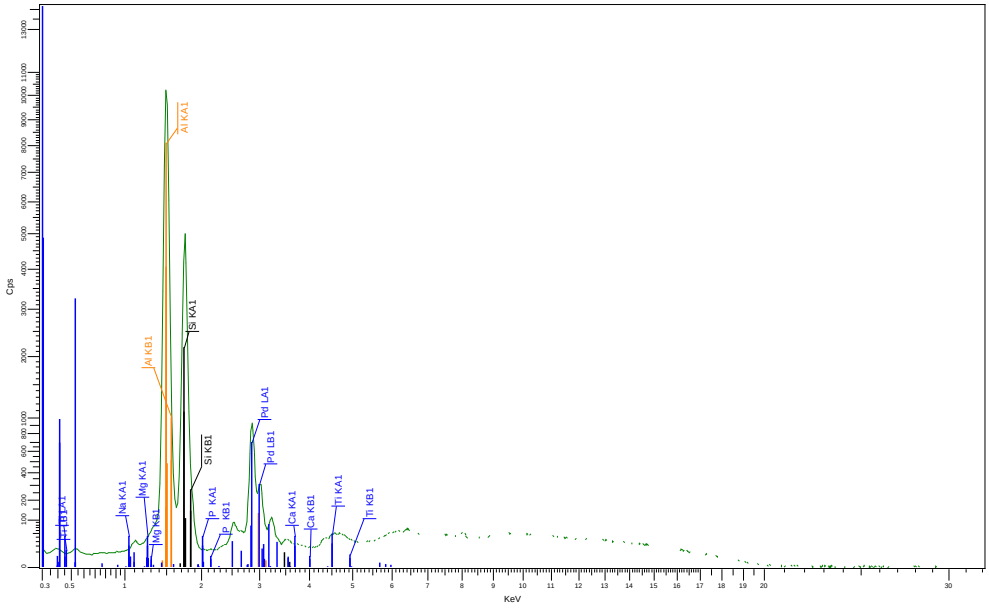
Cps
KeV
Al KA1
Al KB1
Si KA1
Si KB1
Pd LA1
Pd LB1
Ti LA1
Ti LB1
Na KA1
Mg KA1
Mg KB1
P KA1
P KB1
Ca KA1
Ca KB1
Ti KA1
Ti KB1

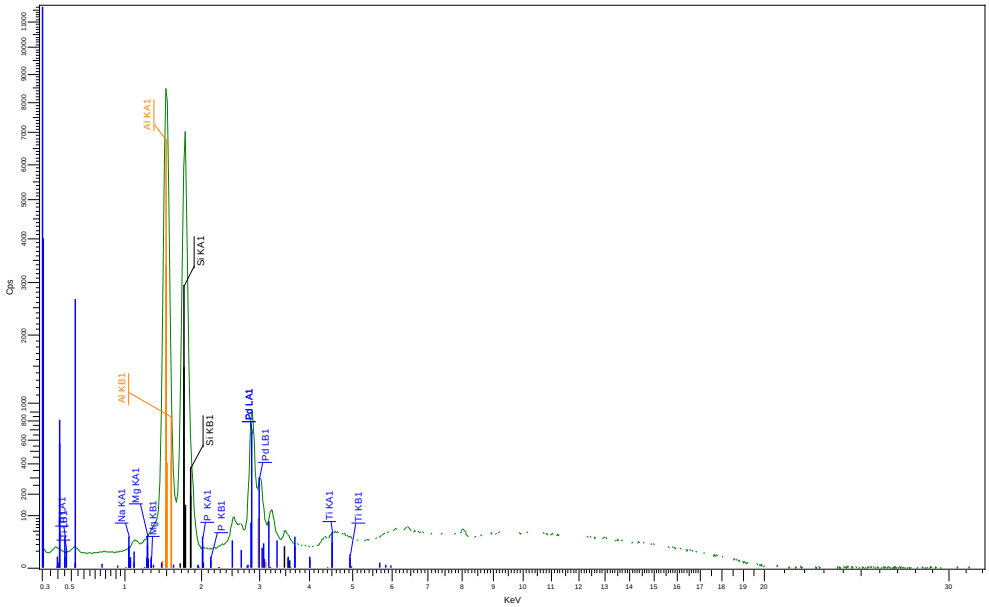
Cps
KeV
Al KA1
Si KA1
Al KB1
Si KB1
Pd LA1
Pd LB1
Na KA1
Mg KA1
Mg KB1
P KA1
P KB1
Ti KA1
Ti KB1

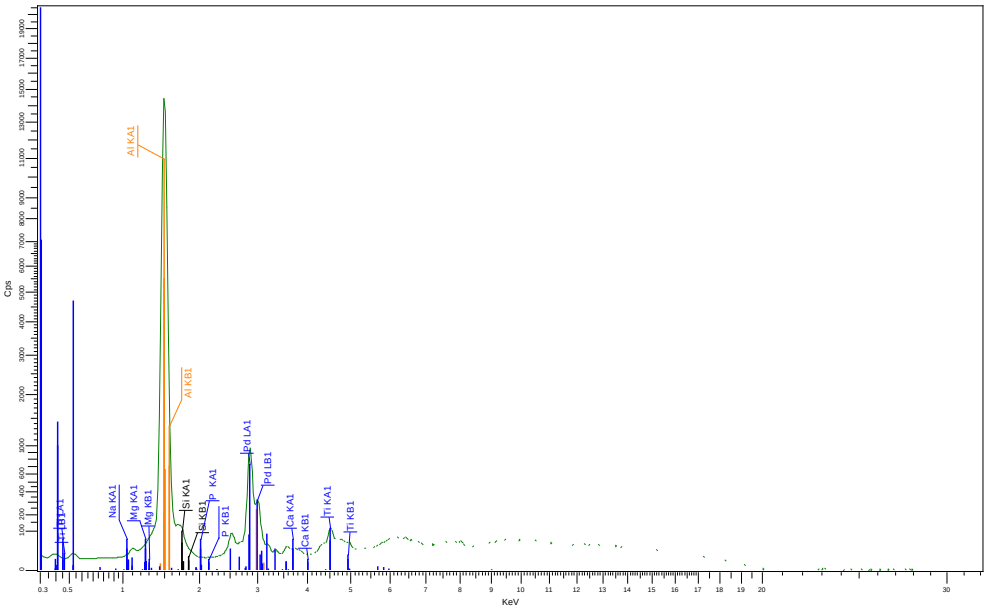
Cps
KeV
Al KA1
Al KB1
Pd LA1
Pd LB1
Na KA1
Mg KA1
Mg KB1
Si KA1
Si KB1
P KA1
P KB1
Ca KA1
Ca KB1
Ti KA1
Ti KB1

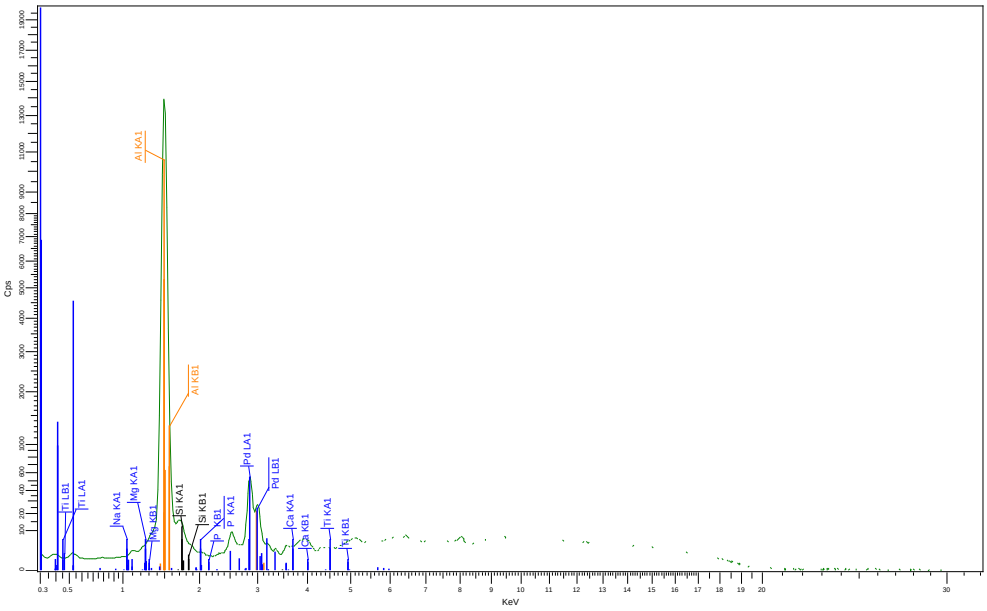

Figure I- 2 XRF for Siral 5(150°C calcined 6h);Siral 10(150°C calcined 6h); Siral20(150°C calcined 6h); Siral30 (150°C calcined 6h), Siral40(150°C calcined 6h); Pural SB(150°C calcined 6h), Pural BT(150°C calcined 6h);

Appendix II

Calculation of B

Catalyst	height(1450cm^{-1})			height(1490cm^{-1})			Lewis:Bronsted acid ratio		
	25 °C	300 °C	400 °C	25 °C	300 °C	400 °C	25 °C	300 °C	400 °C
Siral 1	0.36	0.20	0.13	0.09	0.04	0.03	5.9	11.6	7.3
Siral 5	0.36	0.12	0.07	0.08	0.03	0.02	8.1	5.9	4.4
Siral 10	0.37	0.15	0.06	0.07	0.03	0.02	14.6	11.6	3.3
Siral 20	0.37	0.23	0.13	0.10	0.06	0.05	4.9	5.3	2.6
Siral 30	0.32	0.24	0.15	0.11	0.09	0.05	3.1	2.7	3.3
Siral 40	0.36	0.19	0.15	0.11	0.08	0.06	3.8	2.2	2.4
Pural SB	0.27	0.12	0.07	0.04	0.03	0.04			

Catalyst	Acid site concentration(µmol/g)			Total acid sites (µmol/g)		Weak acid sites (µmol/g)		Medium acid sites (µmol/g)		Strong acid sites (µmol/g)	
	Weak	Medium	Strong	Bronsted	Lewis	Bronsted	Lewis	Bronsted	Lewis	Bronsted	Lewis
Siral 1	368	205	130	102	601	75	293	11	194	16	114
Siral 5	394	326	98	90	728	28	366	43	283	18	80
Siral 10	493	353	92	60	878	25	468	14	339	21	71
Siral 20	453	246	109	136	672	81	372	26	220	30	79
Siral 30	452	489	186	276	851	92	360	139	350	43	143
Siral 40	480	170	170	170	650	65	415	56	114	50	120
Pural SB	337	124	258	0	719	0	337	0	124	0	258

H: Height

B: Brønsted acid sites

L:Lewis acid sites

first use gamma alumina(PURAL SB) for calculating the K1, K2, all of the acid cites in gamma alumina is Lewis acid cites,

L+B=L

$H(1450CM^{-1})$=K1L-------1

$H(1490CM^{-1})$=K2L+K3B----------2

L+B=Total--------3

$H(1450CM^{-1})$=0.27=K1*719

$H(1490CM^{-1})$=0.04=k2*719

We use siral30 to calculate K3, first calculate the Lewis acid cites of siral30 with equation1, bronsted acid sites equates total acid sites minus Lewis acid cites

K1 0.000376

K2 0.0000556

K3 0.000227157

K2/K1 0.14787234 K3/K1 0.604141135

$H(1490CM^{-1})/H(1450CM^{-1})$=K2/K1+K3/K1*(B/L)------4

We used equation 4 to calculate Bronsted:Lewis acid ratios and then calculated Lewis:Bronsted acid ratios

we calculated the bronsted acid sites and lewis acid sites by combining L/B ratios and acidity distribution datas from NH_3-TPD

Appendix III

GC results for the products of the synthesis.

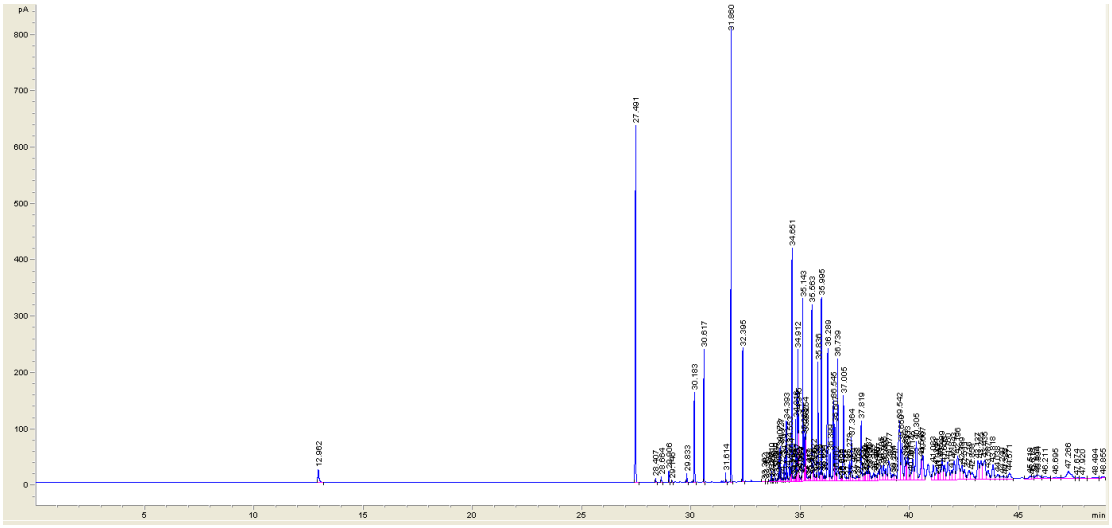

Alkylphenol

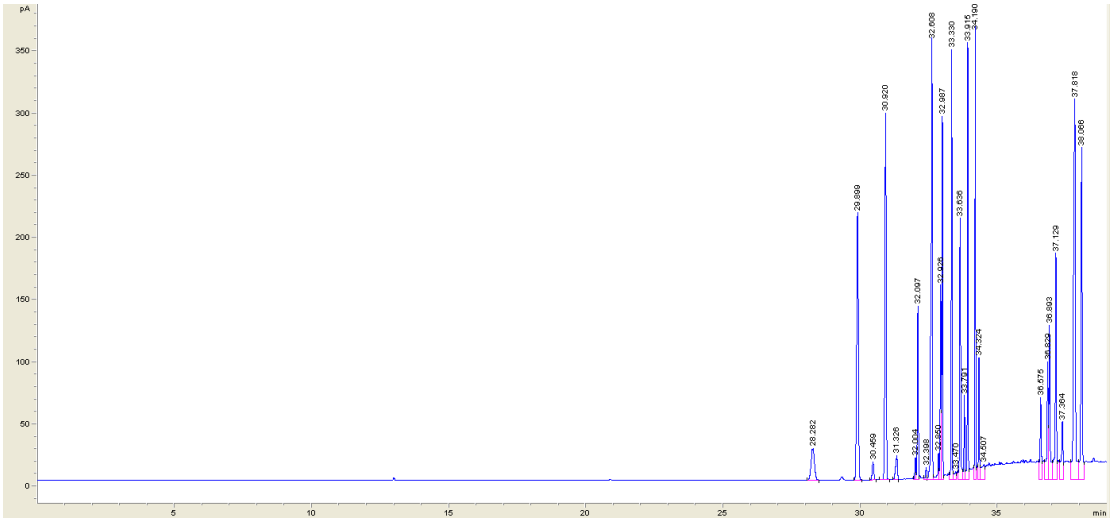

Phenol Ether

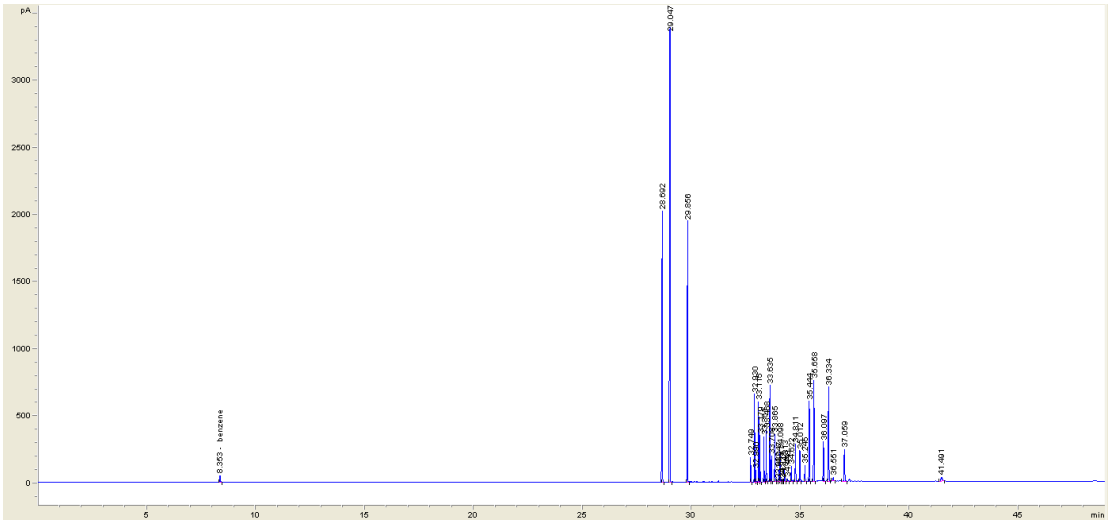

Alkylbenzene(1-Chlorohexane)

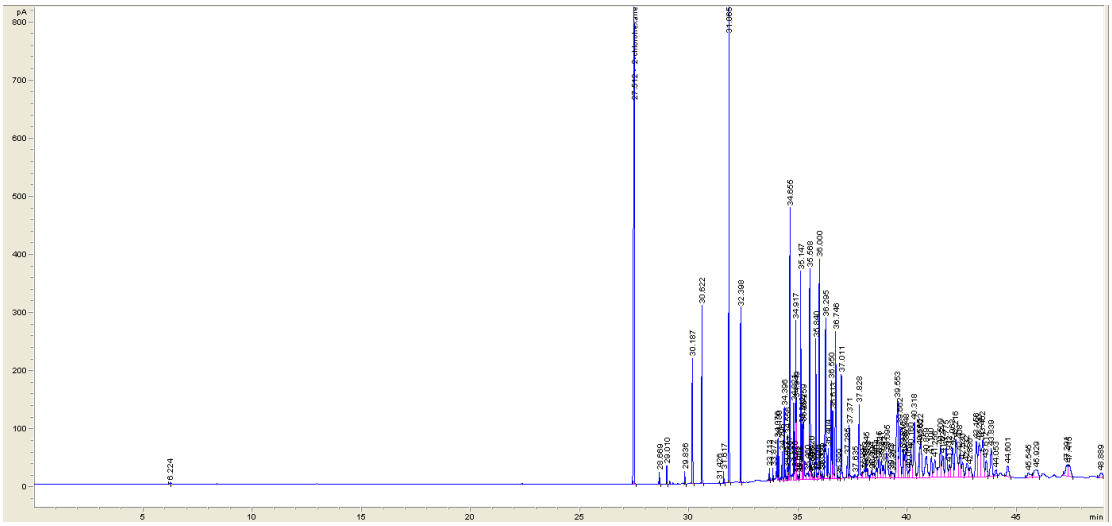

Alkylbenzene(1,6-Dichlorohexane)

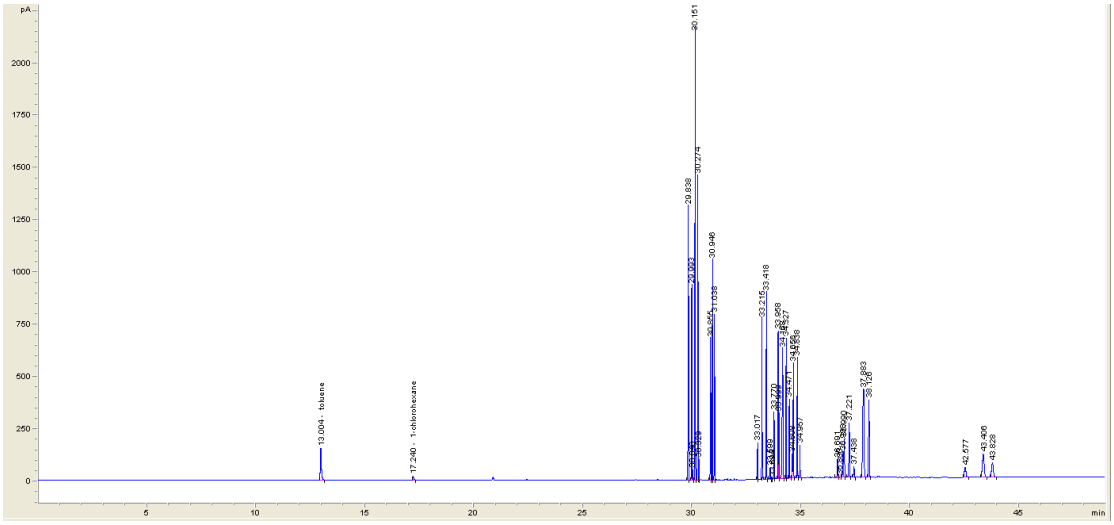

Alkyltoluene(1-chlorohexane)

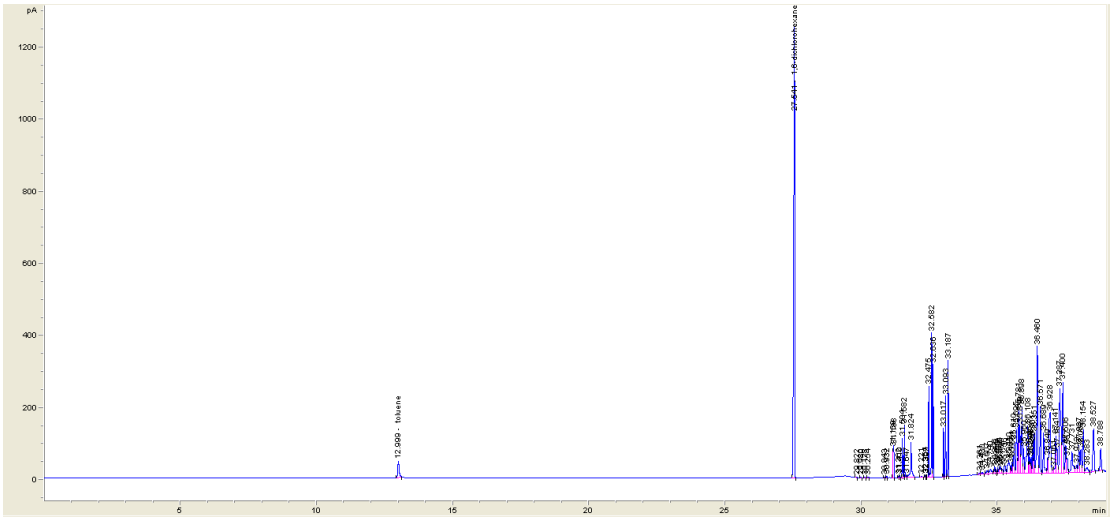

Alkyltoluene(1,6-Dichlorohexane)

Figure III-1 GC for synthesizing reaction products

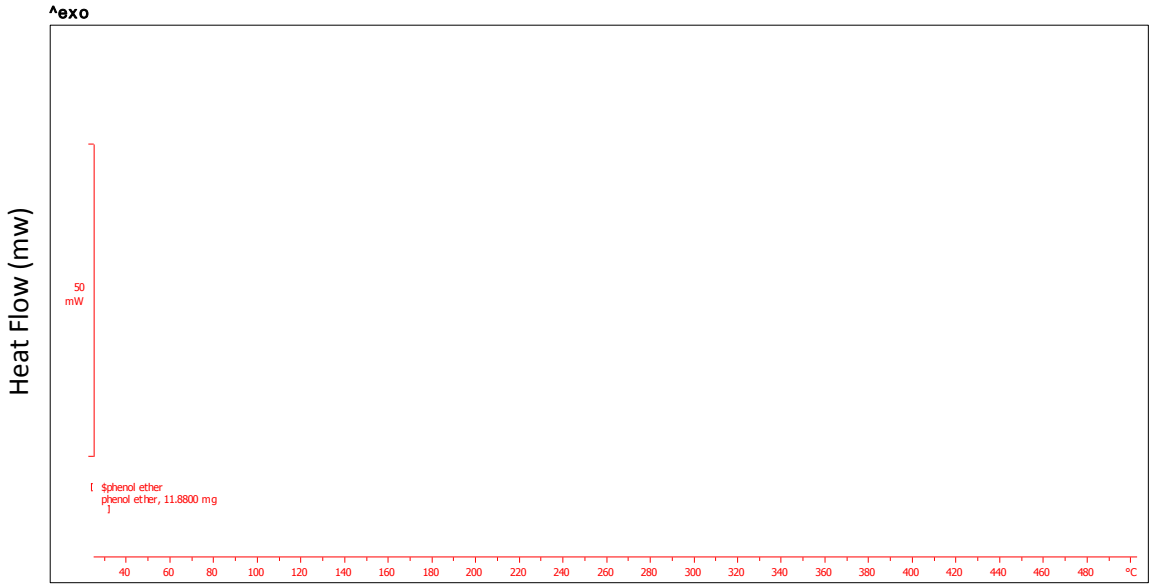

Phenol ether

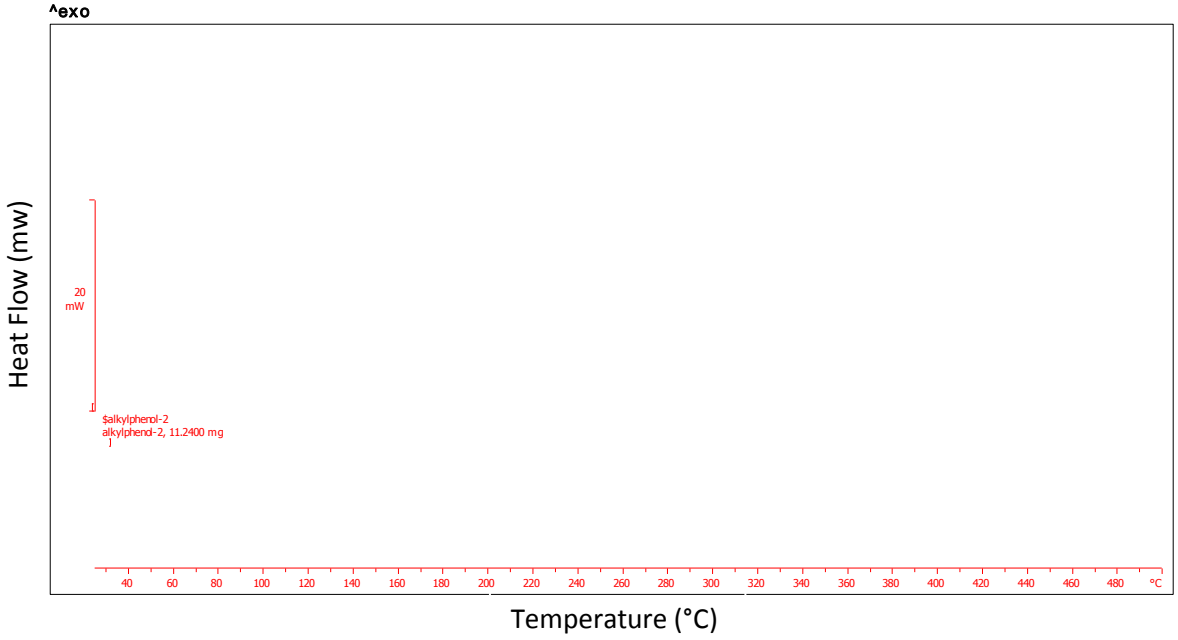

Alkylphenol

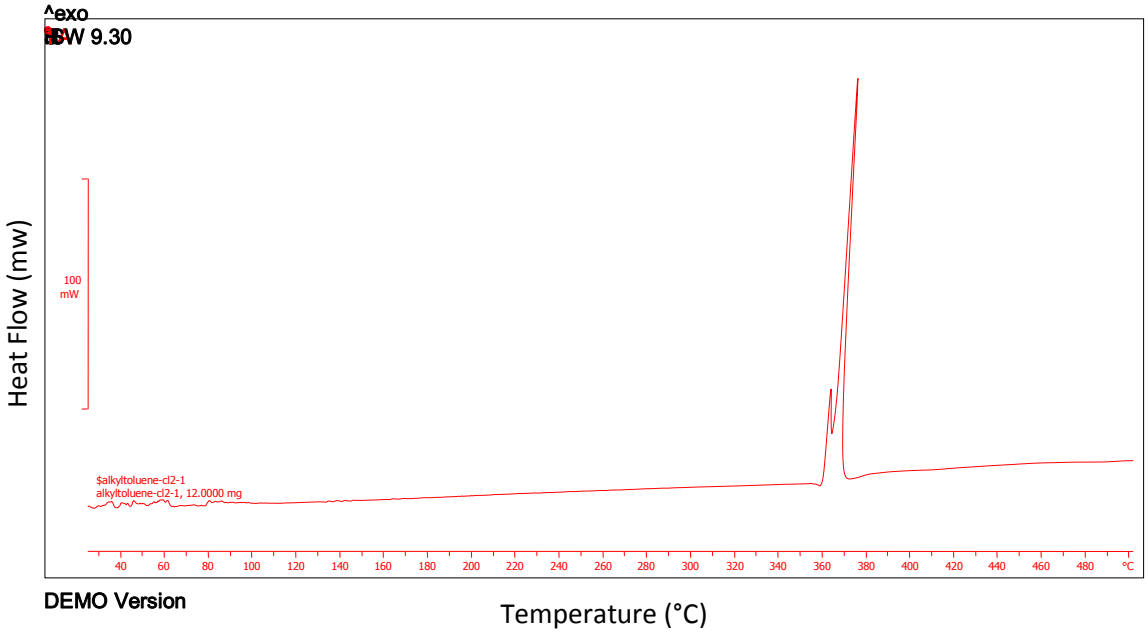

Alkytoluene(1,6-Dichlorohexane)

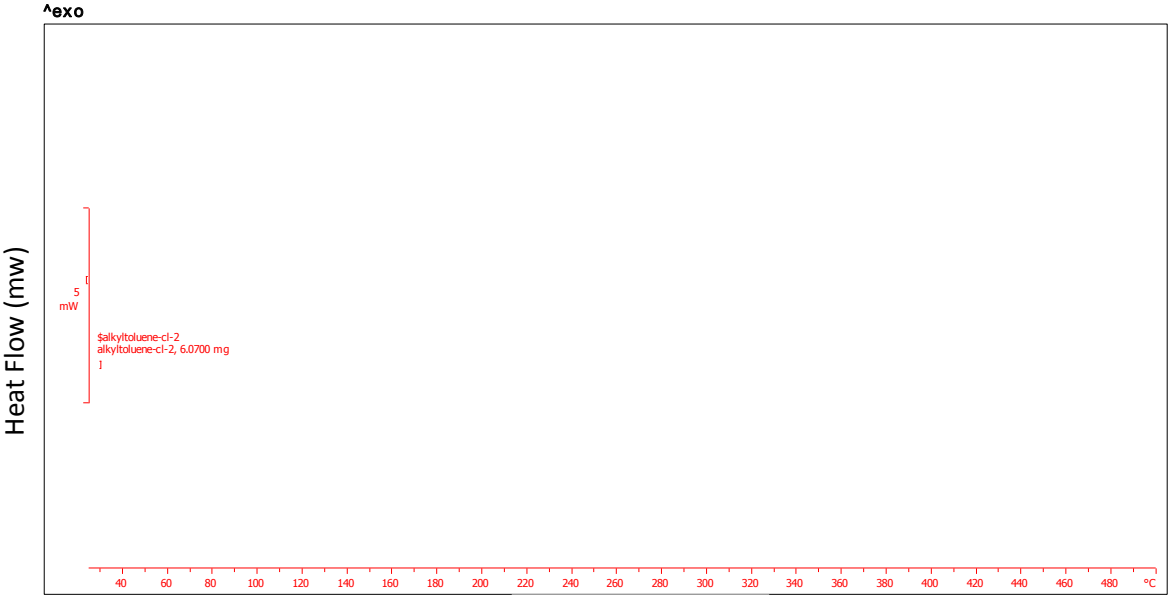

Alkyltoluene(1-chlorohexane)

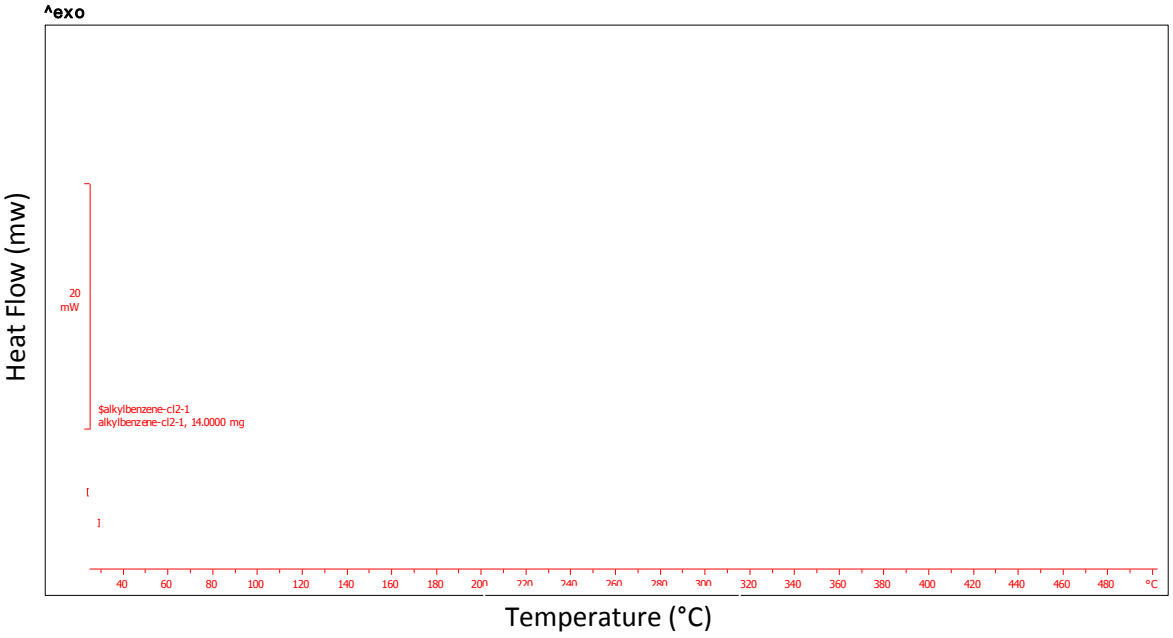

Alkylbenzene(1,6-Dichlorohexane)

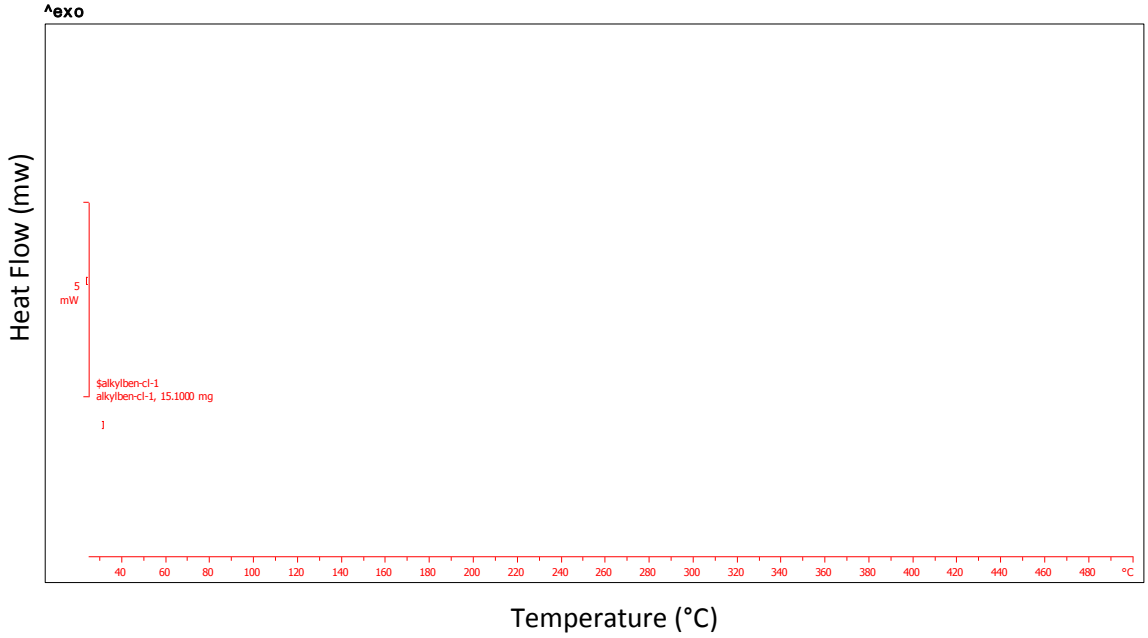

Alkylbenzene(1-chlorohexane)

Figure III- 2 HP-DSC curves for the aromatic alkylation products

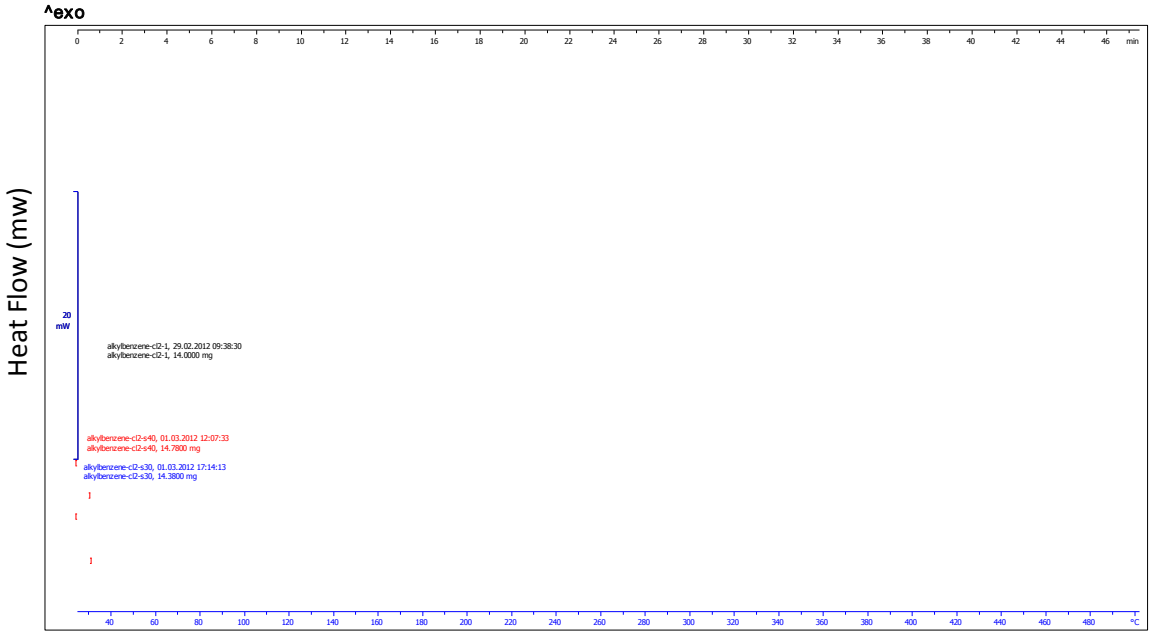

Figure III- 3 Alkylbenzene(1,6-Dichlorohexane) without catalyst(black line);siral30(Blue line); siral40(Red Line)

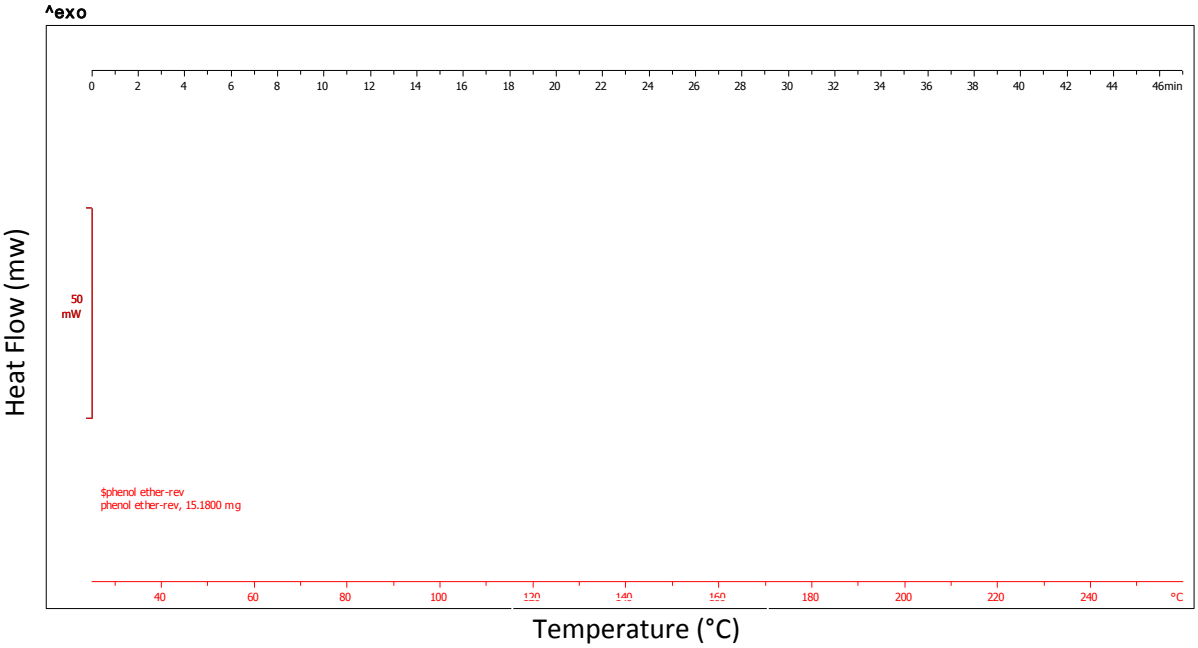

Phenol Ether (25°C to 260°C to 25°C)

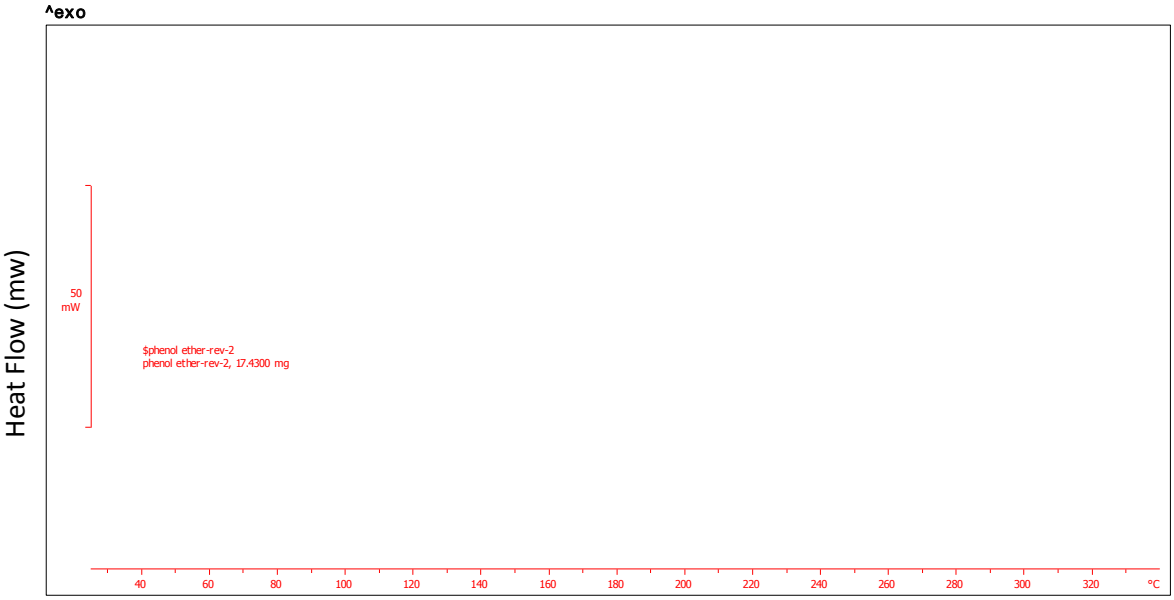

Phenol Ether (25°C to 330°C to 25°C twice)

Figure III- 4 Reversible HP-DSC For Phenol Ether

Appendix IV

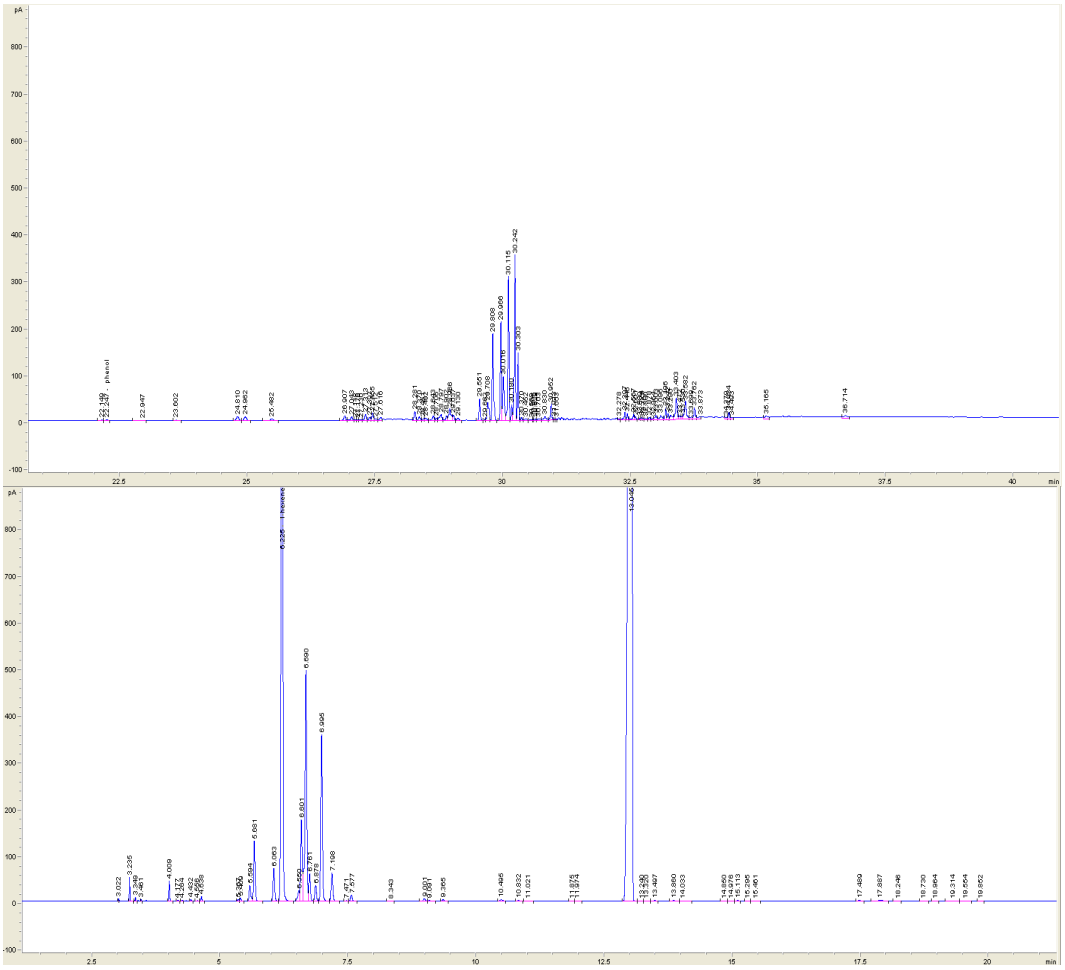

Figure IV- 1 Chromatograms showing toluene alkylation with 1-hexene on Siral 5(Zoom in for different retention time)

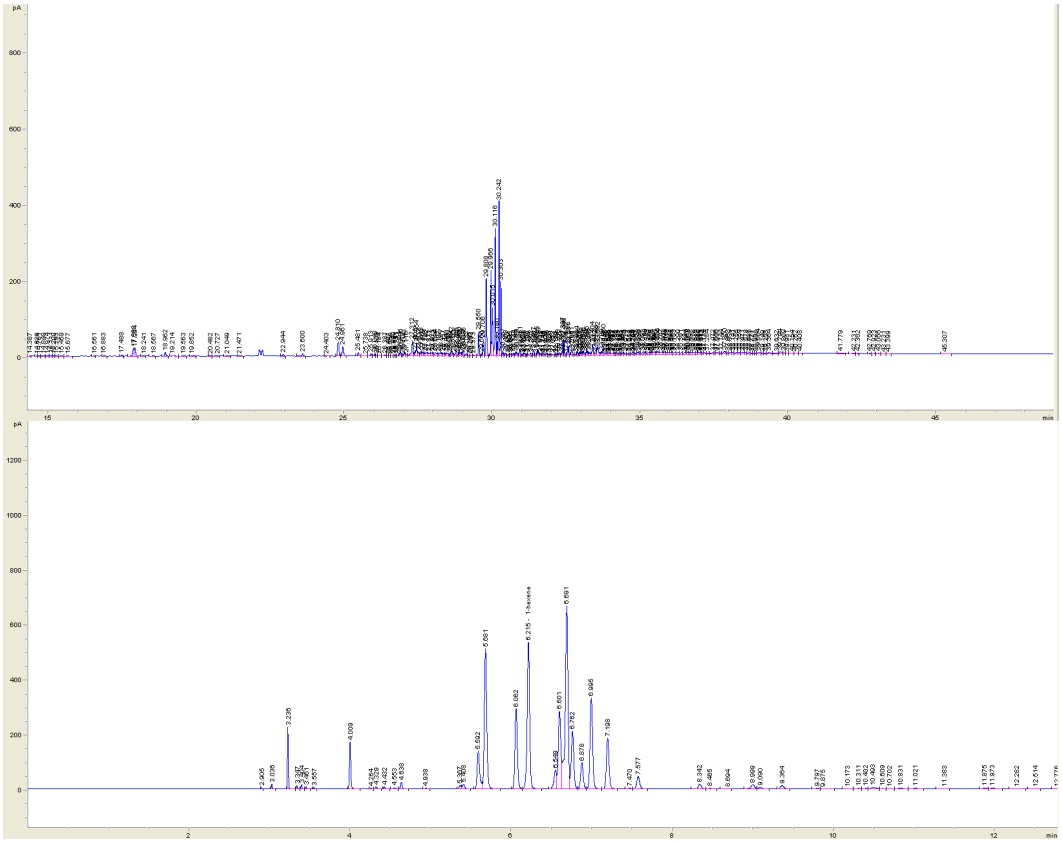

Figure IV- 2 Chromatograms showing toluene alkylation with 1-hexene on Siral 30

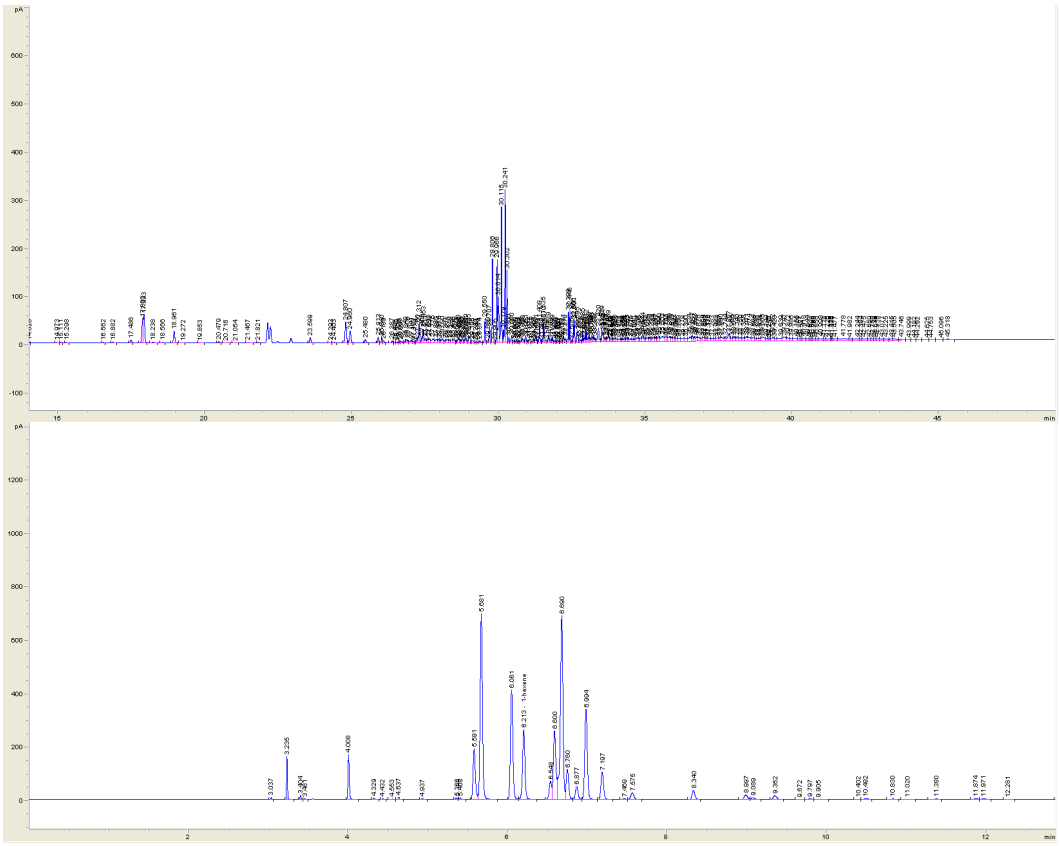

Figure IV- 3 Chromatograms showing toluene alkylation with 1-hexene on Siral 40

Appendix V

GC-MS for product identification

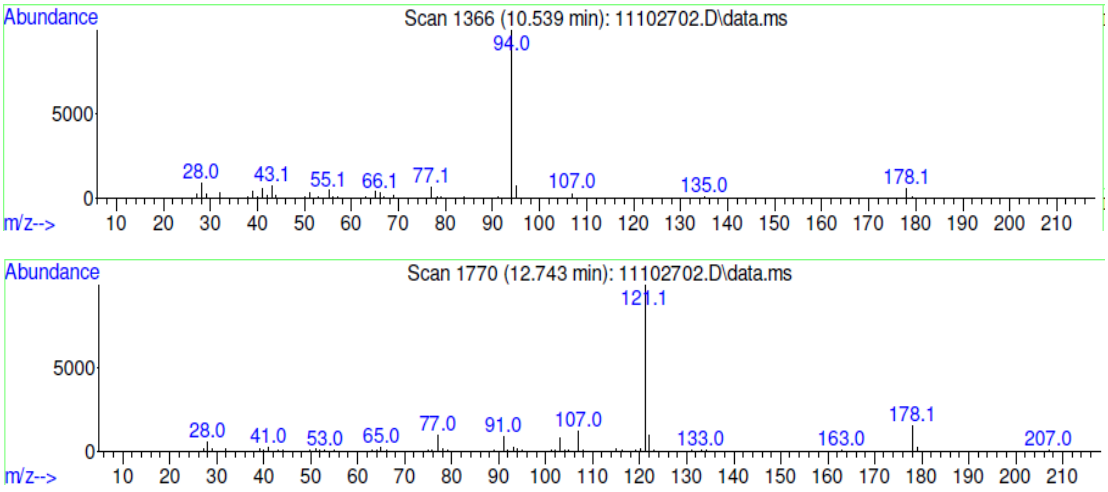

Figure V- 1 Electron impact mass spectra of alkylphenols.

The electron impact mass spectra of the main alkylation products are given in Figure V-1.

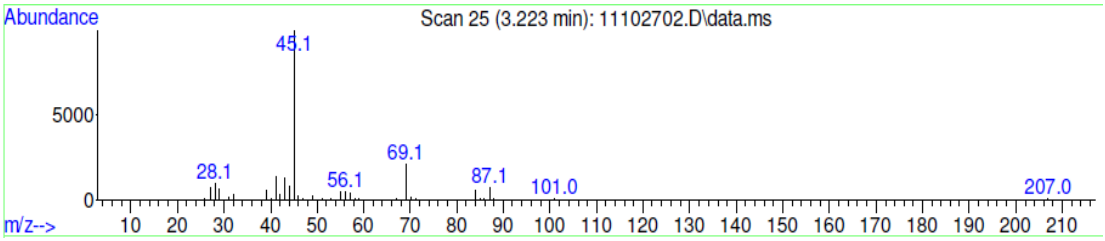

Figure V- 2 Electron impact mass spectrum of hexanol

The compound has a prominent fragment at 45 m/z, which is typical of the CH_3–$CH{=}OH^+$ fragment from the alpha cleavage of 2-alcohols. Based on its mass spectrum and elution time the product is hexanol.